

JAN. - APR. 2000
Volume VI Number 1

ISSN 0859 144X

THE ASEAN JOURNAL OF RADIOLOGY

Published by The Radiological Society and
The Royal College of Radiologists of Thailand,
Bangkok, Thailand

Started through an educational grant from



1955

Leading-Edge Technology and Power

Computed Tomography Systems

Toshiba developed helical scanning which has become the global standard for CT. Other firsts include the real-time reconstruction technology known as AspireCI and other patented innovations creating the heart of the CT scanner. Acting now as a leader in CT technology, Toshiba continues its climb to the top in the area of clinical results.

The half-second CT scanner features a totally new concept in which the gantry has a cylindrical structure. This combines with revolutionary new multislice technology to collect multiple slices simultaneously in a single scan. The result is amazing volume data in a short time over a broad range. The CT has extended its range from diagnosis to treatment, and is now active over a wide range that includes the head region, cardiovascular, lung and abdomen, and limbs. Toshiba will continue to chart new paths in CT technology with new advances.

TOSHIBA

GLOBAL IMAGING • MEDICAL SYSTEMS

- 1998 Achieves cumulative global total of 10,000 systems.
- 1998 Development of multislice helical technology and half-second helical CT.
- 1996 Development of subsecond helical CT.
- 1993 Development of AspireCI real time technology.
- 1987 Obtains patent in Europe for helical scanning.
- 1986 Obtains patent in U.S.A. for helical scanning.
- 1979 Starts research on helical technology.

Half-Second Real-Time Helical CT

- By creating the world's first 0.5 second full scan, Toshiba has realized use in the cardiac region.
- Toshiba has also realized 12 frame/second real-time reconstruction and 0.5 second/frame high-speed reconstruction.
- Equipped with highly definitive 3D display software.
- Designed for multislice technology.



Evolving
Step by Step
Towards
Tomorrow

Made for Life



CMC BIOTECH CO., LTD.

364 Muban Town-in-Town, Soi Ladphrao 94, Ladphrao Road, Wangthonglang, Bangkok 10310

(SOLE DISTRIBUTOR) Tel. (662) 530-4995-6, 559-2179-80, 538-4102, 538-0710, 559-3261-2 Fax: 539-6903

JAN. - APR. 2000
Volume VI Number I

ISSN 0859 144X

THE ASEAN JOURNAL OF RADIOLOGY

Published by The Radiological Society and
The Royal College of Radiologists of Thailand,
Bangkok, Thailand

Started through an educational grant from



1955

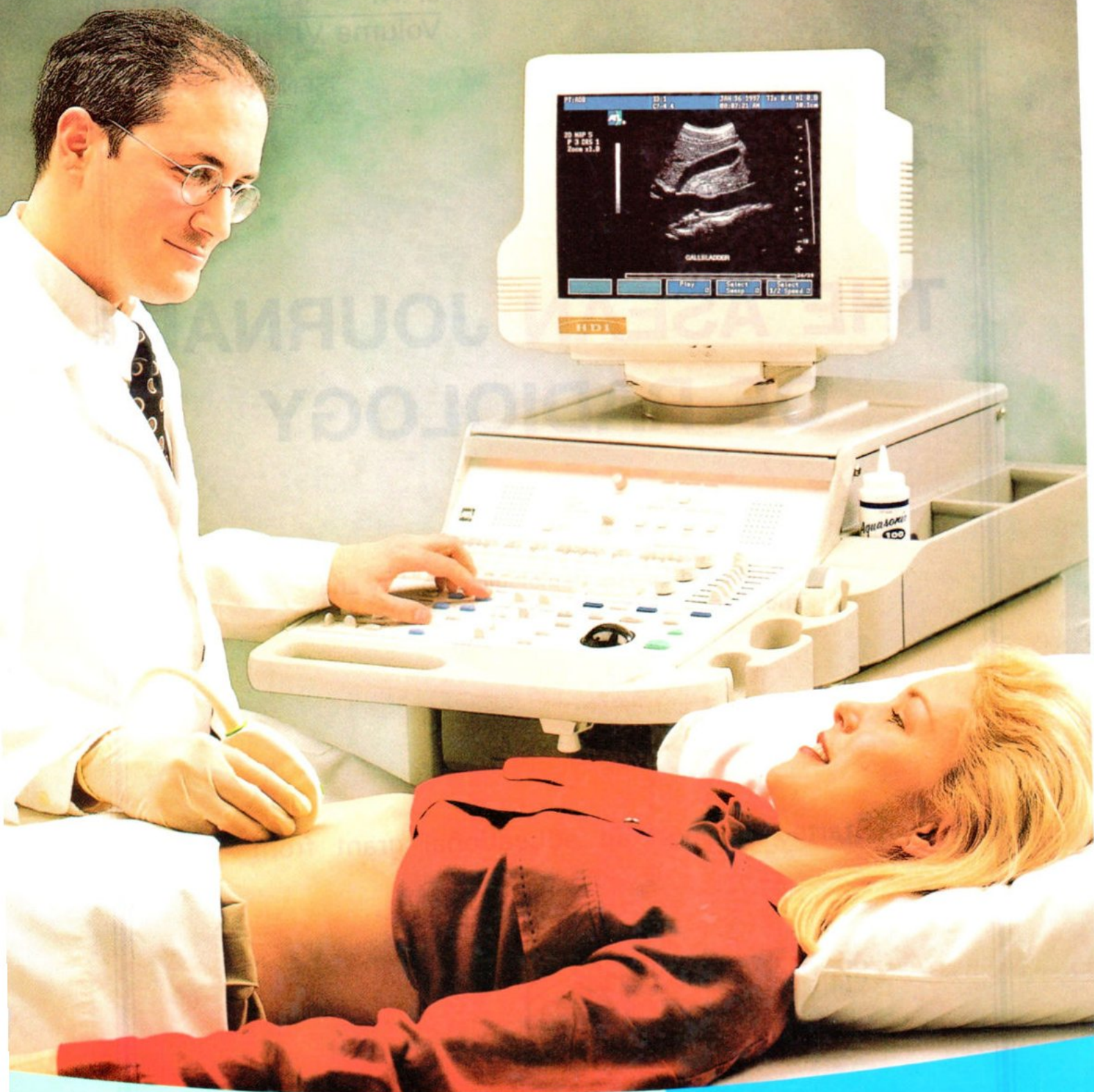
Chief Editor

Professor Kawee Tungsubutra
Kaweevej Hospital, 318 Taksin Road, Dhonburi, Bangkok 10600, Thailand.

WE ARE ULTRASOUND



A Philips Company



FOR MORE INFORMATION PLEASE CONTACT

PHILIPS MEDICAL SYSTEMS

- TEL. 745-4090 Ext. 3332
- FAX. 398-0792

Philips Electronics (Thailand) Ltd.
209/2 Sanpavuth Road, Bangna, Bangkok 10260

☎ 78/2542



PHILIPS

Let's make things better.

CONTENTS

	Page
1. FULL TERM PREGNANCY WITH A HUGE RECURRENT IMMATURE TERATOMA: A CASE REPORT. Chalida APHINIVES, Jitjaroen CHAIYAKUM.	1-4
2. METASTATIC BREAST CANCER IN THE FIRST METACARPAL BONE OF THE NON-DOMINANT HAND: A CASE REPORT. Chalida APHINIVES, Jitjaroen CHAIYACUM, Jaturat KANPITTAYA, Jumpol MITRCHAI.	5-8
3. LANGERHANS' CELL HISTIOCYTOSIS Khomdao BOONCHIT, Jiraporn SRINAKARIN, Dumrongsuk BOONCHIT, Warinthorn BUNCHALEAW.	9-16
4. MAMMOGRAPHIC AND SONOGRAPHIC FEATURES IN PHYLLOIDES TUMOURS Darunee BOONJUNWETWAT, Chunya WILAI, Pichet SAMPATHANUKUL.	17-22
5. ULTRASONIC AND COMPUTED TOMOGRAPHIC APPEARANCES OF PARAGANGLIOMA SIMULATING OVARIAN CANCER Kanjana DANPUKDEE, Piyaporn LIMANOND.	23-26
6. PERCUTANEOUS TRANSLUMINAL ANGIOPLASTY AND WALL STENT PLACEMENT IN THE TREATMENT OF TRANSPLANTED RENAL ARTERY STENOSIS. Krisdee PRABHASAVAT, Saroj VANAPRUKS, Somsak TANAWATTANACHAROEN.	27-34
7. THE FIRST AORTIC STENT-GRAFT PLACEMENT IN THAILAND Jiemjit TAPANEYAKORN, Surasak LEELAUDOMLIPI, Suthus SRIPHONJANART, Sarana BOONBAICHAIPRUCK, Suvipaporn SIRIPORNPITAK.	35-40
8. CT FINDINGS OF RENAL ACTINOMYCOSIS: A CASE REPORT Suprasit CHAROONWATANALAOHA, Linda PANTONGRAG-BROWN.	41-44

THE ASEAN JOURNAL OF RADIOLOGY

Volume VI Number I JAN. - APR. 2000

CONTENTS

	Page
9. PROGNOSTIC VALUE OF CONTRAST ENHANCED CT SCAN COMPARED TO CLINICAL SEVERITY GRADING SYSTEM IN ACUTE PANCREATITIS Kanjana LEELALAWAN, Nittaya CHAMADOL, Chaiyut THANAPAISAL.	45-54
10. PATTERN OF RADIATION THERAPY IN THE TREATMENT OF PEDIATRIC BRAIN TUMORS IN SIRIRAJ HOSPITAL Nan SUNTORNPONG, Supatra SANGRUCHI.	55-61
11. QUALITY ASSURANCE IN NUCLEAR MEDICINE IMAGING Anchali KRISANACHINDA.	63-66
12. ACCEPTANCE TESTING ON A MULTIPLE-DETECTOR SPECT SYSTEM Anchali KRISANACHINDA.	67-72
13. BREAST CANCER DETECTION WITH ^{99m}Tc MIBI IMAGING AND MAMMOGRAPHY Tawatchai CHAIWATANARAT, Chalermchai APINYANURAK, Darunee BOONJUNWETWAT, Kris CHATAMRA, Makumkrong POSHYACHINDA.	73-82
14. GRANULOMATOUS AMEBIC ENCEPHALITIS : REPORT OF TWO CASES WITH NEUROIMAGING FINDING. Arkhom ARAYAWICHANONT, Orasa CHAWALPARIT, Tumtip SANGRUCHI, Vorapun SENANARONG.	83-89

FULL TERM PREGNANCY WITH A HUGE RECURRENT IMMATURE TERATOMA: A CASE REPORT.

Chalida APHINIVES, M.D., Jitjaroen CHAIYAKUM, M.D.

ABSTRACT

Immature teratoma is an infrequent ovarian tumor in reproductive female, especially occurring with pregnancy. This report describes the radiologic findings in a 35-year-old woman, with 32-weeks pregnancy, presented a huge multiloculated cyst in the Cul-de-sac. Thirteen years ago, she was diagnosed to have an immature teratoma, but her treatment was not completed. At this time, cesarean section was performed when her pregnancy reached 36 weeks, but the biopsies of abdominal cysts revealed multicystic peritoneal mesothelioma. No further treatment was done because the patient refused to have.

INTRODUCTION

Any malignancy during pregnancy is rare, with an estimated incidence of 0.07-0.1%.¹ Germ cell tumors are the most frequent ovarian malignancies associated with pregnancy.^{2,3}

Ovarian tumors may cause serious complications during pregnancy and postpartum. Some of these include adnexal torsion and obstruction to vaginal delivery. The most common ovarian tumors are cystic. Beischer and associates (1971) described 164 ovarian tumors diagnosed during pregnancy; one fourth were cystic teratomas. Ovarian tumors complicating pregnancy often are entirely overlooked (Stedman and Kline, 1988). Careful examination of all pregnant women would eliminate some, but not all, of these missed tumors. If an ovarian tumor does not occupy the pelvis, diagnosis through physical examination is especially difficult because abdominal enlargement may attribute to a more advanced pregnancy, multiple fetuses, or hydramnios; and the true condition may not be recognized until after labor. Sonography often provides accurate differentiation between uterine enlargement and an extrauterine cystic mass.

CASE REPORT

A 35-year-old woman presented to another hospital with a larger pelvic mass for gestational age, 32 weeks from the history of menstruation. Ultrasound revealed multiloculated cyst in the Cul-de-sac, 20 cm in diameter. She was referred to Srinagarind hospital, Faculty of Medicine. Her previous medical record, 13 years ago, revealed immature teratoma with incomplete treatment (right salpingo-oophorectomy, 1 circle of VAC) because of her refusal. The MRI revealed huge multiple cystic masses occupying in the pelvic cavity and extending to the middle part of abdomen. The masses contained solid components also, esp. in the anterior aspect (figure 1). There were multiple cystic masses involving right posterior lobe of liver, spleen, and subcutaneous plane at epigastrium and umbilical regions (figure 2-5). There were obstructive hydronephrosis of both kidneys. The diagnosis of malignant cystic masses with pregnancy was suggested. She was performed cesarean section 3 weeks later (36-week gestational age). During this operation, left tubal resection and 2 biopsies of small cysts at abdominal wall and uterus were also performed.

Pathological examinations revealed multicystic peritoneal mesothelioma. Her previ-

ous specimens were reviewed and the diagnosis of immature teratoma was confirmed. Although

her gynecologist suggested further treatment, she again refused to have.

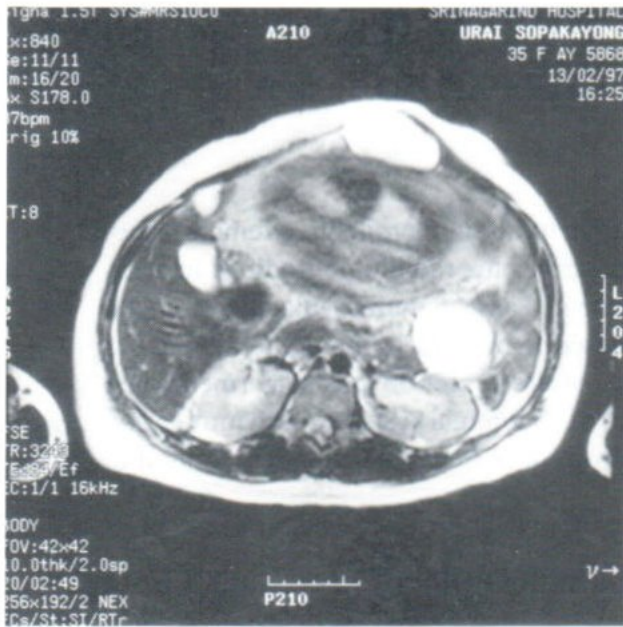


Fig. 1. Axial T2-weighted FSE (TR/TE = 3243/84) revealed 4 x 3 cm intra-abdominal cystic lesion attached to peritoneum anteriorly.

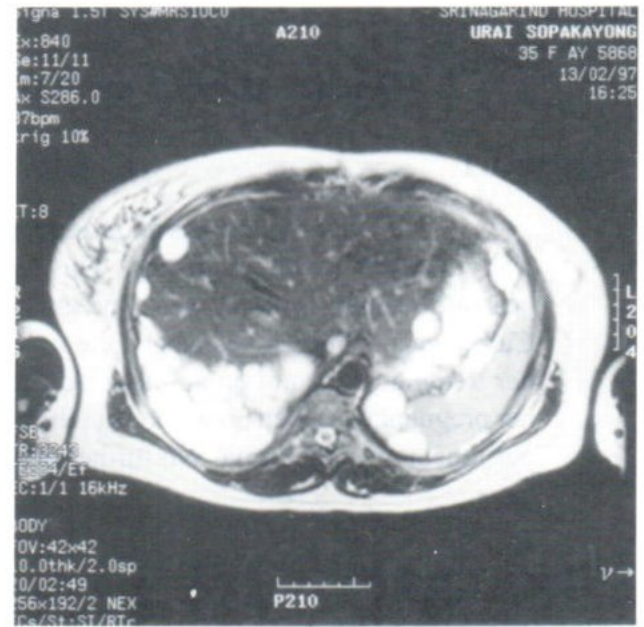
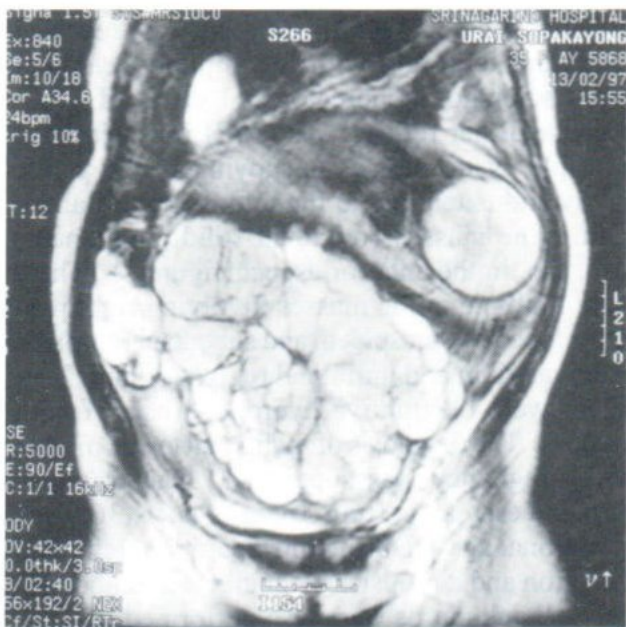
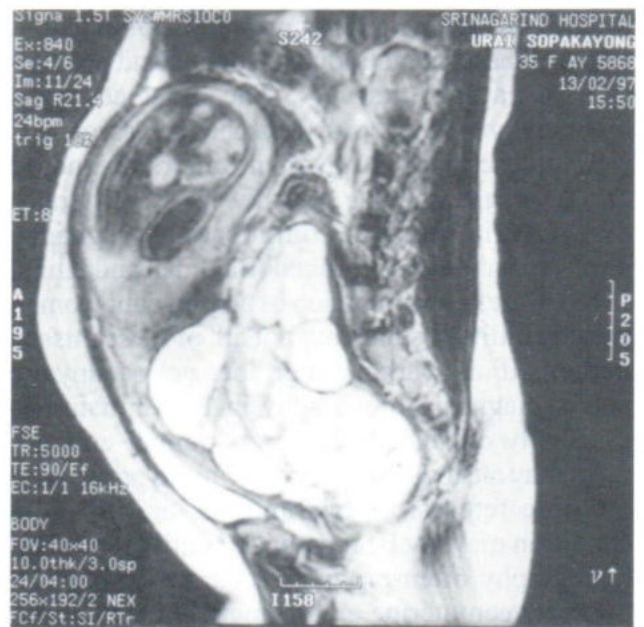


Fig. 2. Axial T2-weighted FSE (TR/TE = 3243/84) revealed multiple cystic components in the right posterior lobe of liver and scattering lesions at segment 3, 7 and around the splenic surface.



3. (Coronal)



4. (Sagittal)

Fig. 3. (Coronal), Fig. 4. (Sagittal): Coronal T2-weighted FSE (TR/TE = 5000/90) revealed multiloculated cystic mass (hypersignal intensity) occupied the entire pelvic cavity displacing the pregnant uterus upward, and the urinary bladder right antero-inferiorly.



Fig. 5. Coronal T1-weighted FSE (TR/TE = 360/20) revealed multi-loculated cystic mass (hyposignal intensity) occupying the entire pelvic cavity and displacing the pregnant uterus upward, while the urinary bladder was also displaced right anteroinferiorly.

DISCUSSIONS

Teratomas are the most common germ cell tumor of the ovary. They can be subclassified into mature teratoma, monodermal teratoma, and immature teratoma. Immature teratomas are composed of tissues derived from the three germ layers; ectoderm, mesoderm, and endoderm; and, in contrast to the much more common mature teratoma, they contain immature or embryonal structures. Mature tissues are frequently present and sometimes may predominate. In these cases, the tumor should be differentiated from a mature teratoma with malignant transformation. The presence of immature or embryonal elements as opposed to the neoplastic transformation of mature tissues can be used to differentiate these two types of neoplasm.⁴

The immature teratoma of the ovary is an uncommon tumor, comprising less than 1% of ter-

atomas of the ovary.⁵ In contrast with the mature cystic teratoma, which is encountered most frequently during the reproductive years but occurs at all ages, the immature teratoma has a specific age incidence, occurring most commonly in the first two decades of life and being almost unknown after the menopause.⁶ These tumors are likely to be large, predominantly solid masses with areas of soft, fleshy, pale pink or tan tissue. The contralateral ovary may be involved if there is extraovarian spread, but these tumors are rarely bilateral. In 10%, the contralateral ovary contains another benign ovarian tumor.⁷ The tumors are graded according to the amount of immature tissue present. Grade 1 tumors have immature glial tissue occupying less than one low power field, grade 2 tumors have immature glial tissue in two to three low power fields in one slide, and grade 3 tumors have four or more fields in one slide.⁸⁻⁹ Peritoneal seeding from these tumors may be represented by mature glial seeding or gliomatosis.

Although ultrasound has been revolutionary, an alternative fetal and maternal imaging technique would be useful when sonography is limited by technical factors. MRI fills this need. Similar to ultrasound, MRI is non-invasive, involving no ionizing radiation, and can provide images in multiple planes. Unlike ultrasound, interference from skeletal, fatty, or gas-filled structures is not a problem with MRI, and imaging of deep pelvic structures does not depend on the presence of an acoustic window. Because tissue characteristics rather than those of acoustic impedance provide the contrast in MRI, it might show features not demonstrable with ultrasound.¹⁰⁻¹¹

In our case, MRI demonstrated a huge multiple cystic masses with solid components occupying almost all peritoneal cavity and involving solid organs (e.g. liver) also. Although the general recommendation for suspected malignancy is laparotomy as soon as possible; this case was delayed until full term pregnancy, because the diagnosis was not made until late in pregnancy (33 weeks) and she was alive longer than usual in the case of immature teratoma. While the prog-

nosis of this tumor with incomplete treatment should be described with 2 years survival,¹² she had survived for 13 years after first diagnosis. During cesarean section, 2 biopsies were taken from the abdominal wall cysts and were reported as multicystic peritoneal mesothelioma, which is a benign tumor. However the first section was confirmed as immature teratoma, but the components in the pathological section mostly contained mature cell with a few component of immature cells. So we made her diagnosis as immature teratoma. At this time, her staging was changed to at least IIIc, so her gynecologist suggested further treatment, such as exploratory laparotomy with tumor resection and adjuvant chemotherapy, but she refused to have any further treatment and went away.

We cannot predict the end of this case. We hope that we shall see her for radiological examinations again, perhaps in a very late stage.

CONCLUSIONS

Immature teratoma in a pregnant woman is rare and the recurrent one after 13 years of the first presentation is even rarer. The first pathological diagnosis was reviewed and confirmed the diagnosis of immature teratoma; even receiving incomplete treatment, she was still alive until this occurrence. Although the histopathological pictures in this second presentation do not absolutely confirm the diagnosis of an immature teratoma, this condition is still the most probable diagnosis, so her obstetricians have advised her to be treated as a recurrent immature teratoma. Unfortunately, she refused to have any more treatment and went away.

REFERENCES

1. Zemlickis D, Lishner M, Degendorfer P, Panzarella T, Sutcliffe SB, Koren G. Fetal outcome after in utero exposure to cancer chemotherapy. *Arch Intern Med*, 1992; 152:573-6.
2. Williams S. Chemotherapy of ovarian germ cell tumors. *Hematol Oncol Clin North Am*, 1991;5:1261-9.
3. Malone J, Gershenson D, Creasy R, Kavanagh J, Silva E, Stringer C. Endodermal sinus tumor of the ovary associated with pregnancy. *Obstet Gynecol*, 1986;68: 86S-9S.
4. Telerman A. Germ cell tumors of the ovary. In: Kurman RJ, ed. *Blaustein's pathology of the female genital tract*. 4th Ed. New York: Springer-Verlag, 1994:876-8.
5. Malkasian GD Jr, Symmonds RE, Dockerty MB. Malignant ovarian teratomas: Report of 31 cases. *Obstet Gynecol*, 1965;25:810.
6. Breen JL, Neubecker RD. Ovarian malignancy in children with special reference to the germ cell tumors. *Ann NY Acad Sci*, 1967;142:658.
7. Wisniewski M, Deppisch LM. Solid teratomas of the ovary. *Cancer*, 1973;32: 440.
8. Thurlbeck WM, Scully RE. Solid teratoma of the ovary. *Cancer*, 1960;13:804.
9. Kojis Z, Urbanski K, Mitus J, Reinfuss M, Pudelek J, Walasek T. Pure immature teratoma of the ovary: analysis of 22 cases. *Eur J Gynaecol Oncol*, 1997;18:534-6.
10. Weinreb JC, Lowe TW, Santos-Ramos R, Cunningham FG, Parkey R. Magnetic resonance imaging in obstetric diagnosis. *Obstet Gynecol*, 1985;154:157-161.
11. Weinreb JC, Brown CE, Lowe TW, Cohen JM, Erdman WA. Pelvic masses in pregnant patients: MR and US imaging. *Radiology*, 1986;159:717-724.
12. Horbelt D, Delmore J, Meisel R, Cho S, Roberts D, Logan D. Mixed germ cell malignancy of the ovary concurrent with pregnancy. *Obstet Gynecol*, 1994;84:662-4.
13. Heslen I, Leveque J, Horyn G, Panel P, Goujon JM, Chahal M, Kerisit J, Pigne A, Magnin G, Grall JY. Immature teratoma of the ovary (Abstract). *J Gynecol Obstet Biol Reprod Paris*, 1994;23:790-6.

METASTATIC BREAST CANCER IN THE FIRST METACARPAL BONE OF THE NON-DOMINANT HAND: A CASE REPORT.

Chalida APHINIVES¹, M.D., Jitjaroen CHAIYACUM¹, M.D.,
Jaturat KANPITTAYA¹, M.D., Jumpol MITRCHAI², M.D.

ABSTRACT

This report describes the radiologic and histologic findings in a 50-year-old woman who presented with an osteolytic lesion of the first metacarpal bone of the non-dominant hand as the result of metastatic breast cancer. The patient is alive and symptoms free at 3 months after curettage with bone graft, adjuvant chemotherapy and radiation therapy (1-year course of treatment).

INTRODUCTION

Metastatic tumors of the hand or foot are rare. The most frequently encountered neoplasms metastasizing to the metacarpal bones originate in the bronchus, kidney, esophagus, colon and rectum, breast, or prostate gland.¹⁻³ They usually occur as pre-terminal events and often are part of a widespread dissemination of metastases. Their incidence is only 0.0021-0.09 percent of all patients with cancer,⁴ while bony metastases present in approximately 25% of all death from malignancy. Failure to recognize these lesions has led to a delayed diagnosis or an inappropriate treatment or both.

We report a case of breast cancer with a metastasis in the first metacarpal bone of the non-dominant hand treated with curettage, bone graft, adjuvant chemotherapy and radiation therapy.

CASE REPORT

A 50-year-old woman who is right-hand

dominant was diagnosed as invasive ductal carcinoma of her right breast (T2N1M0) on August 1994. Her treatment included a modified radical mastectomy right side and an adjuvant chemotherapy (CMF 6 circles). Until July 1997, she developed swelling and chronic pain on her left wrist. After 2-month of medical treatment of joint pain, a plain film showed a geographic osteolytic destruction in the base of the first metacarpal bone of her left hand, ill-defined border, breaking through cortex, soft tissue swelling, without periosteal reaction (figure 1). Her bone scan revealed multiple bony uptakes. Only curettage with bone graft was performed on September 1997 with the aim of tissue biopsy. After a pathologist report of a metastatic ductal carcinoma (figure 2), the patient refused an amputation of her thumb. She had been further treated with the combination of radiation therapy (2,000 cGy) and chemotherapy (CMF 12 circles) since October 1997. She is still alive and symptoms free at 3 months (December 1998) after 1-year course of treatment.

¹ Department of Radiology, Faculty of Medicine, Khon Kaen University, Thailand.

² Department of Pathology, Faculty of Medicine, Khon Kaen University, Thailand.



Fig. 1. The plain film of left hand showed geographic osteolytic destruction in the base of first metacarpal bone (type IC), with breaking through the cortex. No periosteal reaction was seen.

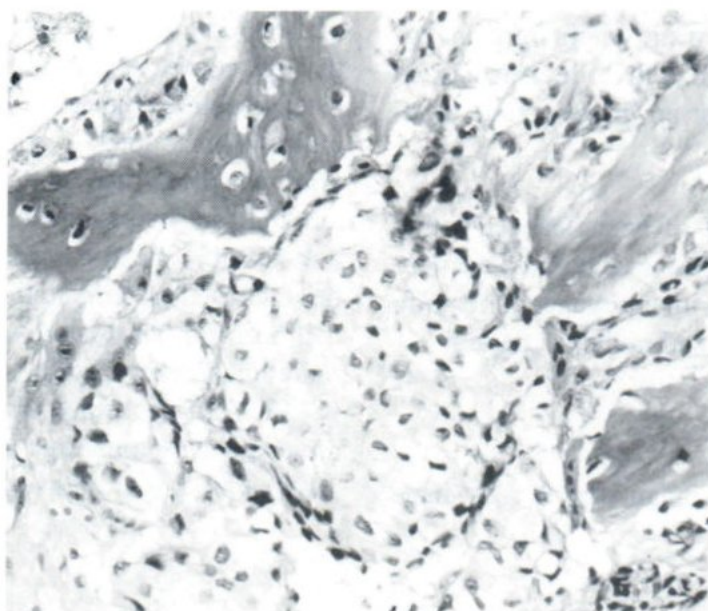


Fig. 2. Well-defined nests of metastatic ductal carcinoma of classical type lie between proliferating bone trabeculae. (x 200)

DISCUSSIONS

The end stages of many malignant neoplasms are associated almost inevitably with metastases and the skeleton is very commonly affected. The most skeletal metastases are hematogenous in origin. Any primary tumor may metastasize to bones, but in woman the most important carcinoma is breast cancer, from which secondary deposits develop in about two-thirds of the cases.

The radiographic appearance of metastatic disease varies from lytic, blastic, or mixed lesions typically in the marrow space. Osteolytic metastases are the most frequent pattern encountered, especially in breast and lung primaries.⁵

As mentioned, the acrometastases (metastatic lesions in the hand or foot) are rare. The clinical findings commonly included pain, swelling, and erythema. There are 2 points of her presentation to be considered: first, this lesion was the first evidence of an occult primary neoplasm; and second, it occurred in the non-dominant hand. Healey, et al¹ found that only 14 percent of all acrometastases presented as the first evidence of metastasis and metastases to the dominant hand were twice as common as to the non-dominant hand (maybe due to more blood flow in dominant hand).

Breast cancer is one of the most common primary tumors in women but its metastasis shows an unusual affinity for bone. The lesions are usually osteolytic and commonly multiple. About 10% of metastases from breast cancer produce osteoblastic lesions and in another 10% the lesions are mixed. Sclerosis may occur in lytic lesions following successful hormone or radiation therapy.⁶

Three patterns of lytic destruction have been described: geographic, type I; moth-eaten,

type II; and permeative, type III. The geographic osteolytic destruction (type I) was divided into 3 types; type IA, well-defined border with sclerosis; type IB, well-defined border without sclerosis around the periphery of the lesion; and type IC, ill-defined border. This case showed to be type IC lesion that showed greater biologic activity and more likely that the lesion was malignant.⁷ The pathological section is well-defined nests of metastatic ductal carcinoma of classical type that lie between proliferating bone trabeculae (figure 2).

The surgical treatment might be inadequate; at least amputation of the first metacarpal bone and thumb was recommended.⁸ However, the combination of radiation therapy and chemotherapy appeared to be quite well in this case. No more lesions, no complication, and symptoms free occurred along 1-year course and 3 months after. The median survival time of hand metastasis was 6.2 months.¹

Finally, if her first physicians recognized this condition, she could be treated appropriately 2 months earlier.

CONCLUSIONS

Metastatic breast cancer in the hand is a rare entity. The presentations of this case are also less common. The combination of radiation therapy and chemotherapy appeared quite well even inadequate resection. This condition should be considered earlier in such a case of joint pain or swelling with a previous history of malignancy.

REFERENCES

1. Healey JH, Turnbull ADM, Miedema B, et al. Acrometastases. *J Bone Joint Surg.* 1986;68:743-6.

2. Kerin R. Metastatic tumors of the hand: A review of the literature. *J Bone Joint Surg*, 1983;65:1331-5.
3. Libson E, Bloom RA, Husband JE, Stoker DJ. Metastatic tumors of bones of the hand and foot: A comparative review and report of 43 additional cases. *Skeletal Radiol*, 1987;16:387-92.
4. Chung TS. Metastatic malignancy to the bones of the hand. *J Surg Oncol*, 1983;24:99-102.
5. Thrall JH, Ellis BI. Skeletal metastases. *Radiol Clin North Am*, 1987;25:1155-70.
6. Watt I. Tumours and tumour-like conditions of bone (1). In: Sutton D, ed. *A textbook of radiology and imaging*. 5th Ed. London: Churchill Livingstone, 1992:128-9.
7. Moser RP, Jadewell JE. An approach to primary bone tumors. *Radiol Clin North Am*, 1987;25:1049-94.
8. Kobus RJ, Leinberry C, Kirkpatrick WH. Metastatic Renal Carcinoma in the hand: Treatment with preoperative irradiation and ray resection. *Orthop Rev*, 1992;21:983-4, 990-5.
9. Bouvier M, Lejeune E, Bonvoisin B, Biron P. Distal bone metastases of the upper limb. (Abstract) *Sem Hop*, 1982;58:2736-9.
10. Drewes J, Sailer R, Schmitt GA. Cancer metastases of the hand. (Abstract) *Hand chirurgie*, 1981;13:296-304.

LANGERHANS' CELL HISTIOCYTOSIS

Khomdao BOONCHIT¹, Jiraporn SRINAKARIN²,
Dumrongsuk BOONCHIT³, Warinthorn BUNCHALEAW⁴

ABSTRACT

Langerhans' cell histiocytosis, previously called histiocytosis X is an inappropriate proliferation and infiltration of various tissues with cells that are morphologically and immunologically similar to normal Langerhans cells that is probably due to an immune regulatory defect.

We report two different cases of Langerhans' cell histiocytosis. First case is a 1 year 5 months old girl presented with left eye lid swelling and erythema. Second case is a 2 years old girl presented with multiple skull masses and diabetes insipidus.

In 1953, Lichtenstein^{1,2} proposed the term histiocytosis X for a group of clinical syndromes of unknown cause characterized morphologically by the proliferation of a unique histiocyte with cytoplasmic inclusions known as X bodies.

In 1980s, it was recognized that the mononuclear cells that populate these lesions were not histiocytes of the usual type, but were in reality a particular cell type: the Langerhans cell³. It has pale eosinophilic cytoplasm and a central nucleus with a characteristic groove that differentiates it from other histiocytes. The distinctive feature of

LCH is proliferation of the Langerhans cell, a tissue based histiocyte that is normally found in skin, some mucous membranes, the T zone of lymph nodes, and thymus⁴. Ultrastructurally, the most characteristic feature of the Langerhans cell is the Birberk granule. In addition there are immunologic features of the Langerhans cell that are typical, including S-100 protein positivity, expression of the HLA-DR antigen, and staining with OKT-6 monoclonal antibody⁴. Regardless of clinical presentation, the diagnosis of LCH is based on the identification of Langerhans cell in typical lesions. (table 1)^{1,6}

LCH = Langerhans' Cell Histiocytosis

TABLE 1 LANGERHANS' CELL HISTIOCYTOSIS

Levels of diagnosis

Presumptive

Conventional histopathology

Diagnosis

Immunohistochemistry (S-100 protein)

Enzymatic activity (adenosine triphosphatase, α -D-mannosidase)

Definitive

Electron microscopy (Birberk granules)

Immunohistochemistry (peanut lectin, OKT-6 antigenicity)

¹ Department of Radiology, Udonthani Hospital, Meung, Udonthani, 41000 Thailand.

^{2,4} Department of Radiology, Srinakarind Hospital, Faculty of Medicine, Khon Kaen University, 40002 Thailand.

³ Department of Plastic and Reconstruction Surgery, Udonthani Hospital, Meung, Udonthani, 41000 Thailand.

There are three well-established clinical subsets of LCH that should be defined at this time: eosinophilic granuloma of bone, Hand-Schuller-Christian disease and Letterer-Siwe disease.

The head and neck region is the most common sites of involvement by LCH.³ Lesions in children are most commonly located in bone or bone marrow.⁵ Orbital involvement of LCH is not uncommon.⁶ It has a predilection for young children 1-4 years old.⁵ The overall incidence of orbital involvement in a large series of 76 children with LCH was 23%.²

CASE REPORTS

CASE 1

1 year 5 months old girl presented with 2 month history of upper eyelid swelling with

erythema and proptosis of left eye.

On examination, she appeared to be healthy and normally developed. Pupils and extraocular movements were normal. The left eye was slightly proptotic, without ecchymosis surrounding the eye.

Orbital CT SCAN without and with contrast enhancement showed an enhancing fairly well-defined extraconal mass, encroaching lacrimal gland with bony destruction at superolateral aspect of left orbit, involving the greater wing of sphenoid bone. (Fig.1a,b)

An incisional biopsy without curettage was done. Histologic examination was diagnosis for LCH.



Fig.1a,b Axial CECT shows enhancing lesion with bony destruction involving the superolateral wall of left orbit

CECT = Contrast Enhancement CT.

CASE 2

2 year-old-girl was admitted to Udonthani hospital in July 1998 with a 4 month history of mass at right temporal region, polyurea and polydipsia. 1 month later, she had another mass at left frontal region.

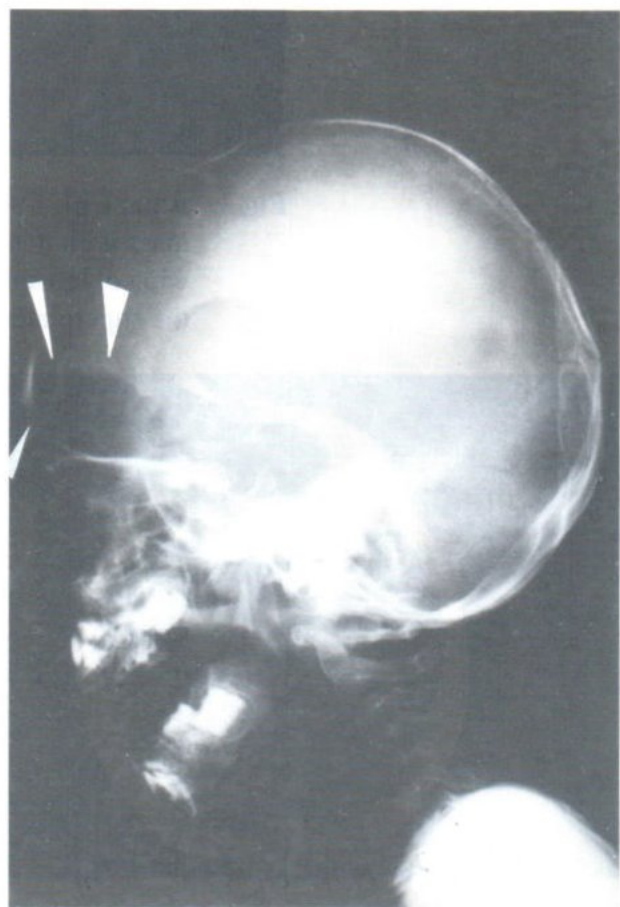
On examination, she appeared to be sick and weak. There were soft tissue masses at right temporal and left frontal regions about 3 and 2 cm. in diameter respectively. Left periorbital swelling was noted. She did not have hepatosple-

nomegaly. Complete blood count, liver function studies were normal. Urine specific gravity test after water dehydration was 1.002.

Skull radiographs showed multiple osteolytic lesions with well-defined margins at the superolateral wall of left orbit, left frontal and right temporal bones. (Fig.2a,b) The chest radiograph was normal. There were no other bony lesions on skeletal radiographic survey. Ultrasound of abdomen showed normal findings.



2A.



2B.

Fig.2a,b Osteolytic lesions with well-defined margins at superolateral wall of left orbit, left frontal and right temporal bones

CT SCAN of the orbits and head without and with contrast enhancement showed an enhancing destructive soft tissue mass centered in the greater wing of left sphenoid bone,

extending into the superolateral aspect of left orbit. (Fig.3) Left frontal and right temporal skull masses were noted with bony destruction. (Fig.4a,b)



Fig.3. Axial CECT shows enhancing soft tissue mass with bony destruction at the greater wing of left sphenoid bone, extending into the superolateral aspect of left orbit



4A.



4B.

Fig.4a,b Axial CECT shows left frontal and right temporal skull masses with bony destruction

The patient underwent MR imaging, on 1.5 Tesla GE Signa Horizon LX™ (GE Medical System Milwaukee WI,USA). Beginning with brain study, axial T1 weighted pre- and post Gadolinium (TR500 ms, TE20ms, 5.0mm.thick section, 2.0 mm. intersection spacing); Sagittal FSE T1 weighted (TR540ms, TE12.2ms, Ef) Axial FSE Proton Density weighted (TR3700ms, TE11.5ms, Ef) T2 weighted (TR3700ms, TE80.8ms, Ef) with 5.0mm.thick section, 1.0mm.intersection spacing were done. The FOV = 12 cm., matrix size = 256 x 160 were taken.

And then pituitary fossa study was performed with coronal, sagittal pre- and post Gadolinium T1 weighted (TR400ms, TE23ms), FSE T2 weighted (TR3000ms, TE92.6,Ef).

Section thickness was 3 mm., with a gap of 0.3 mm. The FOV = 12cm., matrix size = 256x160. Flow compensation technique was used.

The study revealed an enhancing inhomogeneous iso- and hypointense mass involving the greater wing of left sphenoid bone with extension into superolateral aspect of orbital fossa causing mild exophthalmos. (Fig.5) Other cranial vault masses were noted involving inner, outer tables and diploic space at left frontal and right temporal regions. (Fig.6a,b) Areas of hyperintense on all sequence images were identified which represent subacute hemorrhage. Hypothalamus and thickness of pituitary infundibulum were normal. Absent bright spot of posterior lobe of pituitary gland was observed. (Fig.7)



Fig.5 Axial FSE proton density imaging shows mixed iso- and hyperintense (compare with gray matter) extraconal mass at superolateral aspect of left orbital fossa with destruction of adjacent greater wing, sphenoid bone



Fig.6a Axial SE T1W POST Gd imaging shows inhomogeneous iso-hypointense skull masses at left frontal, right temporal regions with peripheral enhancement. Internal areas of hyperintense represent bleeding foci



Fig.6b Axial FSE T2W imaging confirms these skull masses involving inner, outer tables and diploic space with abut on dura. Internal bleeding foci was visualized by areas of hyperintense

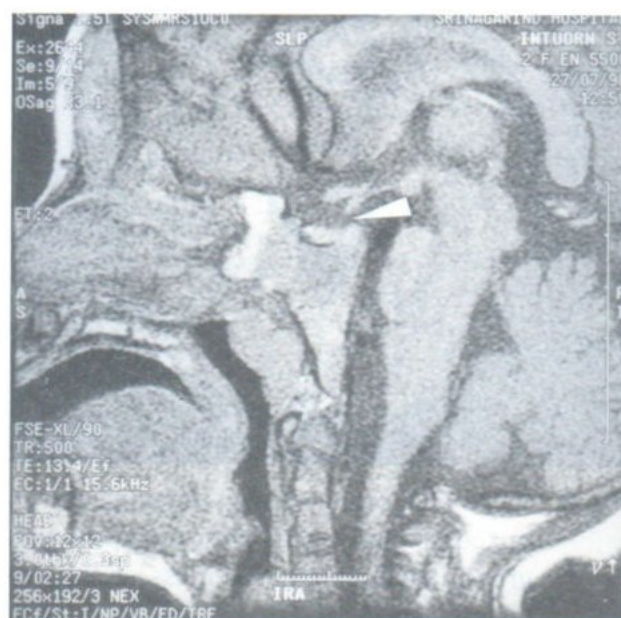


Fig.7 Sagittal SE T1W imaging through pituitary fossa shows absence of bright spot of posterior lobe, pituitary gland. But infundibulum thickness is preserved

Left supraorbital region was incised parallel to an eye brow, disclosing an encapsulated yellowish soft tissue. (Fig.8) An excisional biopsy of left frontal mass was done. Histologic examination was diagnosis for LCH.

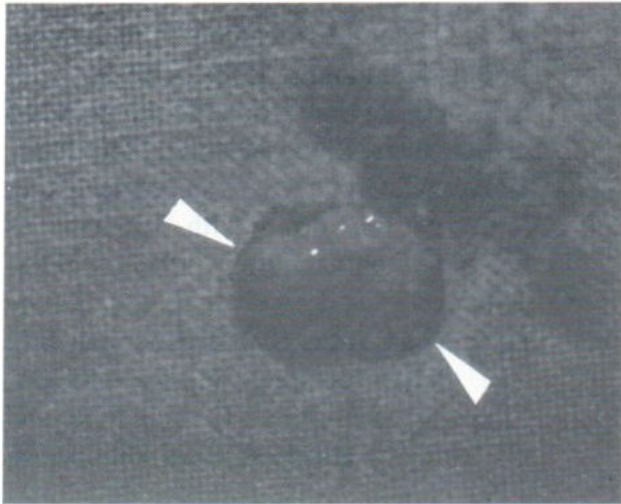


Fig.8 Encapsulated yellowish soft tissue mass

DISCUSSION

LCH most commonly occurs in children. It groups a spectrum of diseases in which, classically, three clinical diseases are: eosinophilic granuloma, Hand-Schuller-Christian disease and Letterer-Siwe disease. Eosinophilic granuloma is a unifocal, rarely multifocal osteolytic lesions normally limited to bone. It accounts for approximately 70% of cases of LCH.⁷ Letterer-Siwe disease is a severe disseminated histiocytosis usually occurring below the age of 3 years with multi-organ involvement and a high mortality rate. Hand-Schuller-Christian disease is a systemic histiocytosis which the original description is the triad of exophthalmos, bony defects of the skull and Diabetes Insipidus,^{2,3,6,8} representing 20% of all cases of LCH.⁷ It is important to rule out disseminated disease that might occur in Letterer-

Siwe or Hand-Schuller-Christian disease, because both proper prognosis and management depend on this initial assessment and the prognosis is excellent in cases of unifocal involvement.⁹

The most common signs and symptoms of the orbital LCH were unilateral or bilateral proptosis, edema, erythema of the eyelid and periorbital pain. Other signs and symptoms are ptosis, optic nerve atrophy and papilledema. The lesions are usually seen in the superior or superolateral wall of the orbit.⁶ The diagnosis should be suspected when a child or young adult presents with a short history of painful, localized swelling and radiographic evidence of bony destruction.^{6,9} Radiographic study characteristically shows circumscribed, lytic lesions without or with surrounding sclerosis.²

CT and MR imaging scans are extremely useful to define the extent of osseous and soft tissue involvement.^{1,6,7,10,11} On post contrast CT and MR imaging scans, lesions demonstrate moderate to marked enhancement.^{6,7,10} MRI characteristics, usually reported, are focal lesions, surrounded by an ill-defined bone marrow and soft tissue reaction considered to represent perilesional inflammation or edema. The focal lesions are described as areas of high signal intensity in T2 weighted images and varies from low to high signal intensity on T1 weighted images.^{7,12,13} On histological examination areas of hemorrhagic changes are seen.^{12,13} There may be dural involvement^{7,14} and extension into the epidural space, as well as in the temporal fossa.⁶

The differential diagnosis of orbital LCH from an imaging viewpoint includes rhabdomyosarcoma, juvenile fibrosarcoma, aggressive fibromatosis, lacrimal gland tumors, leukemic infiltration, granulocytic sarcoma or chloroma, metastatic neuroblastoma, metastatic Wilm's tumor and metastatic Ewing's sarcoma.^{2,6} The diagnosis may, therefore, be in doubt until diagnosis is available.

(table 1) Orbital LCH must be differentiated from other histiocytic disorders which may involve orbit, such as sinus histiocytosis and Juvenile Xanthogranuloma (JGX). They are characterized by localized proliferation of histiocytes, but they usually confined to the orbital soft tissues and do not involve bone, although JGX may rarely result in orbital bony destruction. If there are no other systemic features, it may be difficult to distinguish between LCH and JGX clinically, but they differ in immunohistochemistry, enzymatic activity and electron microscopic features.^{2,6}

Central nervous system involvement in LCH has been reported in 16% of the patients.¹⁵ The most common intracranial sites of involvement are the hypothalamus and the pituitary.¹¹ When deposits of LCH affect the neurohypophysis (posterior lobe), diabetes insipidus may result.³ On MR imaging, T1 weighted, the bright spot of posterior lobe disappears.^{10,16}

REFERENCES

1. Angeli SI, Alcalde J, Hoffman HT, Smith RJH: Langerhans' cell histiocytosis of the head and neck in children. *Ann Otol Rhinol Laryngol* 1995;104:173-180
2. Moore AT, Pritchard J, Taylor DSI: Histiocytosis X: an ophthalmologic review. *Br J Ophthalmol* 1985;69:7-14
3. Devaney KO, Putzi MJ, Ferlito A, Rinaldo A: Clinicopathological consultation Head and Neck Langerhans cell histiocytosis. *Ann Otol Rhinol Laryngol* 1997;106:526-532
4. Herman TE, Shackelford GD, Borders JL, Dehner LP : Unusual manifestations of Langerhans cell histiocytosis of the head and neck. *Pediatric Radiology* 1993;23:41-43
5. Stanley SS: Taking the X out of histiocytosis X. *Radiology* 1997;204:322-324
6. Hidayut AA, Mafee MF, et al: Langerhans' cell histiocytosis and juvenile xanthogranuloma of the orbit: Clinicopathologic, CT, and MR Imaging Features. *The Radiologic Clinics of North America* 1998;36:1229-1240
7. Hermans R, De Foer B, Smet MH, et al: Eosinophilic granuloma of the head and neck: CT and MRI features in three cases. *Pediatric Radiology* 1994;24:33-36
8. Cline MJ: Review article: Histiocytes and histiocytosis. *Blood* 1994;84:2840-2853
9. Glover AT, Grove AS: Eosinophilic granuloma of the orbit with spontaneous healing. *Ophthalmology* 1987;94:1008-1012
10. Bilaniuk LT, Atlas SW, Zimmerman RA: The Orbit. In: Lee SH, Rao KCGV, Zimmerman RA (eds): *Cranial MRI and CT*. McGraw-Hill, 1992, third edition, 178-179, 471
11. Kramer TR, Noecker RJ, Miller JM, et al: Langerhans cell histiocytosis with orbital involvement. *Am J Ophthalmology* 1997; 124:814-824
12. Stull MA, Kransdorf MJ, Devany KO (1992) From the archives of the AFIP: Langerhans cell histiocytosis of bone. *Radiographics* 12;801
13. Hayes CW, Conway WF, Sundaram M (1992) Misleading aggressive MR imaging appearance of some benign musculoskeletal lesions. *Radiographics* 12:1119
14. De Schepper AMA, Ramon F, Van Marck E (1993) MR imaging of eosinophilic granuloma : report of 11 cases. *Skeletal Radiology* 22:163
15. Berry DH, Becton DL. Natural history of histiocytosis X. *Hematol Oncol Clin North Am* 1987;1:23-34
16. Elster AD : Modern imaging of the pituitary. *Radiology* 1993;187:1-14

MAMMOGRAPHIC AND SONOGRAPHIC FEATURES IN PHYLLOIDES TUMOURS

Darunee BOONJUNWETWAT, MD.¹ Chunya WILAI, MD.¹
Pichet SAMPATHANUKUL, MD.²

ABSTRACT

The imaging features of five cases of histopathologically proved phylloides tumours have been reported. Tumor size ranged from 3-16 cm. (mean = 8 CM). Mammographic findings included; well-defined, macrolobulated mass with radiolucent halo, either complete or incomplete. None of them showed associated calcification, skin change or pathologic axillary lymph node. Two showed very large masses, replacing almost entire breast, which one of them occurring in the pregnant woman. Sonographic findings included; heterogenous-coarse, low-level echoic solid mass, well-defined border, macrolobulated contour and minimal posterior acoustic enhancement. Intramural cysts or intramural hypoechoic area, which suggested the characteristic feature of phylloides were seen in 4 cases (80%). These cysts were mainly located at the peripheral region of mass. Color Doppler sonogram was performed in 2 cases. Both of them showed increased vascular flow.

INTRODUCTION

Phylloides tumor is a combined fibroepithelial tumor, like fibroadenoma, but it has stromal component that more hypercellular than fibroadenoma.¹ Clinical and imaging findings cannot be definitely distinguish between two of them. The purpose of this study is to evaluate the imaging features of phylloides tumor. If the diagnosis could be established, the proper surgical treatment should be gained in order to reduce the recurrent rate.

MATERIALS & METHODS

Five cases of histopathologically proved phylloides tumours in Chulalongkorn hospital between 1993-1998 were retrospectively analyzed in aspect of clinical findings and imaging features, related with histopathology. All cases had mam-

mography and sonography performed. Color Doppler was done in 2 cases. Mammogram was examined by GE and Benette equipments in standard MLO and CC views, additional views including spot compression and magnification were necessary for the uncleared lesion. Sonogram was examined by Acuson and GE logic 700, using near field probe (7-13 MHz). Clinical details were including patient's age and symptoms.

Histopathological slides were reviewed and classified into benign, borderline and malignant grading. Mammogram was reviewed by two experience radiologists to determine a mass configuration, density, size, associated calcification as well as axillary nodal status. Sonogram was reviewed to determine the internal echogenicity, margin, size, presence or absence of intramural

¹ Department of Radiology, Chulalongkorn University and Hospital

² Department of Pathology, Chulalongkorn University and Hospital Faculty of Medicine, Chulalongkorn University and Hospital, Bangkok THAILAND

cystic areas, calcification and posterior acoustic properties.

RESULTS

Results were shown in table 1 and 2. The age of patients showed a wide range from 25-61 year-old (mean = 38.5 yrs.). All cases presented with a palpable painless lump of varied sizes; 3-4 cm in 2 cases, 7x8 cm in 1 case and large size occupying almost entire breast in 2 cases. One of the large entire breast mass was a pregnant woman. Mammographic findings showed hyperdense mass in 3 cases (Fig. 1A,B) and isodense mass in 2 cases (Fig. 2). All cases showed macrolobulated con-

tour and well-defined margin. Four cases showed radiolucent halo rim, either complete or incomplete. None of them had calcification or pathologic node. Sonographic findings showed heterogenous-coarse hypoechoic mass with well-defined margin, macrolobulated contour and minimal posterior acoustic enhancement in all cases (Fig.3). Two had echoic rim and edge shadowing features. Four cases showed mass containing small low echoic area (s) or intramural cyst (s) (Fig. 4). Increased vascularity was found in 2 cases by color Doppler study (Fig.5). Histological grading revealed benign in 3 cases and borderline in 2 cases. No malignant case was found in this study.

TABLE 1. Mammographic findings.

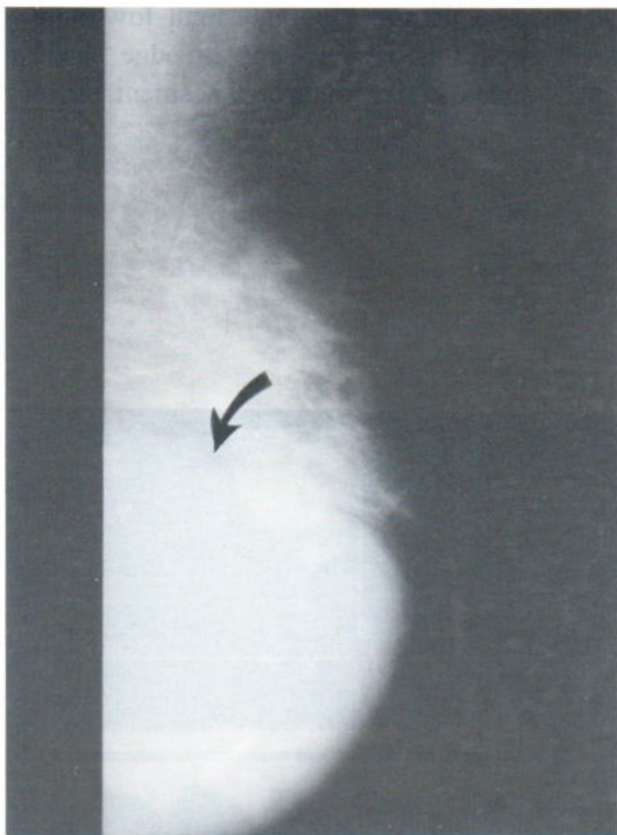
No. of cases	1	2	3	4	5
Side of Breast	Right	Right	Left	Right	Left
Location	Entire	Entire	UOQ	UOQ	LIQ
Size	10 x 6	16 x 8	3 x 4	3 x 2.5	7 x 8
Shape	-	-	Oval	Round	Oval
Contour	Macro L.	Macro L.	Macro L.	Macro L.	Macro L.
Margin	Well-D.	Well-D.	Well-D.	Well-D.	Well-D.
Radiolucent Halo	No	Incomplete	Incomplete	Complete	Incomplete
Mass density	Hyperdense	Hyperdense	Isodense	Isodense	Hyperdense
Calcification	No	No	No	No	No
Skin change	No	No	No	No	No
Axillary LN.	No	No	Yes (benign)	No	No

TABLE 2. Sonographic findings

No. of cases	1	2	3	4	5
1. Echogenicity	hypoechoic	hypoechoic	hypoechoic	hypoechoic	hypoechoic
2. Internal echo pattern (echo texture)	heterog.-coarse	heterog.-coarse	heterog.-coarse	heterog.-coarse	heterog.-coarse
2. Margin	Well-D.	Well-D.	Well-D.	Well-D.	Well-D.
3. Echoic rim	No	Yes	Yes	No	No
4. Edge shadowing	No	No	Yes	Yes	No
5. Post. enhancement	Yes	Yes	Yes	Yes	Yes
6. Calcification	No	No	No	No	No
7. Vascularity	-	-	Increased (RI= 0.6)	Increased (RI= 0.5)	-
8. Anechoic cyst,cleft or intramural hypocho	Yes	No	Yes	Yes	Yes

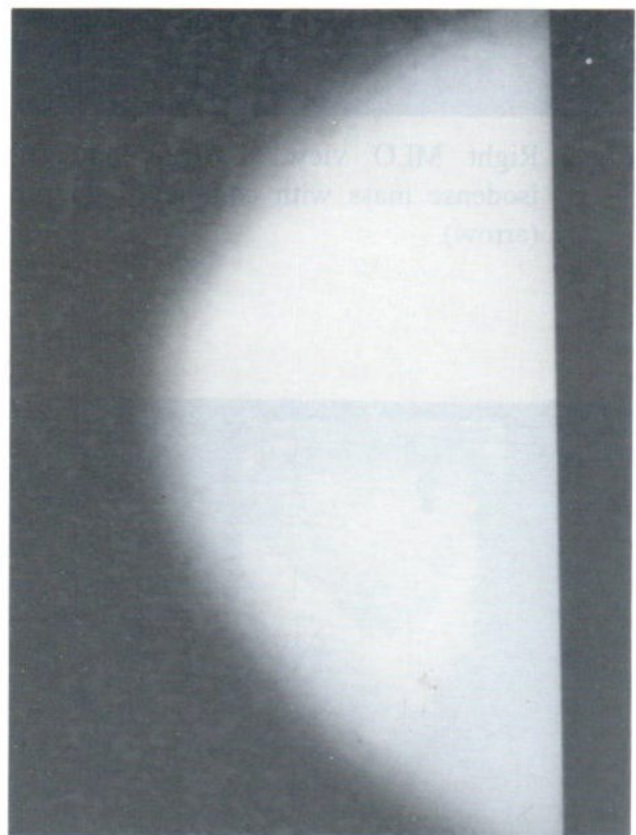
Note ; Macro L. = Macrolobulated contour
Well-D. = Well-defined margin

Heterog. = Heterogenous
- = Not performed



1A.

Fig. 1A. Left MLO view shows a hyperdense mass with well defined border. (arrow)



1B.

Fig. 1B. Right CC view shows huge hyperdense mass occupying the whole breast in the pregnant women.



Fig. 2. Right MLO view shows a lobulated isodense mass with complete halo rim (arrow)



Fig. 3. Ultrasound of left breast shows a lobulated low echogenic mass, heterogeneous coarse echo texture, internal small low echogenic areas, thin echogenic rim with edge shadow and posterior sound enhancement. (arrow)



Fig. 4. Ultrasound of left breast shows a heterogeneous low echogenic mass with intramural cyst at margin. (arrow)

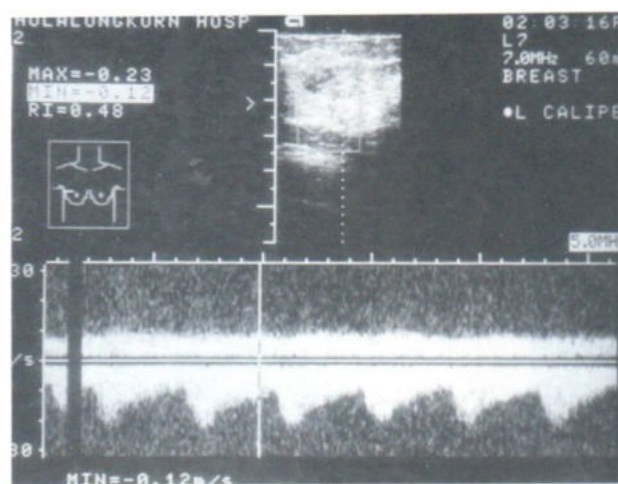


Fig. 5. Color Doppler study shows increased vascularity in the mass.

DISCUSSION

Phylloides tumor is a rare tumor, accounting for 1-2 % of breast neoplasm.² It was first described by Johannes Muller in 1838,³ being a combined fibroepithelial tumor. This tumor occurs over a wide age range.⁴ There is a wide range of tumor's size.⁵ Local recurrence occurs in approximately 20% of cases, usually due to incomplete surgical excision.⁶ Histogenesis of phylloides tumor and fibroadenoma appear to be closely related.⁷ Clinical and radiological findings could not be definitely distinguish phylloides from fibroadenoma, either in mammography or sonography, because both of them show a benign-appearing mass.⁸ However, large phylloides tumors usually are diagnosed correctly on the mammogram due to their size.⁸

In smaller tumors, differential diagnosis is necessary including fibroadenoma, cyst and even well-circumscribed carcinoma.⁸ The density of the mass could be presented both hyperdense and isodense. Sonographic findings typically revealed a well-defined solid mass, containing weak to intermediate echo, which is resemble fibroadenoma or others benign tumors.⁹ But all of our cases showed coarse low-level echogenicity and posterior acoustic enhancement, possibly related to the increased cellularity of the tumors. The thin echoic rim and edge shadowing were found in 2 cases, in which these findings could be benign and malignant features. Presenting of cystic or cleft-like space within a large, lobulated solid mass in sonogram should indicate the diagnosis of phylloides tumors.⁸

In 1991, Buchberger et. al., reviewed 10 cases of phylloides tumors in mamogram and sonogram. Six cases (60%) of benign disease contained 3-10 mm in diameter of intramural cysts.

In our study, 4 cases (80%) contained intramural cysts. According to the study of Buchberger et. al, single or multiple cystic cleft-like space (s) in the mass is characteristic (but not pathognomonic) of phylloides tumors.

Grading of tumors is impossible by imaging.⁸ Differentiation of benign, borderline and malignant is based on microscopic features only.¹⁰ In 1996, Laura et.al. reviewed 51 cases of both benign and malignant phylloides tumors.¹¹ Tumors 3 cm or greater in diameter at mammogram are more statistically significant have malignant grading. In contrast to our study, all cases; both small and large-entire breast masses, none of them were malignant.

Color Doppler sonogram was performed in 2 cases, both of them revealed increased vascularity. This findings paralleled to the study of De Albertist et. al. in 1995. However, this finding of increased vascularity is not the specific feature for phylloides tumors.

In conclusion, by mammography, the phylloides tumours usually present with a large lobulated mass, well-defined border, halo rim and hyper-or isodensity. By sonography, the mass often shows heterogenous coarse echoic mass, well-defined border, lobulated contour and especially containing intramural cyst. The features of coarse echogenicity, lobulated contour, echoic rim and edge shadowing were found in our cases that also being the malignant features. The evidence of intramural cyst (s) could help to diagnose phylloides tumor correctly. Lastly, all masses contain no calcification and lack of secondary metastatic sign.

REFERENCE

1. Hart William R. Cystosarcoma phylloides: A clinicopathologic study of 26 hypercellular periductal stromal tumors of the breast. *Am J Clin Patho* 1977;70:211-216
2. McCrea, ES, Johnson, C& Keramati. Cystosarcoma phylloides. *Southern Medical Journal* 1986;79:543-547
3. Rix DB, Tredwell ST, Forwerd AD. : Cystosarcoma phylloides (cellular intracanalicular fibroadenoma) ; Clinical-pathology relationship : *Can J Surg* 1971; 14:31
4. West, TL, Weiland, LH & Cloget, OT. Cystosarcoma phylloides. *Annual of Surgery* 1971;173:520-528
5. J.E. Page, J.E. Willium. The radiological feature of phylloides tumors of the breast with clinicopathological correlation. *Clinical radiology* 1991;44:8-12
6. Petrek JA, Harris JR, Hellman S, Henderson IC, Kinne DW, eds. *Breast disease*. 2nd ed. Philadelphia, Pa : Lippincott, 1991;791-797.
7. Noguchi et. al. Progression of fibroadenoma to phylloides tumor demonstration by clonal analysis. *Cancer* 1995; 76(10):1779-1785
8. Buchberger W, Strasser K, Heim K, Muller E, Schrocksnadel H. Phylloides tumors : Findings on mammography, Sonography and aspiration cytology in 10 cases. *AJR* 1991;157:715-719.
9. Cole-Beuglet et. al. Ultrasound, X-ray mammography and histopathology of cystosarcoma phylloides. *Radiology* 1983; 146:481-486
10. L. Laura et. al. Benign and malignant phylloides tumors : Mammographic and sonographic findings. *Radiology* 1996; 198: 121-124
11. Al-Jurt A. et. al. Cystosarcoma phylloides. *Surg Gynecol Obstet* 1978 ; 146 : 358-364

ULTRASONIC AND COMPUTED TOMOGRAPHIC APPEARANCES OF PARAGANGLIOMA SIMULATING OVARIAN CANCER

Kanjana DANPUKDEE M.D., Piyaporn LIMANOND M.D.

ABSTRACT

Paragangliomas or extra-adrenal pheochromocytomas are rare tumors affecting about 1/2000000 of the population³. They originate in paraganglia cells lying adjacent to the ganglia and plexuses of the autonomic nervous systems. Most of them arise from the sympathetic chain between the origin of the renal arteries and the aortic bifurcation. There is an association of paragangliomas with Von Hippel Lindau disease, neurofibromatosis and multiple endocrine neoplasia type IIa and IIb².

Paragangliomas usually present with large solid mass located just adjacent to the aorta in the middle age group. Sometimes, central necrosis is found. Mortality rate for surgery in the unsuspected cases is up to 50%. We report a case of an unusually large cystic paraganglioma in the left pelvis simulating an ovarian cancer. Misdiagnosis led to intra-operative hypertensive crisis and post-operative shock. These crises could have been avoided if we had searched for functional activity pre-operatively.

CASE REPORT

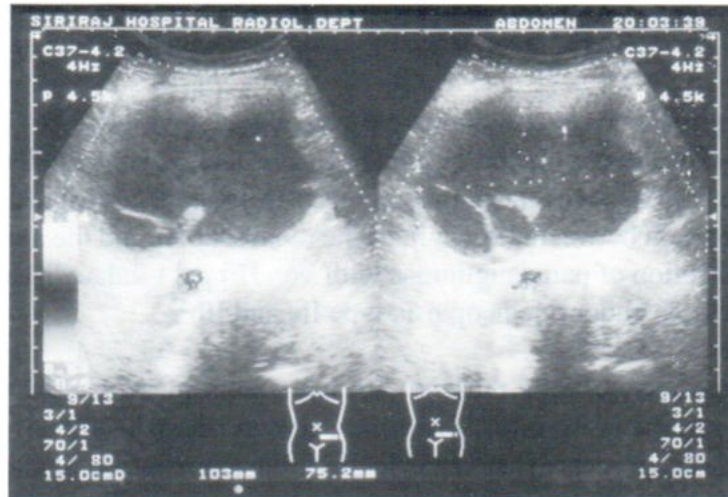
A 72-year-old female patient developed hypertension for 2 years. The physical examination revealed hard mass at left lower quadrant. The pelvic ultrasound revealed well-defined large cystic mass with septation about 10x12cm in the left pelvis. The cyst was homogeneous low echoic with solid papillary growth. Linear wall calcification was observed (Fig. 1). The findings were compatible with ovarian tumor.

Pelvic examination found a high positioned left pelvic mass with difficulty to be palpated. Bilateral adnexa were clear. The findings made a diagnosis of a questionable ovarian cancer so CT scan of the lower abdomen was performed. The scan revealed a well-defined, thin-walled cyst with solid papillary growth. The cyst was 10x13.5x18cm. Linear wall calcification was seen (Fig. 2). The Hounsfield unit intracystic

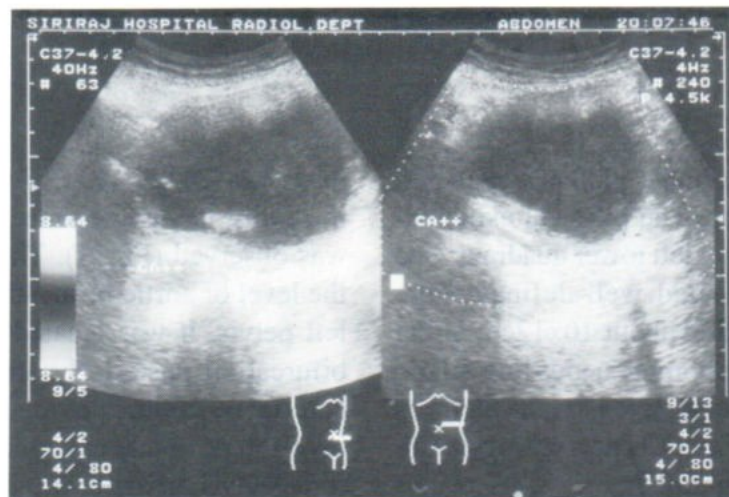
part was 24-28 H.U. Following intravenous injection, intense enhancement of the solid part was observed (Fig. 3). The mass extended from the level of aortic bifurcation downward into the left pelvis. It was located adjacent to the aortic bifurcation posteriorly and the abdominal wall anteriorly. Neither evidence of adjacent organ invasion nor node enlargement was seen. Therefore the ovarian tumor was supposed to be the most likely diagnosis. However, other possible diagnoses were leiomyosarcoma, malignant fibrous histiocytoma, mesenteric cyst and cystic node metastasis. The patient underwent surgical removal in the gynaecologic department. Intra-operative hypertensive crisis occurred immediately after induction to anesthesia (BP 260/180mmHg) and persisted in spite of many vasodilator drugs were given. Operative finding was a large mesenteric root mass with high vascularity. The mass

was totally removed and shown to be a large hemorrhagic cyst. The patient was shock immediately after the removal of the mass. After three hours of vaso-pressive drugs infusion, stable hemodynamic was achieved. Ten days later, the

patient was discharged without complication. Pathological findings were chromaffin tumor cells with cytoplasmic vesicles containing catecholamine compatible with paraganglioma.

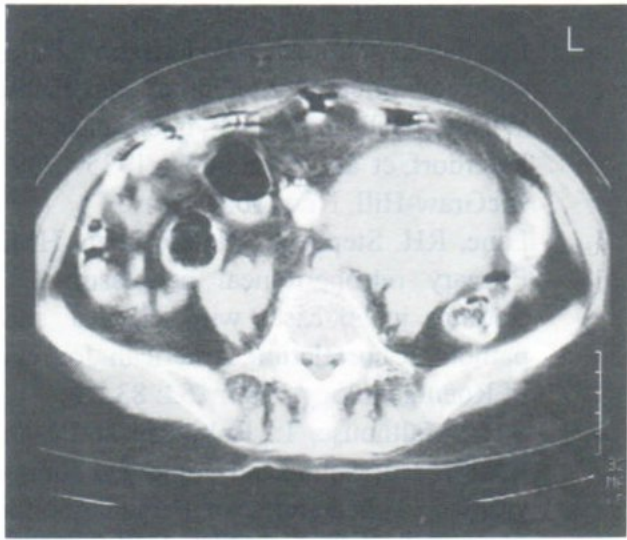


1A.

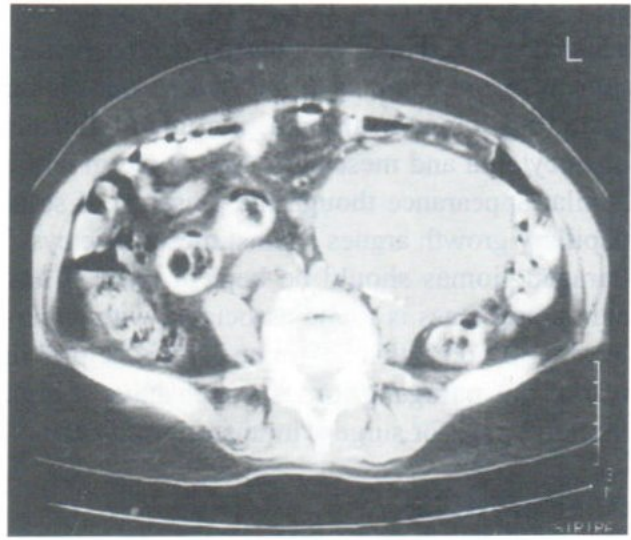


1B.

Fig.1. Ultrasound. (a) Transverse section through the left pelvis demonstrates large cystic mass with papillary growth. (b) Linear wall calcification is seen.



2A.



2B.

Fig.2. Nonenhanced CT scan. (a) Axial image through pelvis reveals well-defined, thin wall cyst 10.0x13.5x18.0cm.with solid papillary growth (b) Linear wall calcification is seen.

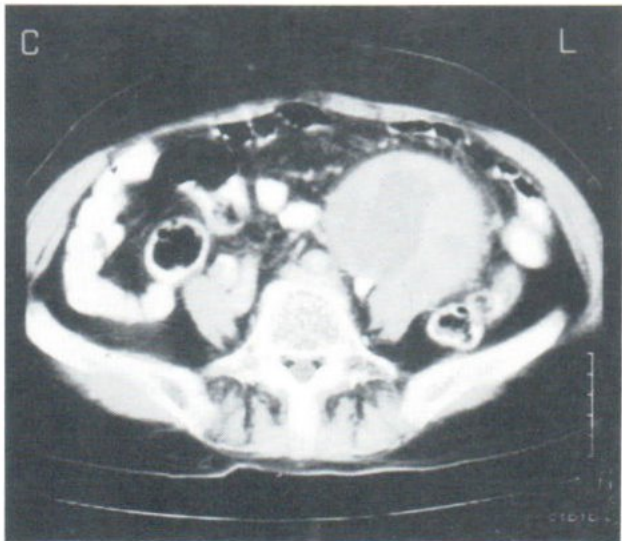


Fig.3. Contrast enhanced CT scan. Intense enhancement in solid part is noted.

DISCUSSION

Paraganglioma is a rare vascular tumor derived from neuroectodermal cells associated with ganglia cells of the autonomic nervous system. They usually lie in the para-aortic region from the level of renal arteries to the aortic bifurcation where the organ of Zuckerkaldle is found¹. The majority of paragangliomas are functionally active⁴. Hayes et al found that 24 of 28 patients had hypertension¹. However, catecholamine levels were elevated in all 18 patients who were studied¹.

Paragangliomas are usually detected by CT scan as large, smooth, well-defined soft tissue mass in the immediate para-aortic region. Most small paragangliomas are homogeneous. However, larger lesions may undergo central necrosis and calcification. We report a case of an unusually large cystic paraganglioma with papillary growth simulating an ovarian cancer in an old woman. Misdiagnosis led to intra-operative hypertensive crisis, which has a mortality rate for surgery of nearly 50%⁴. Retrospective study found

a high positioned mass postulated a diagnosis other than ovarian cancer. Many other neoplasm including leiomyosarcoma, malignant fibrous histiocytoma and mesenteric cyst could give the similar appearance though the presence of solid papillary growth argues against mesenteric cyst.³ Paragangliomas should be kept in mind if any para-aortic mass is found associated with hypertension. Blood catecholamine level is helpful in ruling out paragangliomas which have a high mortality rate for surgery in unsuspected cases.

REFERENCES:

1. Hayes, WS, Davidson, AJ, Grimley, PM & Hartman, DS. Extra-adrenal retroperitoneal paraganglioma: Clinical, pathologic and CT findings. *American Journal of Roentgenology* 1990; 155: 1247-1250
2. Landberg, L & Young, JB. *Harrison's Principle of Internal Medicine*, eds. 1990. Wilson, JD, Braunwald, E, Isselbacher, KJ, Peterdorf, et al. 12th edn, pp. 1735-1739. McGraw-Hill, New York.
3. Lane, RH, Stephens, DH & Reiman, HM. Primary retroperitoneal neoplasm: CT findings in 90 cases with clinical and pathologic correlation. *American Journal of Roentgenology* 1989; 152: 83-89
4. S.R. Malthouse, L. Robinson and S.C. Rankin. Ultrasound and Computed Tomographic Appearances of Paraganglioma Simulating Pancreatic Mass. *Clinical Radiology* 1992; 45(4): 271-272

PERCUTANEOUS TRANSLUMINAL ANGIOPLASTY AND WALL STENT PLACEMENT IN THE TREATMENT OF TRANSPLANTED RENAL ARTERY STENOSIS.

Krisdee PRABHASAVAT, M.D.¹

Saroj VANAPRUKS, M.D.¹

Somsak TANAWATTANACHAROEN, M.D.²

ABSTRACT

PURPOSE: We report our experience with percutaneous transluminal angioplasty (PTA) and endoluminal stent placement in the treatment of transplanted renal artery stenosis (TRAS).

MATERIALS AND METHODS: From February 1998 to February 1999, we performed PTA in 3 patients who were affected by TRAS and besides; 1 Wall stent was successfully implanted in 1 patient affected by transplanted renal artery stenosis. All transplanted kidneys were procured from cadaver donors. The patients were routinely evaluated with color Doppler ultrasonography (CDUS), and when there was the patient in whom the CDUS showed evidence of transplanted renal artery stenosis, the magnetic resonance imaging/angiography (MRI/MRA) and renal angiography would be performed. The mean interval between transplantation and stenosis detection was 9 months (range 4 to 12 months). When serious renal stenosis was diagnosed (stenosis greater than 50%), selected transplanted renal angiography, and endoluminal renal angioplasty had been performed in 3 patients. In 1 patient, an endoluminal metallic Wall stent was placed in the site of stenosis at the anastomotic site.

RESULTS: Clinical outcome was improved in all 3 patients (100 %), the patients became normotensive and there was large amount of urine flow after PTA. The mean residual renal stenosis after PTA was less than 25%. There was no major complication, only in 1 patient there was minor complication, that was a small false aneurysm occurred at the contralateral femoral artery punctured site, which was treated with US probe compression technique.

CONCLUSION: Percutaneous transluminal angioplasty and stent implantation is the initial interventional treatment of choice for high grade transplanted renal artery stenosis, with good clinical outcome, and low complication rate.

Key words: Transplanted renal artery stenosis, kidney transplantation, renal angioplasty, balloon, stent.

¹ Department of Radiology

² Department of Medicine, Faculty of Medicine, Siriraj Hospital, Mahidol University.

Transplanted renal artery stenosis (TRAS) is known to be a cause of severe hypertension, renal allograft dysfunction, or both. TRAS is a serious vascular complication following kidney transplantation. The incidence of TRAS has been reported to be 1.5% - 16 %, which is due to the heterogeneity of the population evaluated. In the large study of 377 patients the incidence was 6.6%. TRAS may be the consequence of arterial damage during donor nephrectomy or kidney perfusion, kinking of a long renal artery, discrepancies of arterial diameter and thickness between donor and recipient vessels, chronic rejection, and immunological factors. The clinical presentations include: poorly control hypertension, serious compromised function of the allograft, a bruit in the iliac fossa over the graft. Intraarterial angiography is the gold standard for diagnosis and is the first step of an angioplasty procedure. However, the color Doppler ultrasonography (CDUS), magnetic resonance imaging/angiography (MRI/MRA) have proved to be simple, noninvasive methods for depiction of vascular complications in the renal transplantation. Percutaneous transluminal angioplasty is currently the first choice of treatment, when transplanted kidney perfusion is reduced by a stenosis greater than 50% or when hypertension is refractory to multidrugs treatment. Chan et al performed the first treatment of an anastomotic ostial transplanted renal artery stenosis by percutaneous placement of an expandable metallic Palmaz stent. We report a series of 3 patients of percutaneous transluminal angioplasty for treatment of transplanted renal artery stenosis and 1 Wall stent placement for the prevention of recurrence renal artery stenosis.

MATERIAL AND METHODS

From February 1998 to February 1999, 2 female and 1 male patients, average age is 36 years (range 31 to 43) were treated with percutaneous transluminal angioplasty with balloon dilatation.

The diagnosis of their transplanted renal artery stenosis was confirmed by color Doppler ultrasonography, magnetic resonance angiography, captopril renogram and renal angiography studies. In 1 patient endoluminal Wall stent was implanted. The mean interval between transplantation and transplanted renal artery stenosis detection was 9 months (range 4 to 12). All of the 3 patients presented with poorly control hypertension, 1 patient with leg edema and oliguria and 1 patient with rising of serum creatinine. All kidneys were procured from cadaver donors. Anastomoses were performed end-to-side to the left external iliac artery in 1 patient, end-to-side to the right external iliac artery in 1 patient, and end-to-end to the left hypogastric artery in 1 patient. During follow up, the patients were evaluated routinely by noninvasive screening methods using color Doppler ultrasonography and magnetic resonance imaging and magnetic resonance angiography (MRA). When a serious transplanted renal artery stenosis (greater than 50 %) was diagnosed, selective angiography and percutaneous transluminal renal angioplasty were performed.

The stenosis was located at the site of anastomosis in 2 patients, at the intra-renal arterial branch that supply to the lower pole of transplanted kidney in 1 patient (patient #3 in the table #1). Angiography was performed via contralateral femoral artery puncture site and via left axillary artery in 1 patient. We used the non-ionic contrast medium, and limited the amount of contrast medium, as lower as possible less than 4 ml/kg, for prevention of its side effect to the transplanted kidney. The diagnostic catheter was cobra-shape tip, and the size of catheter was 5 Frence. The size of uninflated balloon catheter was also 5 Frence. The outer diameter of dilatation balloons were 6 mm. x 2 cm. long in 2 patients (patient #1,2), and 4 mm. x 2 cm. long in 1 patient (no.#3). The transplanted renal artery angioplasty was performed, by

exchange catheter technique across the 0.032 inch conventional guided wire, under fluoroscopy. After the balloon was placed across the stenotic site, the balloon was inflated up to 8-10

atmospheric pressure or until the "waist" of the balloon or stenotic part of the transplanted renal artery disappeared under fluoroscopy for 1 minute x 3 times.



Fig. 1A Pelvic angiography (case # 2 S.NM.) showed 53 % stenosis of the transplanted renal artery at anastomosis of end-to-side to the left iliac artery.

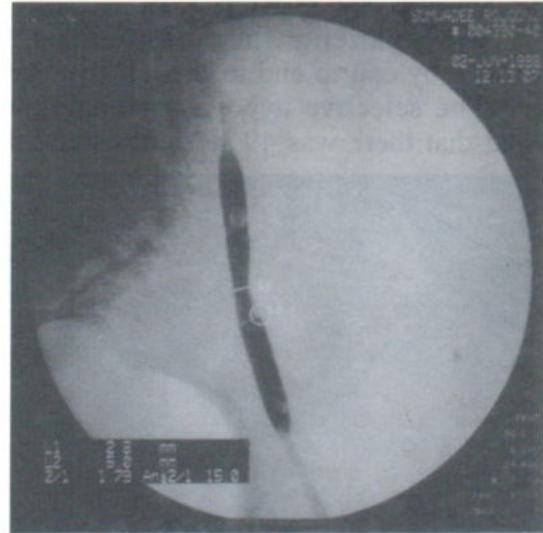


Fig. 1B During angioplasty, there was the narrowed segment or "waist" of the balloon catheter at the stenosis of transplanted renal artery.

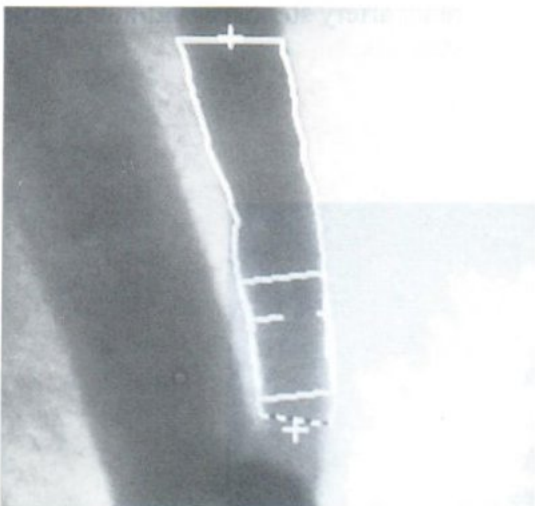


Fig. 1C Magnified angiogram showed stenosis of transplanted renal artery, before angioplasty.

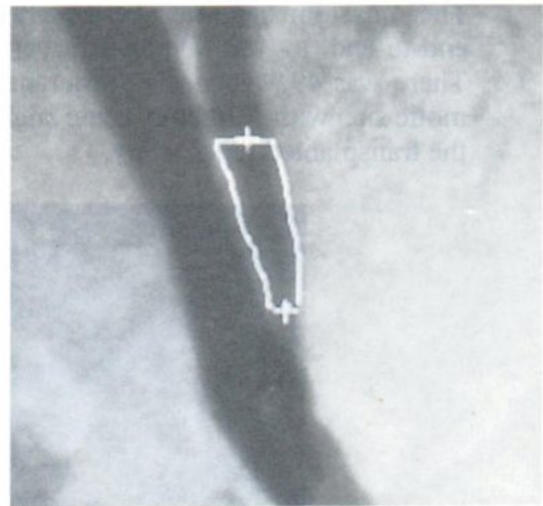


Fig. 1D Magnified angiogram showed no significant stenosis after angioplasty of transplanted renal artery.

During percutaneous transluminal renal angioplasty, 3,000 units of heparin were slowly administered intra-renal artery via the lumen of the balloon catheter. The degree of renal artery stenosis was shown in the table # 1.

In 1 patient, the anastomosis was performed by end to end to the left hypogastric artery. The selective hypogastric angiography showed that there was 49 % stenosis and there

was acute angle and kinking of anastomotic vessel. So after renal balloon angioplasty was performed successfully, the Wall stent, size 8 mm. x 6 cm. was implanted at the anastomosis for reduction of kinking of vascular angle and for prevention of re-stenosis of transplanted renal artery. Then after the angioplasty procedure was complete, the angiography was again performed to assess the degree of residual transplanted renal artery stenosis.



Fig. 2A Pelvic angiography of case #1 (S.R.W.) showed status post-renal transplantation. The anastomosis was performed by end-to-end to left hypogastric artery. There was 49% stenosis at the anastomotic site with kinking acute angle of the transplanted renal artery.

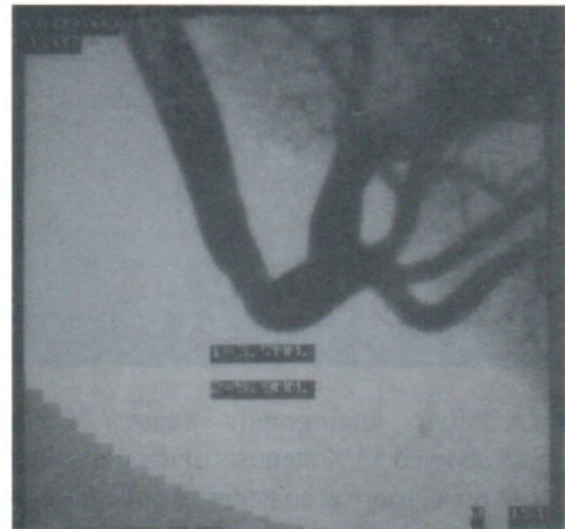


Fig. 2B Selective angiography post-angioplasty showed improvement of the transplanted renal artery stenosis without significant stenosis.

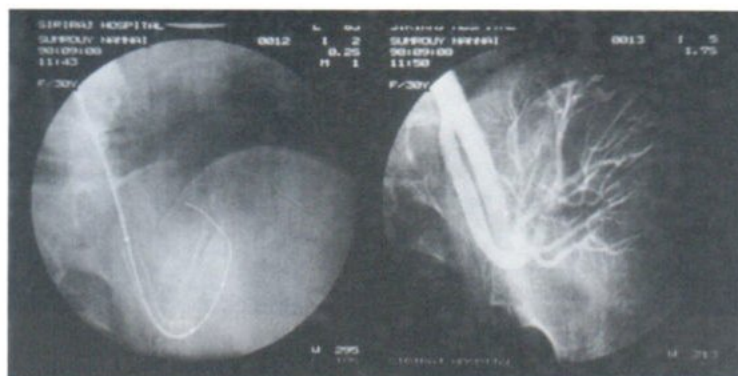


Fig 2C+D Post-Wall stent implantation at the anastomosis, angiography showed reduction of acute vascular angle without significant stenosis.



Fig. 3A Pelvic angiography of case # 3 (C.KT.) showed segmental intra-renal artery stenosis.

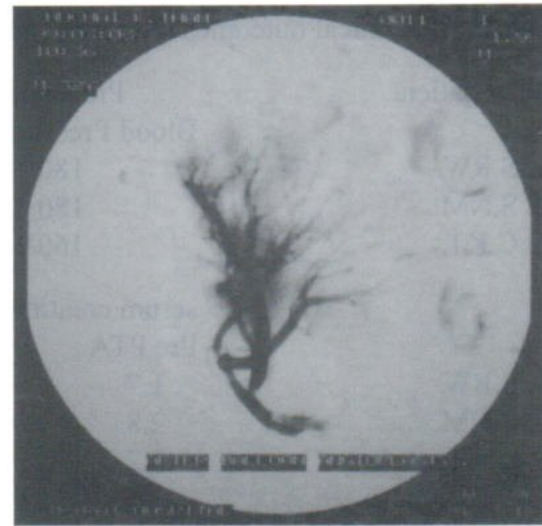


Fig. 3 B Post-angioplasty angiography showed no significant renal artery stenosis.

Appropriate antiplatelet therapy, Aspirin 325 mg. was administered orally, one day before and every day for at least one month period after the procedure.

RESULTS

The degree of transplanted renal artery stenosis before and after renal angioplasty was shown in the table # 1

Table No. 1. degree of renal artery stenosis

No. #	patient age	sex	Pre angioplasty	Post angioplasty.
1. S. RW.	31	F	49%	37% and 27 %*
2. S. NM.	43	F	53%	38% and 25%**
3. C. KT.	33	M	65%	38%

* degree of stenosis after Wall stent implantation.

** degree of stenosis at follow up study 6 months.

On follow up, blood pressure, serum creatinine level and medications are monitored while grafts are evaluated with color Doppler ultrasonography. The technical result of renal angioplasty are evaluated in terms of the extent of renal artery stenosis reduction. A residual post-angioplasty stenosis less than 30 % represents a

satisfactory outcome. Immediate technical success was achieved in all patients.

The clinical findings were good and satisfactory in all patients and was shown in table No.2

Table 2 The clinical outcomes after renal angioplasty.

No. # patient	Pre angioplasty		Post angioplasty.
	Blood Pressure (mm. Hg.)		
#1. S.RW.	180/110		130/80 mm. Hg.
#2. S.NM.	180/100		140/90 mm. Hg.
#3. C.KT.	160/100		140/80 mm. Hg.
	serum creatinine (mg %)		Urine flow /day.
	Pre PTA	Post-PTA	
#1. S.RW.	1.7	2.3	7,000 ml.
#2. S.NM.	2.8	1.6	2,000 ml.
#3. C.KT.	3.2	2.5	3,000 ml.

In patient No.#1 S.RW., there was very good clinical response, after renal angioplasty, there was diuresis phase, with large amount of urine flow of 7,000 ml/day and the edema of her legs disappeared. So satisfactory renal function and good pharmacological control of the blood pressure have been achieved in all patients. However, there was minor complication in one patient (S.RW. No#1). There was a small false aneurysm 1.5 cm. diameter occurred at the contralateral femoral artery punctured site, but the false aneurysm can be treated successfully by ultrasonographic probe compression technique.

DISCUSSION

According to the literatures, the incidence of transplanted renal artery stenosis are 5.8% to 17.7 %, and the interval between transplantation and the diagnosis of transplanted renal artery stenosis ranges from 2 to 45 months. In our series the interval was 4 to 12 months. The cause of transplanted renal artery stenosis is likely to be multifactorial and its etiology may have an immunological component. Tiley et al reported poor resolution of hypertension and graft dysfunction following reparative surgery in patients with chronic rejection and transplanted renal artery stenosis.⁵ Wong et al detected a significantly higher incidence of rejection in a transplanted renal

artery stenosis group versus control group.²⁰

Transplanted renal artery stenosis may occur at the anastomotic ostial site or distal to the anastomosis. There is no difference in stenosis incidence between end-to-side anastomosis to the external iliac artery and end-to-end anastomosis to the hypogastric artery. However, percutaneous transluminal angioplasty (PTA) of stenosis in the end-to-end anastomosis to the hypogastric artery is technically more difficult and results in a higher complication rate with higher allograft loss. Percutaneous transluminal angioplasty results vary according to the length of the follow up. An immediate success rate of 81%, decreasing to 75% at 1 month and to 57 % at 1 year has been reported.¹³ A graft survival rate of 95% after one year and 82% after two years has been reported in a more recent study.¹²

The percutaneous transluminal angioplasty (PTA) has become the first choice in the transplanted renal artery stenosis treatment because of its technical effectiveness and tolerance by the patient. It does not preclude subsequent surgical correction and offers the possibility of implanting endovascular stent if stenosis reoccurs.¹⁴ One limitation of percutaneous transluminal angioplasty that may occur, is restenosis, which may appear 8-12 months after angioplasty,

usually as the result of reactive intimal hyperplasia. Percutaneously introduced vascular stents can improve the long-term results of renal angioplasty. Vascular endoluminal stents were introduced in 1987 for coronary and peripheral circulation.¹⁶ They provide a mechanical scaffolding, prevent elastic recoil and repair arterial dissection if they do occur, while maintaining vessel patency. There are many reports about stent implantation safety and effectiveness. In 1995 Chan et al first reported the successful use of Palmaz stent for the treatment of transplanted renal artery stenosis in women to correct severe stenosis at the ostial site of the end-to-side anastomosis to the right external iliac artery.⁷ They reported a 6-month follow up without any restenosis. The stent were clinically tested in native arteries after inadequate angioplasty or effective endarterectomy,¹⁷ or for ostial lesions of native renal arteries.¹⁸ Palmaz stent is consisted of a slotted stainless steel tube crimped onto the percutaneous transluminal coronary angioplasty balloon catheter after complete inflation of the carrier balloon, the metal stent mesh is incorporated into the arterial wall. Intimal cells and endothelium bridge over the support and completely cover the inner surface of the stent.

However, the Palmaz stent can kink in the acute angle (vessel's angle <90 degree) and it is unbendable. So that we used Wall stent that can be bendable in acute angle, in the patient (S. R. W., No.#1) with end-to-end anastomosis to the left hypogastric artery. And after Wall stent implantation the vascular anastomotic angle was straightened and there was minimal less residual stenosis.

One limitation of the using endovascular stent is that the cost of the stent is high, especially in this IMF period. However, as we compare with the cost of surgery, the stent treatment for renal artery stenosis is more cheaper with high success rate and low complication. And if the stent is more widely use, the cost of stent would be lower in the

following day.

CONCLUSION

Percutaneous transluminal balloon angioplasty and stent implantation is the initial interventional treatment of choice of high grade transplanted renal artery stenosis. The clinical outcomes are better as for blood pressure, graft survival, serum creatinine. There is low minor complication in only one patient. The patient can tolerate the procedure well.

REFERENCES

1. Newman-Sanders, A. P., Gedroye, W. G., al-Kutoubi, M. A., Koo, C. and Taube, D.: The use of expandable metal stents in transplant renal artery stenosis. *Clin. Rad.*, 50:245, 1995.
2. Schacht R.A. Martin, D.G., Karalukulasingam, R., Wheeler. C.S. and Lansing. A. M. Renal artery stenosis after renal transplantation. *Amer. J. Surg.*, 131: 653, 1976.
3. Palmaz, J. C., Windeler, S. A., Garcia, F., Tio, F. O., Sibbitt, R. R. and Reuter, S. R.: Atherosclerotic rabbit aortas : expandable intraluminal grafting. *Radiology*, 160:723, 1986.
4. Kauffman, H.M., Sampson, D., Fox, P.S., Doyle, T. J. and Maddison, F.E. : Prevention of transplant renal artery stenosis. *Surgery*, 81:161, 1977.
5. Tilney, N.L., Rocha, A., Strom, T.B. and Kirkman, R. L. : Renal artery stenosis in transplant patients. *Ann. Surg.*, 199:454, 1984.
6. Macia, M., Paez., A., Tornero, F., De Oleo, P., Hidalgo, L. and Barrientos, A. : Post-transplant renal artery stenosis : a possible immunological phenomenon. *J. Urol.*, 145: 215,1991.

7. Chan, H. W., Ho, Y., Chan, C., Yiu, T., Tong, M. K. and Wong, P. H. : Treatment of anastomotic ostial allograft and renal artery stenosis with the Palmaz stent. *Transplantation*, 59 : 436, 1995.
8. Erley, C.M., Duda, S. H., Wakat, J.P., Sokler, M., Reuland, P., Muller-Schauenburg, W., Lauchart, W. and Risler, T. : Noninvasive procedures for diagnosis of renovascular hypertension in renal transplant recipients-a prospective analysis. *Transplantation*, 54:863,1995.
9. Merkus, J. W., Hoitsma, A. J., van Asten, W.N., Zeebregts, C. J., van der Vliet, J. A., Strijk, S. P., Koene, R. A. and Skotnicki, S. H. : Echo-doppler diagnosis of renal allograft artery stenosis. *Clin. Transplant*, 9:383,1995.
10. Lacombe, M. : Arterial stenosis complicating renal allotransplantation in man : a study of 38 cases. *Ann. Surg.*, 181:283, 1975.
11. Sankari, B. R., Geisinger, M., Zelch, M., Brouhard, B., Cunningham, R. and Novick, A. C. : Post-transplant renal artery stenosis : impact of therapy on long-term kidney function and blood pressure control. *J. Urol.*, 149:980,1996.
12. Benoit, G., Moukarzel, M., Hiesse, C., Verdelli, G., Charpentier, B. and Fries, D. : Transplant renal artery stenosis : experience and comparative results between surgery and angioplasty. *Transplant. Int.*, 3:137,1990.
13. Raynaud, A., Bedrossian, J., Remy, J., Brisset, J. M., Angel, C. Y. and Gaux, J. C. : Percutaneous transluminal angioplasty of renal transplant arterial stenosis. *AJR*, 146:853,1986.
14. Nicita, G., Marzocco, M., Villari, D., Li Marzi, V., Trippitelli, A., Doggweiler, R., Santoro, G. and Grechi, G. : Percutaneous transluminal angioplasty (PTA) in the treatment of transplant renal artery stenosis (TRAS). *J. Urol.*, Part 2, 155 : 686A, abstract 1499, 1996.
15. Grossman, R. A., Dafoe, D. C., Schoenfeld, R. B., Ring, E. j., McLean, G. K., Oleaga, J. A., Freiman, D. B., Najj, A., Perloff, L. J. and Barker, C. F. : Percutaneous transluminal angioplasty treatment of renal artery stenosis. *Transplantation*, 34:339,1983.
16. Sigwart, U., Kaufmann, U., Mirkovitch, V., Joffre, F. and Kappemberger, L. : Intravascular stents to prevent occlusion and restenosis after transluminal angioplasty. *New Engl. J. Med.*, 316:701,1987.
17. Kuhn, F. P., Kutkhun, B., Kock, M., Torsello, G. and Modder, U. : Experience with the strecker stent in the treatment of renal artery stenosis after failed angioplasty or thrombenarterectomy (abstract). *Radiology*, 177:202,1990.
18. Rees, C. R., Palmaz, J. C., Becker, G. J., Ehrman, K. O., Richter, G. M., Noeldge, G., Katzen, B. T., Dake, M. D. and Schwarten, D. E. : Palmaz stent in atherosclerotic stenoses involving the ostia of the renal arteries : preliminary report of a multicenter study. *Radiology*, 181:507, 1991.
19. Wilms, G. E., Peene, P. T., Baert, A. L., Nevelsteen, A. A. Suy, R. M., Verhaeghe, R. H., Vermynen, J. G. and Fagard, R. H. : Renal artery stent placement with use of the wallstent endoprosthesis. *Radiology*, 179:457,1991.
20. Roberts. J.P., Asher, N, L., and Fryd. D. S. : Transplant renal artery stenosis. *Transplantation* . 48:590,1989.

THE FIRST AORTIC STENT-GRAFT PLACEMENT IN THAILAND

Jiemjit TAPANEEYAKORN,¹ Surasak LEELAUDOMLIPI,²
Suthus SRIPHOJANART,² Sarana BOONBAICHAİYAPRUCK,³
Suvipaporn SIRIPORNPITAK¹

ABSTRACT

The first patient in Thailand, a 67 years-old female having liver cirrhosis with an asymptomatic huge infra-renal aortic aneurysm, who has an aortic stent graft, was reported.

INTRODUCTION

Over the past few years, one of the most remarkable innovations in interventional radiology was the development of the intraluminal stent-graft placement. This new technique has recently been used to treat a variety of lesions, including vascular occlusive disease, peripheral aneurysms, vascular injury and aortic aneurysms.¹

Usually, surgical repair is the treatment of choice for an abdominal aortic aneurysm, provided that the patient is a good candidate for operation. The standard surgical repair of the abdominal aortic aneurysm (AAA) using synthetic graft is associated with a perioperative mortality rate of 1.4-6.5%.²

For this reason, the endovascular repair with aortic stent-graft is an attractive alternative treatment for the surgical procedures.

A CASE REPORT

A case of 68 years-old female patient, presented at Ramathibodi Hospital with hematemesis on the 23rd of July 1998. Her physical examination showed evidences of chronic liver disease. Her upper GI study is normal and the

ultrasound study showed liver cirrhosis, splenomegaly and a huge abdominal aortic aneurysm (Fig.1).

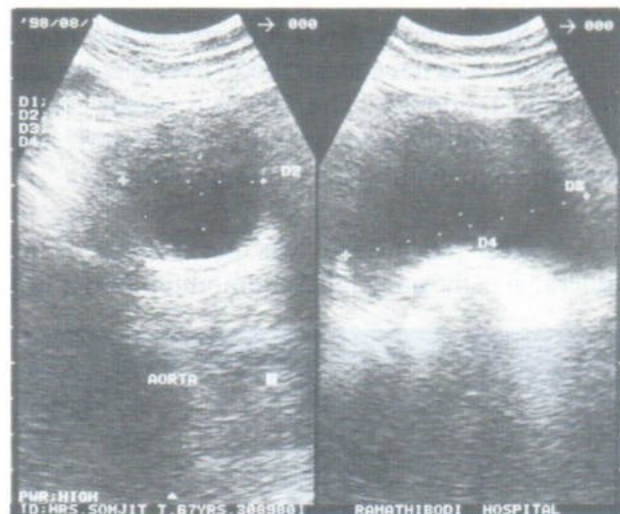


Fig.1. Ultrasound study showed a huge aortic aneurysm.

The hematemesis disappeared after the initial treatment for acute gastritis. The computed tomography angiogram (CTA) was performed to evaluate her asymptomatic aortic aneurysm. It revealed that the size of the aneurysm was about 9 cm in length and 4.8x5cm in its maximum AP and transverse diameters, respectively (Fig.2, 3).

¹ Department of Radiology

² Department of Surgery

³ Department of Medicine, Ramathibodi Hospital

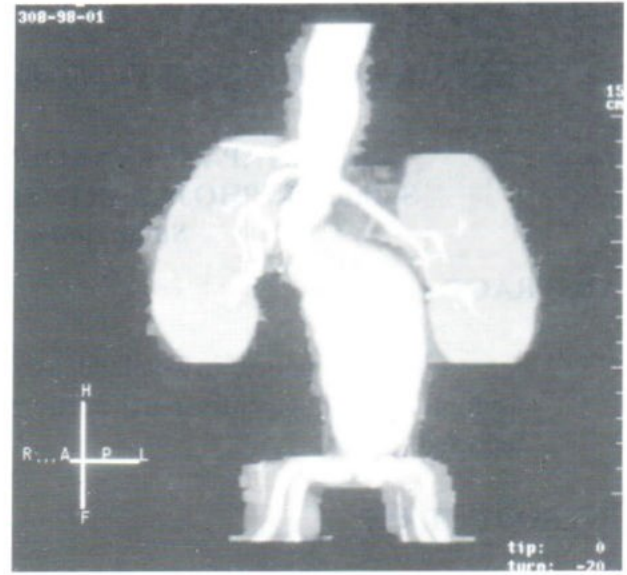
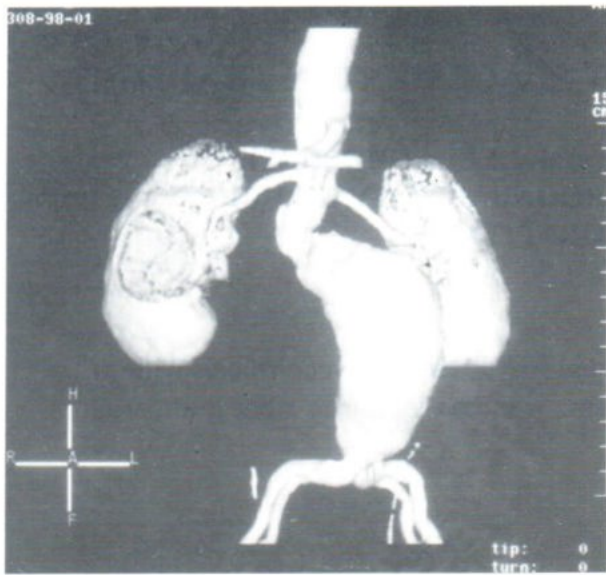


Fig. 2-3. Computed tomography angiogram also showed an infra-renal aortic aneurysm.

PROCEDURE

Since she had risk factors for the major surgery such as her age, cirrhotic liver disease and bleeding tendency. The elective repair of the aneurysm by the endovascular stent graft was performed to avoid the emergency surgery.

The procedure was performed under general anesthesia. Right common femoral artery

was cut down and a 5 French arterial sheath was inserted.

The abdominal aortic angiogram was performed by using a 6 French Pigtail Catheter. Pre-treatment angiogram revealed a huge infra-renal aortic aneurysm (Fig.4) with severe stenosis at its upper neck (Fig. 5).

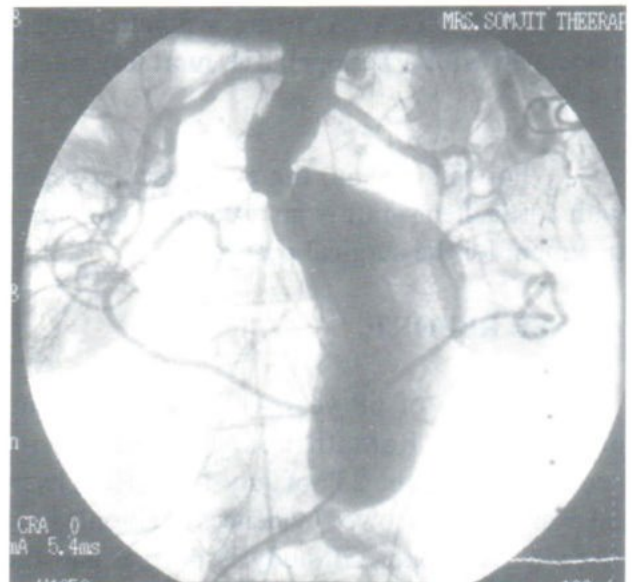
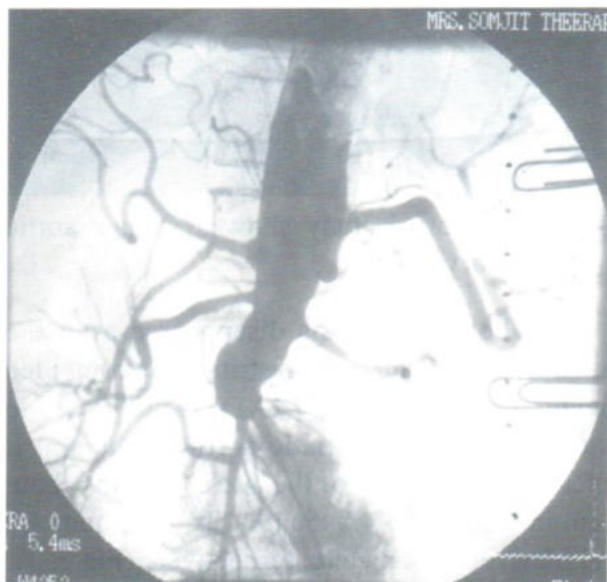


Fig. 4-5. Severe aortic stenosis is noted at the upper neck of the huge infra-renal aortic aneurysm.

The aneurysm was crossed by the 0.35 J-tip Hydrophilic guidewire with difficulty due to the previously mentioned severe aortic stenosis. After successful crossing, the Cobra-2 catheter was inserted by co-axial technique and the Hydrophilic guidewire was changed to 260 cm length, 0.35 Amplatz Super -Stiff guidewire.

The bifurcated aortic stent graft with right leg was placed successfully, (Fig.6, 7) by using the Vanguard Bifurcated Endovascular Graft, which had 26x12mm diameter (Boston Scientific Corporation).

The left leg of the graft was introduced by percutaneous puncture of the left common

femoral artery. The 6 French arterial sheath was placed. The J-tip Hydrophilic guidewire was inserted, crossing over the aortic bifurcation from the right femoral arterial sheath and its tip was snared through the left femoral arterial sheath. The Cobra-2 catheter and 0.35 Amplatz Super Stiff guidewire were changed, respectively and the left leg of the graft was introduced by co-axial technique.

Upper and lower necks of the graft as well as its both legs were dilated by the occlusive balloon to prevent endoleak. The abdominal aortogram, post procedure, revealed a good result (Fig.6, 7).

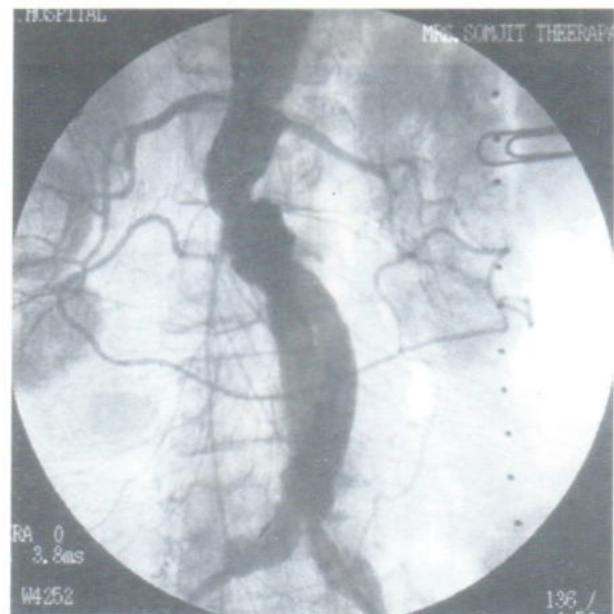
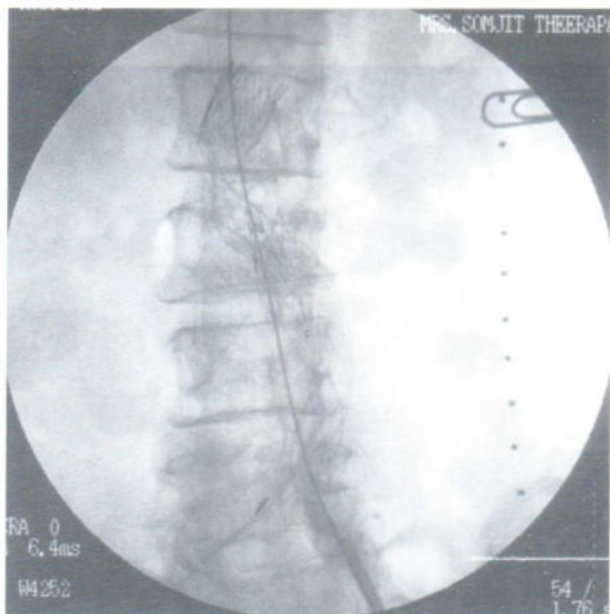


Fig. 6-7. A Vanguard Bifurcated Endovascular Graft (Boston Scientific Corporation) was successfully deployed.

The operative team consisted of a vascular surgeon, a radiologist and a cardiologist. Follow up CTA, at the fourth day post graft placement showed no contrast leakage into the outer

lumen of the graft, which represented the good result (Fig.8, 9,10,11). She was discharged from the hospital five days after the treatment.

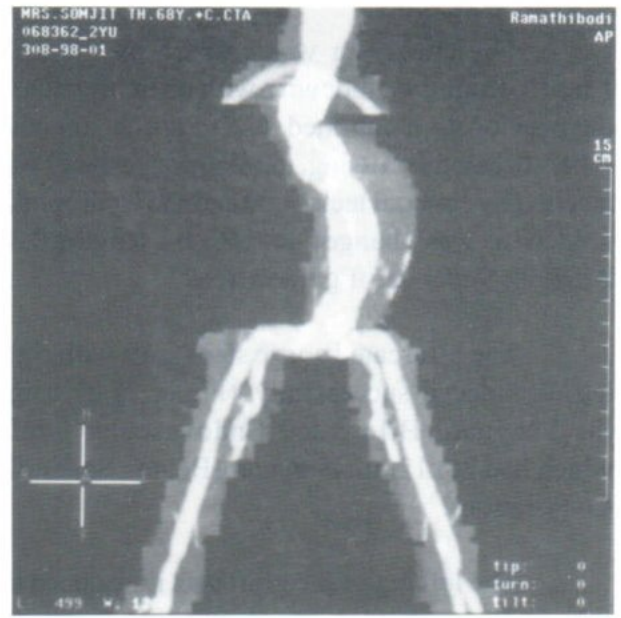
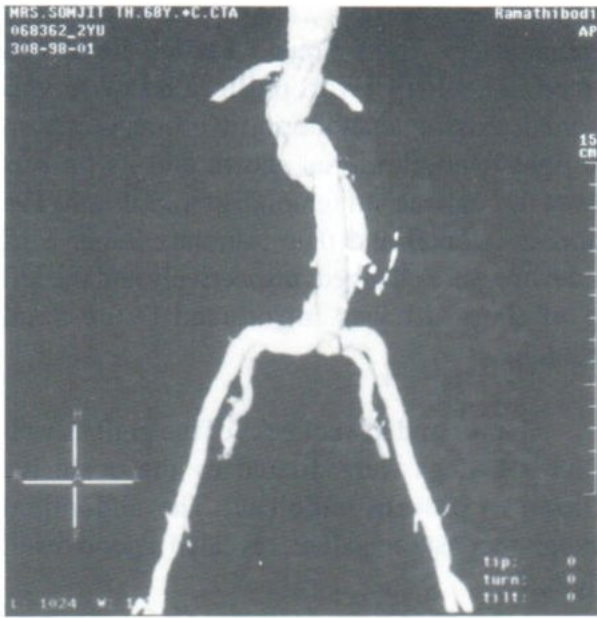


Fig. 8-9. Follow up CTA, four days post the procedure.

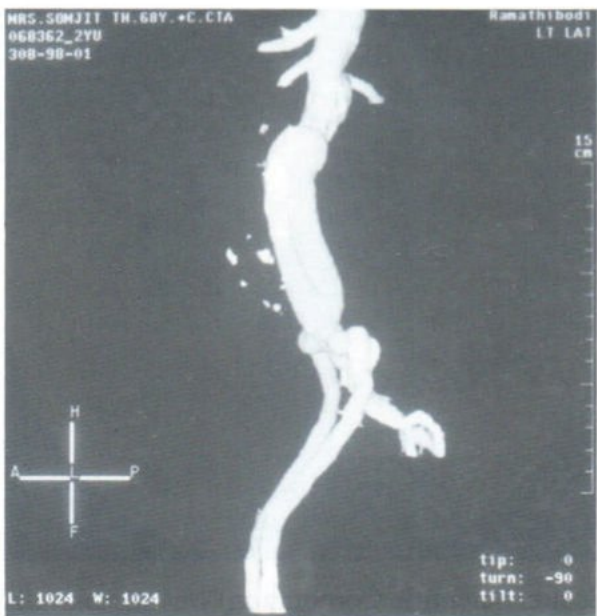


Fig. 10-11. Follow up CTA, four days post the procedure.

DISCUSSION

The surgical treatment for an abdominal aortic aneurysm is associated, however, with a relatively high morbidity and mortality rate. In community hospitals, overall mortality rate is 10-14%.

According to the literature, when elective procedure is performed by an experienced vascular surgeon in excellent centers, the mortality rate is in the range of 3-5%.¹ The mortality rate increases more than 20%³ in patients requiring emergency operative treatment or in patients with advanced age, chronic heart failure, coronary artery disease and chronic obstructive pulmonary disease. It has been recommended to do elective surgical repair even in those patients not at high risk for rupture.¹

The development of covered stents opens a new dimension for non-operative therapy of the aneurysmal disease. Successful endoluminal grafting was performed in different animal model.⁴

The straight grafts in humans for aortic dissection and infra renal aortic aneurysms were first described in 1991 by Parodi et al.³ Since then, endoluminal treatments of aneurysms of the thoraco-abdominal aorta with different types of endoprosthesis have been performed in several centers.⁴

For endovascular repair of an asymptomatic abdominal aortic aneurysm, by the endovascular technologies (EVT) using the endograft was introduced in February 1993.⁴

After initial experience with an endoprosthesis of tubular design, a bifurcated graft was introduced in 1994 and monoiliac system in 1996.⁵⁻⁷

The first bifurcated stent-graft implanta-

tion was performed in good risk patients with the long and straight implantation site in both proximal and distal part of the aneurysm.⁴

By April 1997, over 450 endografts have been utilized worldwide, as part of clinical trials under the supervision of the Food and Drug Administration (FDA) of the USA.

Thoraco-abdominal aneurysms of all Crawford types that usually involve major arterial branches such as the renal or other visceral arteries are not candidates for an endoluminal treatment. However, 75 to 90% of abdominal aortic aneurysms are infrarenal.⁴

The suitable lesions for endoluminal treatment should have a sufficient infra renal neck of 2 to 3 cm in length,⁴ which does not present in about 15% of cases.⁴ The vast majority (90%) of cases does not have a distal aortic neck proximal to the aortic bifurcation. Nearly 50% of cases, there is an involvement of part or the whole segment of unilateral or bilateral common iliac arteries.⁴

Currently, the introduction of large -diameter systems prevents exclusively percutaneous insertion of those devices, which can not be performed by a radiologist alone. This shifts their use to a collaborative effort of both radiologists and vascular surgeons.

CONCLUSION

The use of endoluminal grafts for the treatment of thoracic and abdominal aortic aneurysms has attracted both vascular surgeons and radiologists.

In Thailand, nowadays, the aortic stent graft is quite expensive. But the endovascular aneurysm repair with stent-grafts is an attractive

alternative to surgical procedures, especially in the patients who have high risk of major surgical complications as in this reported case.

REFERENCES

1. Castaneda-Zuniga WR. Vascular stent: Interventional radiology. 3rd ed. Baltimore: Williams&Wilkins, 1997.
2. Ennst CB. Abdominal aortic aneurysm. N Engl J. Med 1993;328:1167-72.
3. Parodi JC, Palmaz JC, Barone HD. Transfemoral intraluminal graft implantation for abdominal aortic aneurysms. Ann Vasc Surg 1991; 5:491-9.
4. Gunther RW, Vorwerk D. Seminars in Interventional radiology 1998;15(1):3-108.
5. Moore WS, Rutherford RB. Transfemoral endovascular repair of abdominal aortic aneurysm: results of the North American EVT phase I trial. J Vas Surg 1996;23:543-53.
6. Balm R, Eikelboom BC, May J, Bell PRF, Swedenborg J, Collin J. Early experience with transfemoral endovascular aneurysm management (TEAM), in the treatment of aortic aneurysms. Eur J Vasc Endovasc Surg 1996;11:214-20.
7. Moore WS. The EVT tube and bifurcated endograft system: technical considerations and clinical summary. J Endovasc Surg 1997;4:182-94.

CT FINDINGS OF RENAL ACTINOMYCOSIS: A CASE REPORT

Suprasit CHAROONWATANALAOHA, MD, Linda PANTONGRAG-BROWN, MD

Abdominal actinomycosis is very uncommon and difficult to diagnose.¹ Within the abdomen, the gastrointestinal tract, particularly colon and appendix, are the most common organs involved.² Recent reports have indicated an increased prevalence of pelvic actinomycosis in women who use intrauterine contraceptive devices.³⁻⁵ Renal involvement is extremely rare, but has been anecdotally reported.⁶⁻⁸ CT findings of renal actinomycosis has been described only once in the English literature.⁸ Therefore, we would like to report a case of renal actinomycosis, emphasizing the CT features that may lead to the diagnosis of this chronic infection.

CASE REPORT

A 17-year-old woman presented with a 2-month history of left flank pain and low-grade fever. She experienced gross hematuria only once during this illness. Previously, she had been healthy, had never used an intrauterine device (IUD) for birth control and had no history of abdominal surgery. Physical examination revealed mild tenderness at the left flank and a palpable but ill-defined mass in the left upper quadrant. The body temperature was within normal limits. The complete blood count and urine analysis were normal.

An excretory urogram was performed which revealed a space-occupying mass in the lateral aspect of the grossly enlarged left kidney with compression of its pelvocalyceal system. The ultrasonography of the abdomen showed a large, heterogeneous, predominantly low-echoic mass involving the left kidney. Plain CT scan of the upper abdomen showed global enlargement of the left kidney with relative preservation of its renal shape (Fig. 1A). After intravenous administration of contrast material, only the superomedial aspect

of the left kidney showed normal nephrogram and excretion. The rest of the kidney was infiltrated and less dense than the normal nephrogram. Slight enhancement within this infiltrated area was noted, presenting a reticular pattern (Fig. 1B). The lesion extended to involve the perinephric fat, renal fascia and anterior pararenal space. The pancreatic tail and the adjacent colon seemed to adhere to the lesion. There was no evidence of thrombus within the left renal vein or inferior vena cava. Based upon the imaging findings, neoplasm such as lymphoma or renal cell carcinoma was suggested.

The patient underwent exploratory surgery. The left renal mass was found to adhere to the spleen, tail of the pancreas, splenic flexure of the colon and left adrenal gland. En bloc resection was performed. The gross pathologic findings showed an ill-defined infiltrative lesion with a yellowish cut surface compressing the left renal pelvis. The resected segment of colon contained a perforated ulcer, measuring about 0.5 cm. in diameter. Microscopic examination of the left

Department of Radiology, King Chulalongkorn Memorial Hospital, Rama IV Road, Bangkok 10330, Thailand

Address for correspondence:

Linda Pantongrag-Brown, MD, Department of Radiology King Chulalongkorn Memorial Hospital Rama IV Road, Bangkok 10330
phone: 256-5364 fax: 256-4417 e-mail: abrown@mozart.inet.co.th

kidney revealed acute and chronic inflammation with scattered foci of actinomycotic abscesses containing colonies with sulfur granule appearance.

The patient was given an extended course of penicillin G and after marked clinical improvement, was discharged from the hospital.

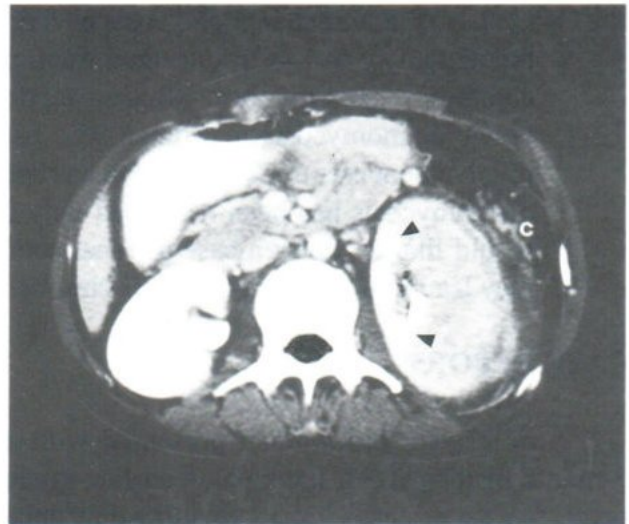
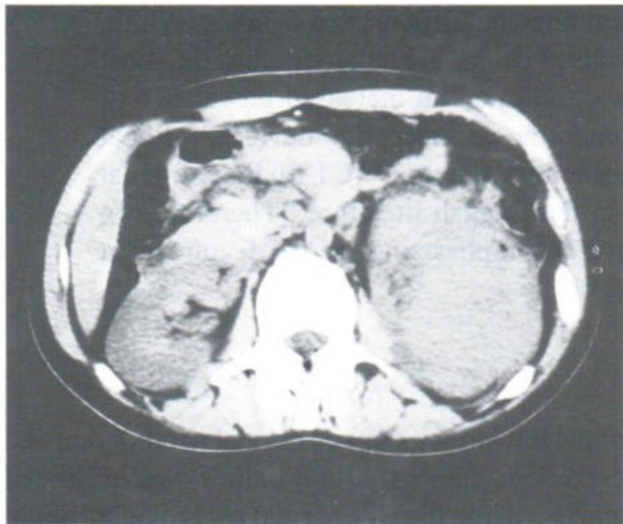


Fig. 1. A 17-year-old female with a 2-month history of left flank pain and low-grade fever.

A. Plain CT shows a global enlargement of the left kidney with relative preservation of its renal shape.

B. CT, after intravenous contrast enhancement, shows low density infiltrative lesion involving almost the entire kidney and extending to perinephric fat, renal fascia, and anterior pararenal space. Slight reticular enhancement within the infiltrative lesion is observed. The descending colon (C) is adhered to the lesion. Note minimal area of normal nephrogram and excretion at the medial aspect of the left kidney (arrowheads).

DISCUSSION

Actinomycosis is a variety of gram-positive, anaerobic or microaerophilic bacterial infection that can affect virtually any site in the body.⁹ Classic actinomycosis is caused most often by *Actinomyces israelii*, which is a normal inhabitant of the gastrointestinal tract.⁹ The pathogenesis of actinomycosis is disruption of the mucosal barrier by trauma, surgery, or bowel perforation

that will permit these organisms to invade surrounding tissues.¹⁰ Not infrequently, the disease occurs without obvious predisposing factors, which makes the diagnosis difficult.²

Most cases of actinomycosis involve the cervicofacial area; the proportion of all cases in this site is as high as 63%.⁴ Abdominal involv-

ement has been reported in approximately 20% of cases, of which the appendix and colon are the most common organs involved.² Pelvic actinomycosis is increasing and is associated with use of intrauterine devices.³⁻⁵ Renal involvement is extremely rare, but can occur as a result of hematogenous dissemination from a cryptic or defined, non-contiguous source, or from direct extension within the peritoneum.⁶⁻⁸ In our case, we believe that the perforated left-sided colon, found on surgery, was a source of contiguous spread of the infection to the left kidney, although there were no clinical symptoms suggestive of this prior to the time of operation.

Diagnosis of abdominal actinomycosis is always a challenge. It has been called "the most misdiagnosed disease", and part of the reason is because of its rarity.¹¹ In our case, CT correctly identified the infiltrative mass within the left kidney with evidence of transfascial involvement. By virtue of its invasiveness and long clinical course, neoplasm was highly suggested. Chronic infection or inflammation was not even in the differential diagnosis. Retrospectively reviewed in our case, CT actually showed a clue that the lesion might have been an infectious process. On contrast-enhanced CT scan, there was a reticular pattern of enhancement within the infiltrative lesion. This pattern may reflect multiple small abscesses clustering together. This CT observation has not been described in an anecdotal report of renal actinomycosis.⁸ In that report, renal actinomycosis was described on CT as an infiltrative lesion with invasion of normal anatomic barriers.⁸ These findings were also noted in our case, but could not be differentiated from neoplasm. As detected retrospectively in our case, we propose that CT images be carefully scrutinized for a reticular pattern of enhancement within the infiltrative lesion, if found, the infectious etiology is more likely. A suggestion of infection by the radiologist may be important, since the wider differential diagnosis may influence the

clinician to perform percutaneous biopsy instead of nephrectomy. Actinomycosis usually responds very well to antibiotics, thus its diagnosis may allow the patient to avoid sacrifice of the kidney. Unfortunately, this was not the case in our patient and nephrectomy was performed.

In conclusion, although rare, actinomycosis should be in the differential diagnosis of an indolent intrarenal lesion, along with tuberculosis, fungal infection and neoplasm. CT scan is a good imaging modality for determining invasiveness of the process and, if accompanied by a reticular enhancement pattern in the invasive lesion, infectious etiology, should be highly considered.

REFERENCES

1. Weese WC, Smith IM. A study of 57 cases of actinomycosis over a 36-year period. A diagnostic "failure" with good prognosis after treatment. *Archives of Internal Medicine* 1975;135:1562-1568.
2. Berardi RS. Abdominal actinomycosis. *Surgery, Gynecology & Obstetrics* 1979; 149:257-266.
3. Henderson SR. Pelvic actinomycosis associated with an intrauterine device. *Obstetrics & Gynecology* 1973;41:726-732.
4. Maloney JJ, Cho S. Pelvic actinomycosis. *Radiology* 1983;148:388.
5. O'Connor K, Bagg MN, Croley MR et al. Pelvic actinomycosis associated with intrauterine devices. *Radiology* 1989;170: 559-560.
6. Anhalt M, Scott, Jr. R. Primary unilateral renal actinomycosis; case report. *Journal of Urology* 1970;103:126-129.
7. Fowler RC, Simpkins KC. Abdominal actinomycosis: a report of three cases.

- Clinical Radiology 1983; 34:301-307.
8. Ha HK, Lee HJ, Kim H et al. Abdominal actinomycosis: CT findings in 10 patients. American Journal of Roentgenology 1993; 161:791-794.
 9. Bartlett JG. Agents of Actinomycosis. In: Gorbach SL, Bartlett JG, Blacklow NR, eds. Infectious Diseases, 2nd ed. Philadelphia: W.B.Saunders, 1998:1973-1980.
 10. Brown JR. Human actinomycosis. A study of 181 subjects. Human Pathology 1973; 4:319-330
 11. Cope VZ. Visceral actinomycosis. British Medical Journal 1949; 2:1311-1316

PROGNOSTIC VALUE OF CONTRAST ENHANCED CT SCAN COMPARED TO CLINICAL SEVERITY GRADING SYSTEM IN ACUTE PANCREATITIS

Kanjana LEELALAWAN¹, M.D. Nittaya CHAMADOL¹, M.D.
Chaiyut THANAPAISAL², M.D.

ABSTRACT

Purpose: To evaluate the prognostic value of contrast enhanced CT (CECT) in predicting the severity of acute pancreatitis and compared it to the prognostic signs as detectable clinically. Other signs on plain film radiography and sonography were also analyzed.

MATERIALS AND METHODS

Twenty patients with clinical diagnosis of acute pancreatitis at Srinagarind hospital, Khon Kaen University between January 1993-January 1999, who underwent CECT study of pancreas, were reviewed retrospectively. CECT grade, degree of necrosis and severity index (Balthazar) were determined. Ranson's objective prognostic signs, duration of hospitalization, morbidity, mortality and etiology were evaluated.

RESULT

The CT grading was grade A in 1 patient (5%); grade B, 2 patients (10%); grade C, 0 patient (0%); grade D, 6 patients (30%); and grade E, 11 patients (55%). Pancreatic pseudocyst occurred in 4 patients. Surgical drainage was required in 1 patient.

Pancreatic abscess developed in 1 patient, which improved clinically by conservative treatment. Two patients with CT grade E had pancreatic necrosis more than 50%. The mean

duration of hospitalization in patients with pancreatitis grade A, B, D, E were 7, 7.5, 7.3, 11.82 days respectively. The severity of pancreatitis was also graded by clinical's prognostic signs as 0-2 signs in 12 patients (70.58%), 3-4 signs in 3 patients (17.64%), 5-6 signs in 1 patient (5.88%), and 7 or more signs in 1 patient (5.88%). The patients who had 3 or more early objective prognostic signs were in CT grade E category, and 80% of them had gland necrosis. In this study, the patient had 10% morbidity and no mortality. The plain film radiography and ultrasonography findings were also shown.

CONCLUSION

CECT provides excellent anatomic, morphologic representation of the pancreas and peripancreatic tissue. The patient who were categorized as having pancreatitis in Balthazar's grade E were clinically more severe, had more morbidity and longer hospitalization than the other grades.

¹ Department of Radiology, Srinagarind Hospital, Khon Kaen University, Khon Kaen Province, Thailand.

² Department of Surgery, Srinagarind Hospital, Khon Kaen University, Khon Kaen Province, Thailand.

Correspondent. Kanjana Leelalawan, M.D. Department of Radiology, Srinagarind Hospital, Khon Kaen University Maung, Khon Kaen Province 40002 THAILAND Telephone, Fax 66-43-348389

INTRODUCTION

Previous reports^{1,2} in the literatures showed that severe pancreatitis was missed in 30 to 40 percent of the patients if based on the clinical and laboratory data. In the remaining cases, the disease was diagnosed at the time of laparotomy or at postmortem examination.

The most common etiologies of acute pancreatitis are heavy alcohol abuse and cholelithiasis. The pathophysiology is controversial but appears to be related to a temporary or permanent blockage of the pancreatic duct leading to a sudden release of enzymes into the adjacent interstitial tissue. Alcohol has a toxic effect and chemical alteration of the exocrine secretion with the development of protein precipitates within the pancreatic ducts. The activated enzymes lead to autodigestive fat necrosis and nonspecific inflammation of the pancreas and peripancreatic tissues.

Acute pancreatitis has been conveniently classified into acute interstitial (edematous) and acute hemorrhagic or necrotizing pancreatitis. Acute edematous pancreatitis is a mild, self-limiting disease while the necrotizing variety is a severe, life-threatening condition associated with frequent complications and high mortality.³

A careful history taking and physical examination will often raise clinical suspicion of acute pancreatitis in the differential diagnosis of a patient presenting with acute abdominal pain. Accurate diagnosis including the extent of disease is needed for appropriate management.

The aim of CT scan in patients with acute pancreatitis is not to make a diagnosis, as this can usually be done on the basis of clinical findings, laboratory data, and more simple imaging methods such as ultrasonography and plain film radiography, but rather to predict its complications.

The CT scanning can accurately confirm and offer excellent anatomic and morphologic representation of the pancreas and peripancreatic tissue.

Balthazar et al.⁴ noted that a grading system of abdominal CT scan obtained early in the course of acute pancreatitis has considerable predictive value in identifying patients at high risk of developing serious complication.

The purpose of this study was to evaluate the prognostic value of CECT in acute pancreatitis and correlate it with the clinical severity and complication as proposed by Ranson. Other signs on conventional radiography and sonography were also evaluated.

MATERIALS AND METHODS

The CECT of the pancreas in 20 patients with clinical diagnosis of acute pancreatitis at Srinagarind hospital, Khon Kaen University between January 1993 – January 1999, were reviewed.

The diagnosis of acute pancreatitis was based on the history and clinical findings such as abdominal pain penetrating to the back, nausea and vomiting, abdominal tenderness and guarding, and high level serum and/or urine amylase.

The severity of pancreatitis was graded using Ranson's prognostic sign (Table 1): 0 to 2 positive signs; 3 to 4 positive signs; 5 to 6 positive signs; and 7 or more positive signs.

A dynamic CT scan was performed after a bolus injection of 100 ml, 300% contrast medium, using GE 9800 scanner or a spiral CT (Toshiba Exvission) taken at 60 seconds after initiation of injection of the contrast medium by mechanical

injector at the rate of 3 cc/sec.

CECT grade, degree of necrosis and severity index (Balthazar's criteria) (Table 2) were determined.

The patients included 14 men and 6 women with a mean age of 41.6 years, range from 23 – 76 years. The mean age of men and women are 38.24, and 49.37 years respectively.

The etiology of acute pancreatitis was chronic alcohol abuse in 14 patients, obstructive jaundice in 2, cholelithiasis in 1, DM in 1, post ERCP in 1, and miscellaneous in 2 patients.

Ranson's prognostic signs, duration of hospitalization, morbidity, mortality and etiology were analyzed.

RESULTS

CLINICAL COURSE

Nineteen patients recovered and were discharged from the hospital without local pancreatic complications requiring surgery. Pancreatic pseudocyst developed in 4 patients, (20%). One of them had persistent pancreatic pseudocyst that required operation. Pancreatic abscess occurred in one patient (5%) which improved by conservative treatment. The diagnosis in this patient was the presence of gas bubble in the collection and the small bowel study excluded a fistula to the gastrointestinal tract.

CECT AND CLINICAL COURSE

The relationship between the CECT grading, CT severity index (CTSI) and clinical course is shown in Table 3 and 4 respectively. There were pancreatitis grade A in 1 patient; grade B, 2 patients; grade D, 6 patients; grade E, 11 patients. No patient was classified as grade C. In

grade E pancreatitis, the average hospital stay was 11.32 days while grade A, B and D were 7, 7.5 and 7.3 days respectively. Six patients with CT grade E had pancreatic necrosis. Four of them (66.66%) had gland necrosis less than 30% and 2 patients (33.33%) had gland necrosis more than 50%. The mean duration of hospitalization in patients with CTSI 0-3, 4-6 and 7-10 were 5.88, 12.22 and 11.5 days respectively.

CT AND PROGNOSTIC SIGNS.

The Ranson's early objective prognostic signs were evaluated in 17 patients. The severity of pancreatitis was graded by prognostic signs as 0-2 signs in 12 patients (70.58%), 3-4 signs in 3 patients (17.64%), 5-6 signs in 1 patient (5.88%), 7 or more signs in 1 patient (5.88%). The occurrence of local pancreatic complications related to the CECT grading and number of prognostic sign was shown in Table 5. Four of five patients (80%) who had 3 or more prognostic signs had pancreatic necrosis, were in CT grade E category. Pancreatic abscess developed in the patient who had 7 prognostic sign. The abscess was detected after the patient was discharged for 28 days. The relationship between Ranson's prognostic signs and clinical course was shown in table 6. The mean duration of hospitalization in the patients with 0-2, 3-4, 5-6, and 7 or more prognostic signs were 7.75, 14, 10, 15 days respectively.

In this study, the patients had 10% morbidity and no mortality.

The findings on plain film radiography and ultrasonography are shown in Table 7 and 8.

Table 1. Ranson's early objective prognostic signs.

Admission diagnosis	During initial 48 hours
Age > 55 years	Hematocrit falls greater than 10 % points
White blood cell count >16,000/mm ³	Blood urea nitrogen rise > 5 mg/100 ml
Blood glucose > 200 mg/ml	Serum calcium level < 8 mg/100 ml
Serum lactic dehydrogenase > 350 IU/L	Arterial pO ₂ < 60 mm Hg
Serum glutamic oxaloacetic Transaminase > 250 IU/100ml	Base deficit greater than 4 mEq/L
	Estimated fluid sequestration > 6 L

Table 2. Balthazar's CECT grading and scoring system.

CT grade	Score	Definition
A	0	Normal pancreas
B	1	Focal or diffuse pancreatic enlargement/ heterogeneity
C	2	Intrinsic pancreatic abnormality/ haziness/ streaky in peripancreatic fat
D	3	Single, ill-defined fluid collection
E	4	Two or multiple ill-defined fluid collection or pancreatic or or peripancreatic or peripancreatic gas
Gland Necrosis %	Necrotic score	Definition
None	0	Uniform pancreatic enhancement
< 30	2	Non-enhancement of region(s) of gland equivalent in size to the pancreatic head
30-50	4	Non-enhancement of 30% to 50% of the gland
> 50	6	Non-enhancement of over 50% of the gland

Severity index = grade score + necrotic score

Table 3. Relationship between CECT grading and clinical course

CT grade	Number of Patient (%) (n=20)	Mean hospital stay (days)	Abscess (%)	Pseudocyst (%)
A	1 (5)	7	0	0
B	2 (10)	7.5	0	0
C	0 (0)	-	0	0
D	6 (30)	7.3	0	0
E	11 (55)	11.32	1 (5)	4 (20)

Table 4. Relationship between CTSI and clinical course

CTSI	Number of Patient (%) (n=20)	Mean hospital stay (days)	Abscess (%)	Pseudocyst (%)
0-3	9 (45)	5.88	0	0
4-6	9 (45)	12.22	1 (5)	3 (15)
7-10	2 (10)	11.5	0	1 (5)

Table 5. The occurrence of local pancreatic complication related to the initial CT findings and number of positive prognostic signs.

CT Grade	Positive prognostic signs									
	0	1	2	3	4	5	6	7	8	*
A	0									
B	00									
C	00	0	0							00
D	PP	PN0		0nn		P+N		A+n		n

0 = no complication; P = pancreatic pseudocyst; A = pancreatic abscess;

n = pancreatic necrosis < 30%; N = pancreatic necrosis > 50%

* = Ranson's prognostic signs were not available to evaluated.

Table 6. Relationship between prognostic signs and clinical course

Ranson's score	Number of Patient (%) (n = 17)	Mean hospital stay (days)	Abscess (%)	Pseudocyst (%)
0-2	12 (70.58)	7.75	0	2 (11.76)
3-4	3 (17.64)	14	0	2 (11.76)
5-6	1 (5.88)	10	0	0
7 or more	1 (5.88)	15	1 (5.88)	0

Table 7. Radiographic findings

Plain films	No of patient (%) (n = 18)
Normal	5 (27.78)
Bowel ileus	4 (22.22)
Pleural effusion (bilateral) (left)	3 (16.67) 1 (5.56)
Widening of gastrocolic space	4 (22.22)
Colon cut off	3 (16.67)
Pancreatic calcification	2 (11.11)
Gassless abdomen	1 (5.56)
Gastric distention	1 (5.56)

Table 8. Ultrasound pattern

Ultrasound pattern	No of patient (%) n = 15
Normal finding	6 (40)
Inhomogenous hypoechoic of the pancreas	5 (33.33)
Fluid collection	5 (33.33)
Enlarged pancreas	4 (26.67)
Pancrease was obscured by bowel gas	2 (13.33)

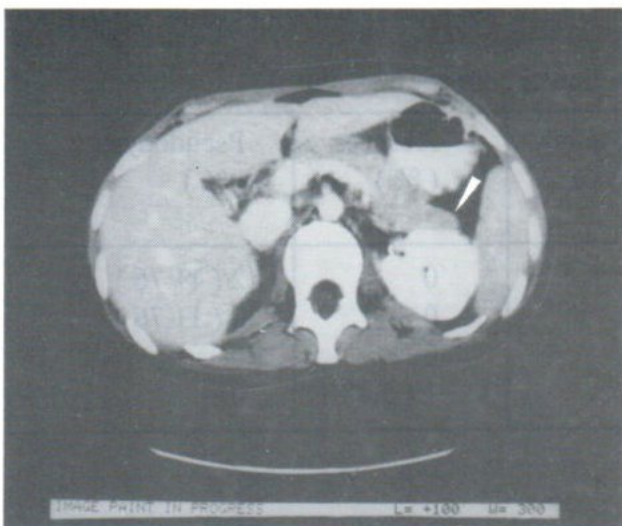


Fig. 1. CT study demonstrating a normal pancreas in a patient with clinical pancreatitis (grade A).

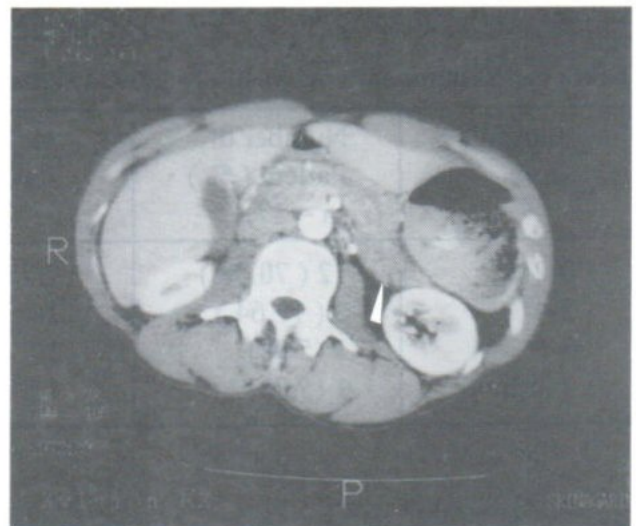


Fig. 2. CT study showing diffuse enlargement of the pancreas without peripancreatic inflammatory changes or fluid collection (grade B).



Fig. 3. CT study of a patient with pancreatitis showing fluid collection (arrow) in the left anterior pararenal space (grade D). Associated fatty liver is noted.

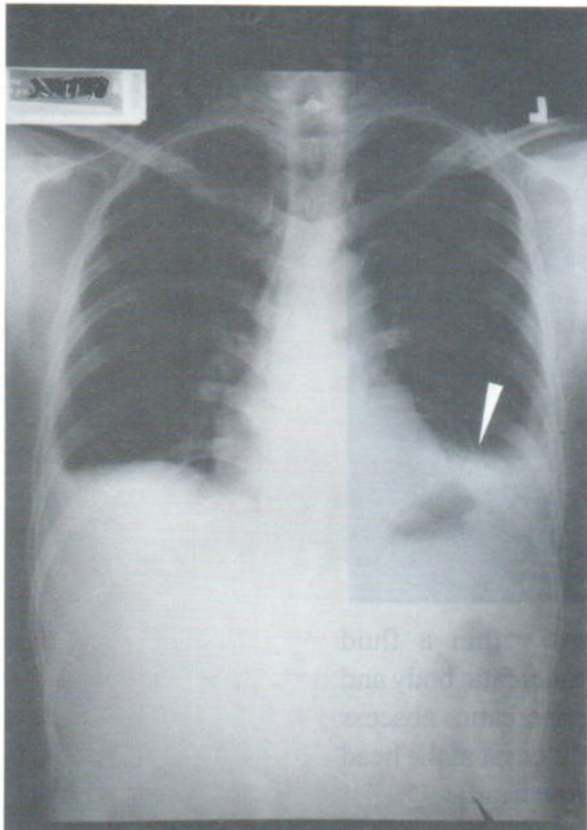


Fig. 4A. Conventional chest film shows left pleural effusion.

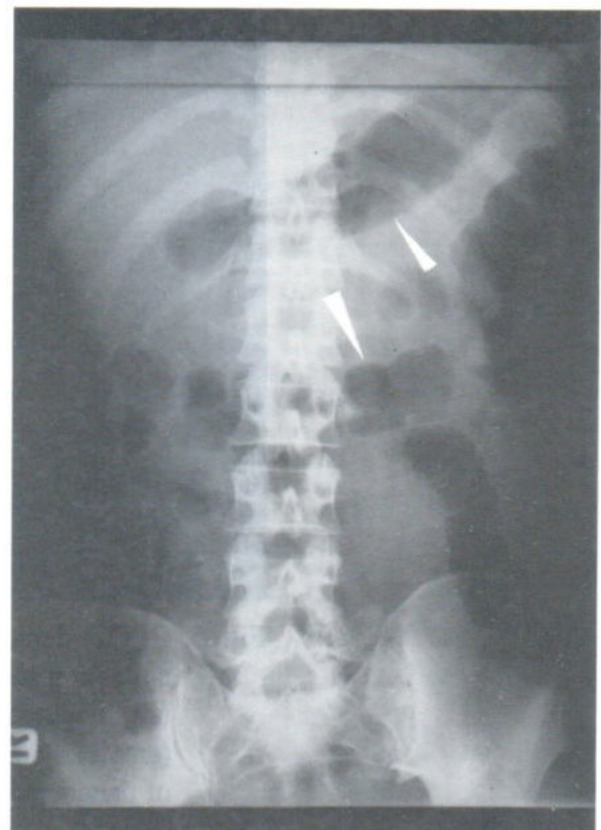


Fig. 4B. Conventional radiograph of the abdomen shows widening of gastrocolic space.



Fig. 4C. Axial sonogram shows diffuse enlargement of the pancreas with inhomogeneous decrease parenchymal echo pattern.

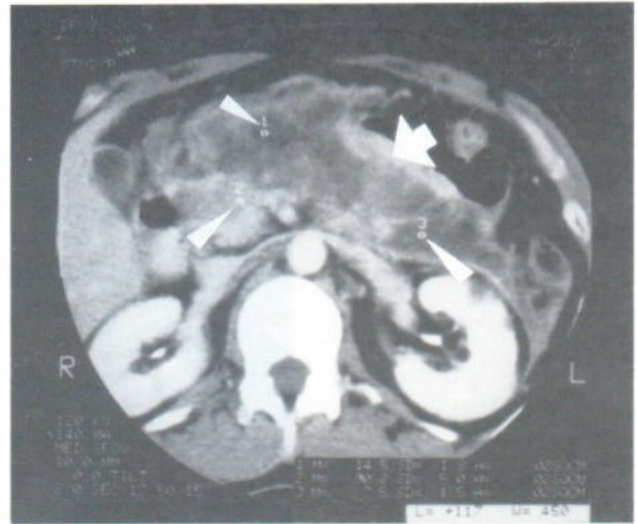


Fig. 4D. CECT demonstrate diffuse enlargement of the pancreas with area of decreased enhancement at body and tail (arrow) (grade E with pancreatic necrosis >50%)

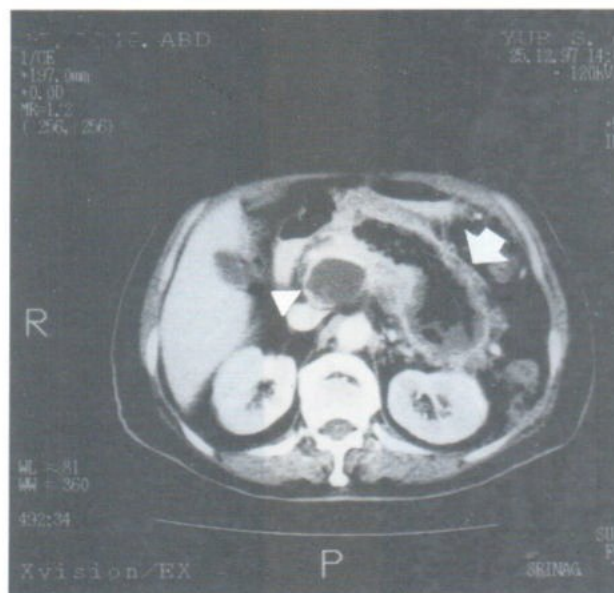


Fig. 5. CECT demonstrate gas within a fluid collection at region of pancreatic body and tail, suggestion for pancreatic abscess (arrow). Pancreatic pseudocyst at the head of pancreas is note (arrow head).

DISCUSSION

In this study, 55% of the patients was classified as pancreatitis grade E. However, since pancreatitis is a clinical diagnosis, only the severe cases were investigated by CT scan.

The reported success of ultrasonography in demonstrating the pancreas in patients with acute pancreatitis is as high as 74.5%.⁵ However, gas-filled loop of bowel may obscure the pancreas from full ultrasonographic evaluation. A comparison between ultrasonography and computed tomography⁶ in patients with pancreatitis have shown that CT scan is significantly more accurate in this setting.

Potential roles for CT evaluation in patients with acute pancreatitis are : 1) to confirm or refute the clinical diagnosis of pancreatitis; 2) to identify early in their course the patients with a high risk of local complication; 3) to diagnose the occurrence of local complications.

A spectrum of morphologic changes on CECT, depends on the severity of the inflammatory process. Balthazar et al.⁷ have categorized this spectrum into five grades: grade A- normal pancreas; grade B- pancreatic enlargement; grade C- gland enlargement and peripancreatic soft tissue inflammatory changes; grade D- enlarged gland, peripancreatic inflammatory changes and single peripancreatic fluid collection; and grade E- two or multiple fluid collections or the presence of gas in or adjacent to the pancreas (abscess formation).

For disease staging, the presence of gland necrosis is important. Bradley et al.⁸ and Johnson et al.⁹ found that pancreatic necrosis can be detected by dynamic CT as a focal or diffuse area of diminished parenchymal contrast enhancement.

Balthazar et al.⁴ have combined the CT-based staging of acute pancreatitis with the

presence of necrosis to generate the CT severity index. Patients with a high CTSI had 92% morbidity and 17% mortality; patients with a low CTSI had 2% morbidity and no mortality.

Ranson et al.¹⁰ conducted a prospective study and found that increasing number of Ranson's prognostic signs correlates significantly with the more severe form of pancreatitis. The mortality associated with 0-2 prognostic signs is less than 1%, 3-4 prognostic signs = 16%; 5-6 signs = 40%; and 7 signs or more = 100%.

These indicators have prognostic importance. They help to identify a subgroup of patients at risk of increased morbidity and mortality, who should be targeted for more drastic and specific therapeutic measures.

Balthazar et al.⁴ found the relationship between prognostic signs and severity of pancreatitis. Increased CT grade score correlated with the increasing number of prognostic signs. Infected abscess occurred with an increased incidence in patients with several prognostic signs.

Ranson et al.¹¹ noted that the radiographic detection of gas within a fluid collection may be an extremely valuable sign of infection. While this finding can be due to communication of the fluid collection with the gastrointestinal tract. Gas was present in 22% in his series at the time of diagnosis of pancreatic abscess. The incidence of pancreatic abscess increased with increasing clinical severity.

In Varnacchia's study¹², no clear prognostic value of CTSI in predicting pancreatic abscess was demonstrated on the baseline CT scan in his patient's population.

One of our patients who was categorized

as severe (7 or more prognostic signs) according to Ranson's prognostic sign developed pancreatic abscess. However, the number is limited, no conclusion could be drawn.

CONCLUSION

CECT severity staging correlates favorably with the severity of clinical signs. The patients who were categorized clinically as having 3 or more prognostic signs were in CT grade E category, and highly correlated to gland necrosis. CECT also offers excellent anatomic, morphologic representation of the pancreas and peripancreatic tissue. Pancreatitis in Balthazar grade E had higher morbidity, requires longer hospitalization than the other grades.

REFERENCE

1. Peterson LM, Brooks JR. Lethal pancreatitis, a diagnostic dilemma. *Am J Surg* 1979;137:491-496
2. Trapnell J. The natural history and management of acute pancreatitis. *Clin Gastroenterol* 1972;1:147-166
3. Balthazar EJ. CT diagnosis and staging of acute pancreatitis. *Radiol Clin North Am* 1989;27:19-37
4. Balthazar EJ, Robinson DL, Megibow AJ, Ranson JHC. Acute pancreatitis: Value of CT in establishing prognosis. *Radiology* 1990;174:331-336
5. McKay AJ, Jmrie CW, O'neill J, Duncan JG. Is an early ultrasound scan of value in acute pancreatitis? *Br J Surg* 1982;69:369-372
6. William S, Michael BI, Michael CH, Jamie B. Diagnostic imaging of acute pancreatitis: Prospective study using CT and sonography. *AJR* 1981;137:497-502
7. Balthazar EJ, Ranson JHC, Naidich DD, et al. Acute pancreatitis: prognostic value of CT. *Radiology* 1985;156:767-772
8. Bradley EL, Murphy F, Ferguson C. Prediction of pancreatic necrosis by dynamic pancreatography. *Ann Surg* 1989; 210:495-503
9. Johnson CD, Stephens DH, Sarr MG. CT of acute pancreatitis: Correlation between lack of contrast enhancement and pancreatic necrosis. *AJR* 1991;156:93-95
10. Ranson JHC. Etiological and prognostic factors in human acute pancreatitis: a review. *Am J Gastroenterol* 1982;77:633-638
11. Ranson JHC, Balthazar EJ, Caccavale R, Cooper M. Computed tomography and the prediction of pancreatic abscess in acute pancreatitis. *Ann Surg* 1985;201:656-665
12. Vernacchia FS, Jeffrey RB, Federle MP, et al. Pancreatic abscess: Predictive value of early abdominal CT. *Radiology* 1987; 162:435-438

PATTERN OF RADIATION THERAPY IN THE TREATMENT OF PEDIATRIC BRAIN TUMORS IN SIRIRAJ HOSPITAL

Nan SUNTORNPONG, M.D.
Supatra SANGRUCHI, M.D.

ABSTRACT

A retrospective study was performed to review the management by radiation therapy (RT) for several types of pediatric brain tumors in a single institution. Of seventy-three children treated at Division of Radiation Oncology, Department of Radiology, Siriraj Faculty of Medicine from January 1990 to August 1999, 9 were equal to or younger than 3 years. The most common pathology was medulloblastoma. The modalities of treatment and the techniques of RT depend on age, pathology and location of tumors with 50% of brain stem tumors and 41% of pineal region tumors were irradiated without tissue diagnosis.

INTRODUCTION

Brain tumors constitute the most common solid neoplasms in childhood.^{1,2} These consist of several histological types and location of lesions with different frequency of individual groups from those in adults. The common types of tumors in children are low-grade glioma and primitive neuroectodermal tumor (medulloblastoma). Approximately 50% of brain tumors in children more than 1 year old develop infratentorially. Due to the diversity of these diseases and age-influenced therapeutic modalities especially in radiation therapy (RT), this study was performed to review the conventional management and present some recent approach in RT for individual types of brain tumors in a single institution.

METHODS & MATERIALS

The pediatric patients with brain tumor treated with RT at Division of Radiation Oncology, Department of Radiology, Siriraj Hospital from January 1990 to August 1999 were eligible for this study. All available treatment records were reviewed to collect for the patient characteristics, histopathology of primary tumors, modalities of treatment and techniques of RT.

RESULTS

The total number of patients in this study was 73, of which 9 were equal to or younger than 3 years. The number of patients distributed by age and histopathology of primary tumor according to the World Health Organization classification⁽³⁾ is shown in Table 1.

Table 1 The number of patients distributed by age and pathology of primary tumor

Characteristics	Number of patients
Age : <= 3 years	9
>3 years	64
Pathology: Astrocytoma Grade I	6
Grade II	6
Anaplastic astrocytoma	3
Glioblastoma multiforme	4
Medulloblastoma	16
Ependymoma Low grade	2
High grade	2
Germ cell tumor: Germinoma	9
Nongerminoma	4
Primitive neuroectodermal tumor	2
Craniopharyngioma	1
Choroid plexus papilloma	1
Unknown	17

The median age at diagnosis was 9 years (range 1/3 to 15 years). The most common pathology in this study was medulloblastoma. The tissue diagnosis cannot be obtained from certain location including brain stem lesions in 7, pineal region lesions in 9 and posterior fossa lesion in

1 infant.

The treatment for these tumors depended on location and pathology of tumors. The modalities of treatment are summarized in Table 2.

Table 2 The modalities of treatment for primary tumors

Pathology	Number of patients			
	Sx+RT	Sx+RT+CT	CT+RT	RTalone
Astrocytoma Grade I	4			2
Grade II	1			5
Anaplastic astrocytoma	2			1
Glioblastoma multiforme	4			
Medulloblastoma	14	2		
Ependymoma Low grade	2			
High grade	1	1		
Germ cell tumor: Germinoma	9			
Nongerminoma	2	2		
Primitive neuroectodermal tumor	2			
Craniopharyngioma	1			
Choroid plexus papilloma	1			
Unknown			1	16

Of 14 patients who were diagnosed of brain stem tumor, all were treated by RT alone except one with partial removal prior to RT. Of 7 (50%)

patients who were biopsied for tissue diagnosis, the distribution of pathologic results in brain stem tumors is shown in Table 3.

Table 3 The distribution of pathology in brain stem tumors

Pathology	Number of patients	
	Sx+RT	RT alone
Astrocytoma Grade I		1
Grade II		4
Anaplastic astrocytoma	1#	1
Glioblastoma multiforme		
Unknown		7

Partial removal of tumor

Of 22 patients with pineal region tumors, 13 (59%) were confirmed for pathology. The

increasing tendency to perform biopsy in the years during this study is shown in Table 4.

Table 4 The tendency to perform biopsy for pineal region tumors by years.

Year	No. of Patients	
	No biopsy performed	Biopsy performed
1990	-	1
1991	2	1
1992	1	1
1993	-	1
1994	3	-
1995	-	-
1996	1	-
1997	1	6
1998	-	2
1999	1	1

The distribution of pathologic subtypes and treatment in germ cell tumors are shown in Table 5.

Table 5 The distribution of pathologic subtypes and treatment in germ cell tumors.

Pathology	Number of patients			
	Sx+ RT	Sx+CT+RT	CT+RT	RT alone
Germinoma	8			1
Nongerminoma	2	2		
Unknown			1	8

One of the patients in this group received chemotherapy prior to RT without tissue diagnosis due to highly increased serum tumor marker.

The technique of RT (volume, total dose for primary tumors) are summarized in Table 6 and Table 7.

Table 6 The volume of RT

Pathology	Number of patients		
	CSI	WB & reduced field	local brain
Astrocytoma: Grade I		4	2
Grade II	1	2	3
Anaplastic astrocytoma		2	1
Glioblastoma multiforme		1	2
Medulloblastoma	16		
Ependymoma : Low grade	1	1	
High grade	2		
Germ cell tumor : Germinoma	5	4	
Nongerminoma	4	1	
Peripheral neuroectodermal tumor	2		
Craniopharyngioma			1
Choroid plexus papilloma	1		
Unknown : at brain stem	1		6
at pineal region	5	4	
posterior fossa	1		

CSI= Craniospinal Irradiation , WB= Whole brain

Table 7 The total RT dose @

Pathology	Number of patients			
	Dose at primary (Gy)		Dose at spine(Gy)	
	<=50	>50	<=30	>30
Astrocytoma : Grade I	5	1		
Grade II	2	3		1
Anaplastic astrocytoma	1	2		
Glioblastoma multiforme	1	3		
Medulloblastoma	6	7	9	4
Ependymoma : Low grade	1	1		1
High grade	1	1	1	1
Germ cell tumor: Germinoma	7	1	4	1
Nongerminoma	2	3	1	3
Primitive neuroectodermal tumor	1			
Craniopharyngioma		1		
Choroid plexus papilloma				
Unknown: at brain stem	5	2	1	
at pineal region	5	1	1	2
at posterior fossa	1		1	

@ Exclude 9 patients with incomplete RT .

DISCUSSION

Brain tumors represent the most common solid neoplasm in children treated each year at Siriraj Hospital.⁴ The modalities of treatment depend on age at diagnosis, location and pathology of the tumor. Surgery has been traditionally used as the definitive diagnosis and initial therapeutic intervention except for unresectable tumors. The extent of resection is also clearly associated with the outcome for several types of brain tumors in children.⁵ RT is acceptable modality as an adjuvant postoperative or definitive treatment in unresectable or inoperable cases.

The patients younger than 3 years account for 12.3 % of all children in this study. The current therapeutic strategies in this group differ from those in older children. In addition to the higher rate of surgical morbidity, RT has consistently been

associated with severe neuropsychological sequences in developing nervous system.⁶⁻⁸ The chemotherapy has been investigated to be primary or primary postoperative treatment to delay, diminish or omit RT.⁹ However, morbidity from chemotherapy alone was also reported in young children.¹⁰

For the lesions with high risk of open biopsy or resection such as brain stem or pineal region tumors, RT alone has been the alternative treatment without tissue diagnosis. However, a variety of new techniques such as CT- or MRI-guided stereotactic biopsy can manipulate this problem at present.

Of all 13 patients with brain stem tumors in this study, almost 50% were treated without

tissue diagnosis. The total dose to primary tumors varied from 40 to 56 Gy due to certain factors such as performance status of patients, volume and location of tumor and imaging characteristics. The distinction between subtypes and grading of brain stem gliomas can be apparent on magnetic resonance imaging (MRI). The subtypes classified by imaging findings consist of focal, dorsal exophytic, cervicomedullary and diffuse intrinsic tumors.¹¹ For the patients to whom biopsy can be accomplished safely, complete resection was not recommended in some cases. The hyperfractionated RT has not been performed in any patient with brain stem tumor in this study due to lack of significant benefit. Pediatric Oncology Group recently reported the result of phase III trial that hyperfractionated RT neither improved survival nor decreased morbidity of treatment compared to those of conventional RT.¹²

Due to the development of current microsurgical approaches, the treatment for pineal region tumors also has been changed. The tissue diagnosis and total resection should be obtained when possible to differentiate the radioresistant or RT not-required tumors such as teratoma. All except 1 patient in this study were biopsied after 1993. The delivery of test dose RT as primary treatment to rule out germinoma from other germ cell tumors has a tendency to markedly decrease at present.

In addition to treatment for the patients with existing neuraxis dissemination detected by MRI and/or cerebrospinal fluid cytology, the prophylactic RT to the entire craniospinal axis is demanded in certain tumors with striking propensity to spread throughout cerebrospinal fluid. These consist of high grade medulloblastoma, high grade ependymoma, pineoblastoma, germinoma, malignant germ cell tumor and primitive neuroectodermal tumor.¹³⁻¹⁶ The other 2 patients in this study diagnosed with subependymal giant cell astrocytoma and choroid plexus papilloma

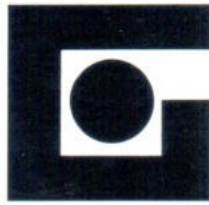
also received craniospinal irradiation due to ventricular involvement.

The recommended total dose by conventional RT to primary brain tumors in childhood varies from 45 to 60 Gy depended mainly on pathology and location. The reduced volume of RT to primary tumor only is required during the treatment course because diffuse white matter change and intellectual decline can be apparent following full brain dose of 30–35 Gy.^{17,18} Concerns in morbidity should be more emphasized in certain types of tumor which required combined RT with chemotherapy.^{19,20}

REFERENCES

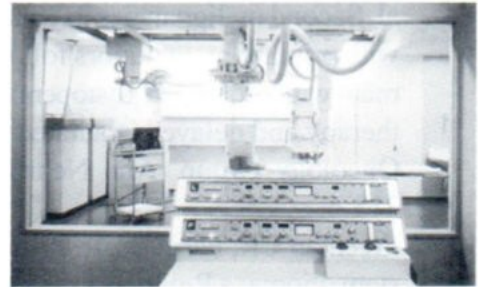
1. Pollack IF. Brain tumors in children. *N Eng J Med* 1994;331: 1500-07.
2. Young JL. Cancer incidence, survival and mortality for children younger than 15 years. *Cancer* 1986;58: 561-68.
3. Central Nervous System. In : von Essen CF, Nair MK, eds. *Radiotherapy in Cancer Management : A Practical Manual*. Chapman & Hall Medical, London 1997: 229-49.
4. Tumor Registry. Siriraj Cancer Center. Statistical report 1998. Faculty of Mahidol Siriraj Hospital
5. Pollack IF. Treatment approaches for pediatric gliomas. In: Perry MC, ed. *American Society of Clinical Oncology Educational Book* 1999: 1987-94.
6. Kun LE. Brain tumor in infants and young children In: Perry MC, ed. *American Society of Clinical Oncology Educational Book* 1999: 574-77.
7. Jenkin D, Danjoux C, Greenberg M. Subsequent quality of life for children irradiated for a brain tumor before age 4 years. *Med Pediatr Oncol* 1998;31:506-11.

8. Kun LE. Brain tumors: Challenges and directions. *Pediatr Clin North Am* 1997; 44:907-17.
9. Castello MA, Schiavetti A, Varrasso G et al. Chemotherapy in low grade astrocytoma management. *Childs Nerv Syst* 1998; 14:6-9.
10. Duffner PK, Krischer JP, Horowitz ME et al. Second malignancies in young children with primary brain tumors following treatment with prolonged postoperative chemotherapy and delayed irradiated a Pediatric Oncology Group. *Ann Neurol* 1998;44: 313-6.
11. Freeman CR, Farmer JP. Pediatric brain stem glioma: a Review . *Int J Radiat Oncol Biol Phy* 1998;40: 265-71.
12. Mandell LR, Kadota R, Freeman CR et al. There is no role for hyperfractionated radiotherapy in the management of children with newly diagnosed diffuse intrinsic brain stem tumors: results of a Pediatric Oncology Group phase III trial comparing conventional VS hyperfractionated RT. *Int J Radiat Oncol Biol Phy* 1999; 43: 959-64.
13. Prados MD, Edwards MS, Chang SM et al. Hyperfractionated craniospinal radiation therapy for primitive neuroectodermal tumor: results of a phase II study. *Int J Radiat Oncol Biol Phys* 1999;43:279-85.
14. Schild SE, Nisi K, Scheithauer BW et al. The results of radiotherapy for ependymomas: the Mayo Clinic experience. *Int J Radiat Oncol Biol Phys* 1998; 42: 953-8.
15. McLaughlin MP, Marcus RB Jr, Buati JM et al. Ependymoma: Results, prognostic factor and treatment recommendations. *Int J Radiat Oncol Biol Phys* 1998;40:45-50.
16. Aoyama H, Shirato H, Yoshida H et al. Retrospective multiinstitutional study of radiotherapy for intracranial nongerminoma germ cell tumors. *Radiother Oncol* 1998; 49: 55-9.
17. Schultheiss TE, Kun LE, Ang KK et al. Radiation response of the central nervous system. *Int J Radiat Oncol Biol Phys* 1995; 31:1093-1112.
18. Packer RJ, Zimmerman RS, Bilaniuk LT. Magnetic resonance imaging in the evaluation of treatment related central nervous system damage. *Cancer* 1986;58: 635-40.
19. Reddy AT, Packer RJ. Pediatric central nervous system tumors. *Curr Opinion Oncol* 1998; 10: 186-93.
20. Fauladi M, Grant R, Barachel S et al. Comparison of survival outcome in patients with intracranial germinoma treated with radiation alone versus reduced-dose radiation and chemotherapy. *Childs Nerv Syst* 1998; 14: 596-601.



Nippon Electric Glass Co., Ltd. Radiation Shielding Lead Glass

- Observation window for CT scanning room
- Observation window for angiography room
- Observation window for X-ray diagnosis room



จำหน่าย กระจกตะกั่วกันรังสี แผ่นตะกั่วเรียบหนา 1 มม.-
10 มม. รับกรุแผ่นตะกั่วที่ผนังห้องเอกซเรย์ รับทำบาน
ประตูไม้อัด ประตูเหล็กบุแผ่นตะกั่ว ยินดีให้คำชี้แนะ

สอบถามได้ที่

ผู้แทนจำหน่ายในประเทศไทย

ห้างหุ้นส่วนจำกัด วิมิตรกิจ เอ็นจิเนียริง
VIMITKIJ ENGINEERING LTD., PART.

42 ซอย 96/3 ถ.จรัญสนิทวงศ์ บางอ้อ เขตบางพลัด กทม. 10700
42 CHARANSANITWONG 96/3, BANG-AW, BANGPLAT, BANGKOK 10700

 (02) 424-9775, 424-1009, 424-0977

FAX : 435-7870, 424-1009

E-mail : napana@access.inet.co.th

QUALITY ASSURANCE IN NUCLEAR MEDICINE IMAGING

Anchali KRISANACHINDA, Ph.D.

INTRODUCTION

Nuclear medicine uses tracers, tiny amounts of radioactive substances, to diagnose or treat the disease. These substances pass harmlessly through the body. As they are radioactive, their movement can be detected with special devices, yielding a wealth of information about bodily processes. The essence of nuclear medicine is that it can visualize changes in the function and biochemistry of body organs and tissues. Measurement of such changes offer unique information for diagnosis and therapy that can't be obtained through other tests. One of the great benefits of nuclear medicine is that regional abnormalities in the body often can be detected before an abnormality is noted in overall organ function, before the patient feels something is wrong. Similarly, regional chemical changes can be measured before abnormalities can be found in the concentration of chemical constituents in blood or urine. Early detection allows a disease to be treated before it becomes advanced, when these are generally a better outcome.

The technology for detecting radiotracers in the body advanced rapidly. In 1957, a Geiger Muller counter was used to discriminate hot and cold thyroid nodule, which helped to decide the likelihood that the nodule was benign or malignant. Later the motor-driven scintillation detector was designed by Benedict Cassen to produce images of distribution of radioactivity from thyroid gland. One year later, in 1958, Hal O. Anger invented the scintillation camera, an imaging device which made it possible to conduct rapid dynamic studies. It also improved static images and, when used with Tc-99m, reduced the radiation dose to the patient. Over the past half-century, radiation detectors have evolved into sophisticated Positron Emission Tomography (PET) and Single Photon Emission Computed Tomography (SPECT) scanners with their associated computer processing and display systems.

QUALITY ASSURANCE AND QUALITY CONTROL: DEFINITIONS

Quality Assurance in diagnostic nuclear medicine has been defined by WHO in 1980 in three objectives as:

1. Improvement in quality of the diagnostic information.
2. Use of the minimum amount of radio-nuclide activity to ensure the production of the

desired diagnostic information.

3. Effective use of available resources.

In Thailand, quality in health care is currently being addressed, followed by the project on Hospital Accreditation which includes the quality standards for hospital services and nuclear

medicine in the near future.

Although formulated differently from different viewpoints, the objectives of the above concern quality assurance leading to **the best care with the least radiation burden to the patient.** A quality assurance program that meet these objectives covers the total diagnostic process from the request to perform the procedure to the report and follow-up. These include nuclear medicine service, organization, facilities, staffing, radio-pharmaceuticals, instrumentation, pro-cedure, evaluation of results and training.

Quality Control in nuclear medicine started in 1977 and covered wider issues and human aspects of quality assurance. (Rhodes 1977).¹ Various organizations such as American Association of Physicists in Medicine (AAPM), Hospital Physicist's Association UK (HPA) the International Atomic Energy Agency (IAEA)² the World Health organization (WHO)³ had prepared the recommendation for quality control procedures of imaging devices. Recommendations were made for quality control of all nuclear medicine instrumentation.

Quality control testing falls into three basic levels

ACCEPTANCE TESTING

The first, crucial step in quality control of an instrument is the initial evaluation or acceptance testing. Acceptance testing means not only confirming that the instrument performs according to specifications, but also means evaluation performance under conditions that will be encountered in clinical practice. Manufacturer's specifications only provide a few essential performance characteristics, so that a full set of acceptance tests, covering the range of clinical needs, has to be developed. The users should not accept an instrument that fails to conform to specifications. An

instrument that fails to operate correctly at installation has a great likelihood of never being satisfactory. Acceptance testing should be carried out before the instrument is put into clinical use.

Acceptance tests can be difficult especially for an inexperienced user. A user may be confronted with unfamiliar instruments and computer software. Special test devices or phantoms are needed. Quantitative studies are essential in order to compare results with specifications and to provide baseline values for future comparison. It is recommended that the acceptance tests should be performed by the user and the representative of the vendor. If there is only inexperience, then employ an experienced, qualified consultant to assist with the tests.

REFERENCE TESTING

A reference test is a test of an instrument whose results proved a measure against which future performance of an instrument may be comprehensively assessed. (WHO 1982).³ The tests may be identical to acceptance testing, or may be simplified versions. These reference tests form part of the initial testing program. There after they form periodic tests to be made if malfunction is suspected, after a major failure has been repaired, after component replacement, and after an instrument is moved to another site. Since they are made periodically, exact details of the test need to be documented along with the results, so that the test can be reproduced and results compared with the previous results.

ROUTINE TESTING

The purpose of the routine test is to assure that a level of quality is maintained and to determine deterioration with time. An instrument may fail or perform malfunction at any moment, but routine test supplies a degree of confidence in the instrument performance up to the last routine

test performed and assessed. Routine testing should be simple, test of the total system, be sensitive to small changes in component performance, and not be time consuming. Not only is a comparison of results with previous test but also a comparison of results obtained over a period of weeks. Subtle changes can occur which may only become evident by such comparisons.

Quality control is, however, not the actual act of doing the test, but the immediate evaluation and action upon its result. The most important aspect of routine testing is that it does not just become daily exercise, the results of which are stored away unheeded.

RECORD /LOG BOOK

Assurance of quality requires that a record or logbook be started at installation to document the history of an instrument. This record may be the only means of following recurring malfunction, obtaining maintenance satisfaction or providing commencing evidence of the need for component replacement. Such a record ideally includes:

- Details of problems and their solutions.
- Environmental and operational conditions at the time of malfunction
- Service response time
- Details of service carried out
- Maintenance reports and reference test results.

This log should also record whether a patient's nuclear medicine study showed artifacts, was compromised, could not be completed, or could not be started due to the instrument failure.

ACTION THRESHOLDS

The final stages of any quality control are the decision-making and follow-up processes, which determine whether or not the instrument is

functioning properly and can be used, or whether it needs repaired. For the evaluation to serve its purpose, objective quality control assessment and limits of acceptability that provide action thresholds are required. This implies objective comparison of quality control test results with reference standards that represent optimum performance. Prior knowledge is required of what is optimum, what is measurable, and how much deterioration from optimum is acceptable for the completion of the clinical procedures. The latter is, perhaps, the most illusive part of quality control: when does deterioration in instrument performance lead to clinically misleading results?

INTERLABORATORY COMPARISON STUDIES

One way to assess the quality of the clinical use of imaging instrument is through interlaboratory comparison studies, using hardware or software phantoms. This is a quality control method that permits assessment of the total imaging performance on a national or international level. The laboratory measures or images the phantom using its usual clinical method, evaluated and reports its results. In this way the instruments as well as the persons performed the test and those evaluation results are tested. Comparison of an individual's results with those from others and feedback of individual performance enables a laboratory to reappraise and improve its performance.

QUALITY ASSURANCE OF NUCLEAR MEDICINE SOFTWARE

Software quality control monitors programs at installation, after program modification, after system modification and in case of suspected failure. For testing a particular clinical software package, clinically validated patient studies are needed. These enable comparison of results from different computers and algorithms,

definition of radionuclide patterns and quantitative parameters for normal function and typical disorders. Such clinical studies are "Software Phantoms".⁴ Phantoms could also consist of mathematics simulations and data acquired from hardware phantoms that simulate clinical data. However, real patient studies are essential because they provide authentic data and read biological variation that the software will encounter in practice.

HOSPITAL ACCREDITATION

Quality Assurance of nuclear medicine imaging is only a small part of the broader quality assurance objectives. In order to implement a total quality assurance program, quality standards for the whole service must be defined. Accreditation is then a means of recognizing compliance with the quality standards. For nuclear medicine, these quality standards apply to organization structure, staffing, facilities, purchase and storage of materials, radiopharmaceuticals preparation, quality control and servicing of equipment, all activities concerning a patient study, personnel training and quality assurance evaluation.

CONCLUSION

Quality assurance has until now been

voluntary, but legislation is imminent. Each person and each aspect of the service contributes to the quality of the patient care provided by a department. The radiation protection of the patient is an additional factor, so that the diagnostic information is obtained with the least administered radiation. A wellplanned and performed quality control program for instrumentation and software is just one step towards achieving this. The most essential ingredients are the human aspects, which include continual care, awareness, observation and readiness to act when any deficiency is encountered. To achieve continuous quality improvement, motivation of personnel is perhaps the most vital ingredient of all.

REFERENCES

1. Rhodes BA. Quality control in nuclear medicine. The CV Mosby Company, St Louis, 1997.
2. IAEA Quality control of nuclear medicine instrumentations. IAEA-TECDOC-602 IAEA, Vienna, 1991.
3. WHO. Quality assurance in nuclear medicine. World Health Organization Geneva, 1982.
4. Britton KE, Busemann ES. COST-B2 : Why and wherefore. Euro. J. Nucl. Med. 1992. 19;563-568.

ACCEPTANCE TESTING ON A MULTIPLE-DETECTOR SPECT SYSTEM

Anchali KRISANACHINDA,Ph.D.

ABSTRACT

Single Photon Emission Computed Tomography (SPECT) system is a nuclear medicine imaging device using a rotating scintillation camera and a computer system to acquire, reconstruct and process a patient tomographic images in transverse-axial, coronal and sagittal planes. The system can have one detector or more. The advantage of multiple detectors is the higher sensitivity, shorter time study and the ability to perform more patient studies per day.

Acceptance testing of the SPECT system by the physicist is an important step towards the acquiring of images of the highest possibility quality over the operating life of the instrument. The test should be performed after the system is installed, carefully tuned, clinical operative, and before patient studies are initiated. The major purpose of the acceptance test is to assure the user that the system is performing according with the specifications as quoted by the manufacturer. The National Electrical Manufacturers Association (NEMA) has prepared a protocol detailing test conditions to be used by manufacturers. The document provides specific protocol to measure the performance parameters and traceability from manufacturer to user. Two test methods, performance standards and class standards are measured in the acceptance testing which include the intrinsic and system resolution, spatial linearity, energy resolution, flood field uniformity sensitivity and count rate performance. Furthermore, whole body imaging, multiple window spatial registration (MWSR) must be included that in the acceptance test of single and multiple detectors. SPECT phantom study, will offer the information on the SPECT performance in terms of tomographic uniformity, contrast, resolution and lesion detectability. Images should be compared from each detector and all detectors. Best image quality should be obtained from all detectors.

In this paper, the result of the acceptance test of the triple detector SPECT, TRIAD XLT 20 will be presented. All the results are within acceptable limit under NEMA Standards and manufacturer guidelines. The acceptance testing of a system is a critical step towards the achievement of high quality performance of any damage, deficiencies or flaws before the warranty has expired. No instrument should be put into routine use unless it has been shown through acceptance testing to be performing optimally. An instrument that does not perform correctly at installation has a high likelihood of never doing so.

INTRODUCTION

Single Photon Emission Computed Tomography (SPECT) system is a nuclear medicine imaging device using a rotating scintillation camera and a computer system to acquire, reconstruct and process a patient tomographic images in transverse-axial, coronal and sagittal planes. The system can have one detector or more. Triple detector SPECT system is shown in Figure 1. The advantage of multiple detectors is the higher sensitivity, shorter time study and the ability to perform more patient studied per day.

Acceptance testing of the SPECT system by the physicist is an important step towards the acquiring of images of the highest possible quality over the operating life of the instrument. The test should be performed after the system is installed, carefully tuned, clinical operative, and before patients studied are initiated. The major purpose of the acceptance test is to assure the user that the system is performing in accordance with the specifications as quoted by the manufacturer. This is extremely difficult to do in a rigorous manner. For the most part, the system performance has been measured by the manufacturer under test conditions which are impossible for the user to duplicate. The manufacturer uses specialized equipment and test procedures which are not openly documented and which vary from manufacturer to manufacturer. After the camera has been shipped, performance measurements as initially done in the factory are impossible to repeat as the specialized equipment is not available to field service representatives. Further, many manufacturer's specifications are class standards, indicating that they are not measured on each and every system, and therefore may never have been measured on a given system.

In an effort to encourage more complete and uniform performance specifications, the National Electrical Manufacturers Association¹ (NEMA) has prepared a protocol detailing test conditions to be used by manufacturers. These standards detail the equipment and techniques to be used in measuring a set of performance parameters. The document provides the user with specific protocols to allow them to measure the

same set of performance parameters and thus provide traceability from manufacturer to user. Two types of standard, class standard as defined earlier and performance standards, which represents test measurement specifications that apply to and must be met by every system covered by the specification, are measured in the acceptance testing.

Tomographic techniques are very sensitive to inadequate calibration procedures. In order to ensure artifact free images, the first performance task conducted should be the center of rotation calibration and correction and the uniformity correction. There should be coincidence of both collimator and detector axes of rotation. Separate centers of rotation should be acquired for each detector. In addition, each detector must have its own unique reference flood. The collimators should be uniquely identified so that the reference floods for uniformity correction will be applied to the correct collimator. The acceptance test of a multiple detector system is more critical than a single detector system as it is essential that response of all detectors be matched to each other. All calibration factors and centroid locations should be within 0.5% of each other. Quantitative comparisons should be performed for each detector separately and then after the responses of all detectors have been added together to ensure that the added image has not been degraded. The system sensitivity variation between each detector must not be greater than 5%. SPECT performance study using JASZCZAK phantom filled with Tc-99m solution should be acquired and reconstructed for each detector and for all detectors. Transverse – axial slices from each reconstructed image should be compared which the image contrast should stay the same but the signal-to-noise ratio should improve. Carefully examine the section of solution which represents tomographic uniformity and noise, no ring artifact should be observed in this region. Sphere and rod sections represent tomographic resolution and contrast. The smallest cold sphere of diameter 9.5 mm and at least the 7.9 mm cold rod diameter should be visualized. The collimator hole

angulation measurements² should be added in the SPECT acceptance testing.

LOG BOOK

A permanent record book should be initiated at the time of acceptance testing of a new system. The user should record all available performance data obtained from the manufacturer, the results of the test including the labeled images and all information necessary for the reference test at some later date. Subsequent quality control, component failure and maintenance records should be kept in the same log book.

MATERIAL AND METHOD

Radioactive sources

- Point source Tc-99m, Co-57, Ga-67
- Line source Tc-99m, Co-57
- Flood or sheet source Tc-99m, Co-57, Ga-67

Phantom and accessories

- Jaszczak phantom
- SPECT System Spatial Phantom

- Solid acrylic scatter phantom
- Resolution (Bar) phantom
- Orthogonal Hole Test Pattern (OHTP)
- Useful Field Of View (UFOV) Mask
- Copper Absorber 13 plates 2 mm thick
- Bubble level and level protractor
- Equipment

A triple detector SPECT TRIAD XLT-20, rectangular detectors with useful field of view (UFOV) 18x23", center field of view (CFOV) 15x20" and 3/8" NaI(Tl) crystal thickness, has been tested under NEMA protocol and manufacturer's guideline for the planar and tomographic specifications.

RESULT

- A. Physical inspection for damage and production flaws PASS
 - B. Planar study
- Result on planar study is shown in Table 1 for Class Standards and Table 2 for Performance Standards.

Table 1 Result on planar study for Class Standards

	Class Standards	Result			Worst Case
		Head 1	Head 2	Head 3	
C1	Intrinsic count rate performance in air.				
	20% observed count rate loss,cps	104,000	101,000	102,000	<60,000
C2	System count rate performance in scatter				
	Collimator LEUR_PAR				
	20% observed count rate loss		34,300		<30,000
	Dead Time (microsecond)		5.2		N/A
C3	System spatial resolution with scatter				
	FWHM (mm)	6.34	6.94	7.44	7.60
	FWTM (mm)	13.74	13.92	14.39	14.65
	Collimator ME_PAR				
	FWHM (mm)	9.83	9.53	9.67	11.90
	FWTM (mm)	20.15	18.61	19.87	23.93
C4	System spatial resolution without scatter				
	Collimator LEUR_PAR				
	FWHM (mm)	6.65	6.68	7.07	7.20
	FWTM (mm)	12.69	12.46	12.55	12.95
	Collimator ME_PAR				
	FWHM (mm)	9.46	9.26	10.07	11.20
	FWTM (mm)	16.90	17.09	16.66	20.10

Table 2 Result on planar study for Performance Standards

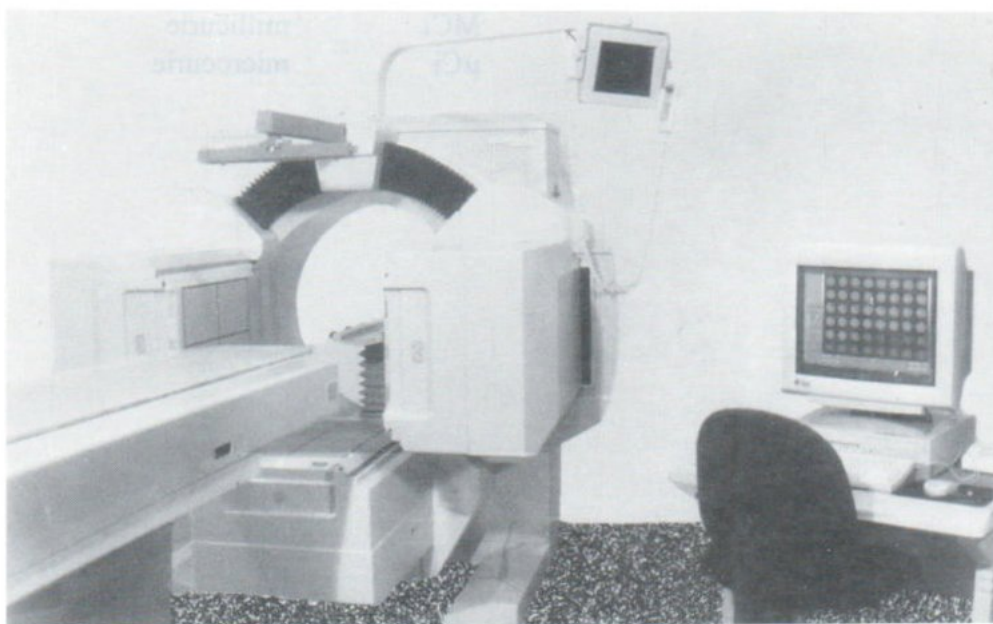
	Performance Standards	Result			Worst Case
		Head 1	Head 2	Head 3	
P1	Intrinsic Flood Field Uniformity				
	Integral UFOV	1.6%	2.0%	1.5%	2.5%
	CFOV	1.6%	1.8%	1.5%	2.0%
	Differential UFOV	1.3%	1.7%	1.3%	2.0%
	CFOV	1.3%	1.4%	1.0%	1.5%
P2	Intrinsic Energy Resolution (Tc-99m)				
	FWHM(%)	9.5%	9.8%	9.8%	9.9%
P3	Intrinsic energy Resolution				
	FWHM(mm) UFOV	4.0	3.9	4.0	4.0
	CFOV	3.7	3.7	3.7	3.8
	FWTM(mm) UFOV	7.5	7.4	7.5	7.8
P4	Intrinsic Spatial Linearity				
	Absolute(mm) UFOV x	0.41	0.33	0.38	0.60
	y	0.42	0.31	0.31	0.60
	CFOV x	0.24	0.33	0.31	0.40
	y	0.27	0.30	0.31	0.40
	Differential (mm) UFOV x	0.12	0.14	0.14	0.20
	CFOV y	0.20	0.11	0.14	0.25
	CFOV x	0.12	0.14	0.14	0.20
	y	0.19	0.11	0.14	0.20
P5	Intrinsic Maximum Count Pate. keps	131	124	125	110
P6	Maximum Window Spatial	0.49	0.32	0.29	1.0
	Registration (mm)				
P7	System Sensitivity (cpm μCi^{-1})				
	Collimator LEUR_FAN	200	199	199	N/A
	System Variation		0.87%		5.0%
	Collimator LEUR_PAR	141	138	141	N/A
	System Variation		2.66%		N/A
	Collimator ME_PAR	161	159	160	N/A
	System Variation		1.23%		N/A
P8	Angular Variation of Flood Field Sensitivity				
	Maximum Sensitivity Variation		0.10%		2.5%

D. Tomographic study.

Result on tomographic study is shown in Table 3

Table 3 Result on Tomographic study

T1	Center Of Rotation (COR) Correction and Calibration			
	Angle Dependent Maximum Deviation after x-y alignments, mm			
	x	0.09	0.11	0.10
	y	0.10	0.10	0.10
T2	System Spatial Resolution with Scatter (mm)			
	Tangential	6.7		7.3
	Radial	9.3		9.8
	Central	10.4		10.4
T3	SPECT Performance Study Jaszczak phantom Transverse-Axial slices			
	Visualized minimum sphere diameter (mm)	9.5		N/A
	Visualized minimum rod diameter (mm)	7.9		N/A

**Fig. 1.** Triple Detector SPECT System

DISCUSSION AND CONCLUSION

The Acceptance testing of a system is a critical step towards the achievement of high quality performance. It should be carried out immediately after the installation, so that the supplier can be informed of any damage, deficiency or flaws before the warranty has expired. The results from this study show that all of the values are within the acceptance level of the manufacturer's worst case. The instrument should not put into routine

use unless it has been shown through acceptance testing to be performing optimally. An instrument that does not perform correctly at installation has a high likelihood of never doing so.

ACKNOWLEDGEMENT

The author wishes to acknowledge The Chicago Medical School and Trionix Research

Laboratory, Inc. for the facilities, document, advice and kind support during this study.

REFERENCES

1. National Electrical Manufacturers Association. NEMA Standards Publications No. NU 1-1994. Performance Measurements of Scintillation Cameras. Washington D.C. 1994
2. American Association of Physicists in Medicine. AAPM Report No.22. Rotating scintillation camera SPECT acceptance testing and quality control. New York 1987.

ABBREVIATION

CFOV	Central Field Of View
UFOV	Useful Field of View
Cpm	counts per minute
Cps	counts per second
FWHM	Full Width at Half Maximum
FWTM	Full Width at Tenth Maximum
LEUR_PAR	Low Energy Ultra high Resolution Parallel hole collimator
LEUR_FAN	Low Energy Ultra high Resolution Fan beam collimator
ME_PAR	Medium Energy Parallel Hole Collimator
MCi	millicurie
μCi	microcurie

BREAST CANCER DETECTION WITH ^{99m}Tc MIBI IMAGING AND MAMMOGRAPHY

Tawatchai CHAIWATANARAT¹, Chalermchai APINYANURAK²,
Darunee BOONJUNWETWAT¹, Kris CHATAMRA³,
Makumkrong POSHYACHINDA¹

ABSTRACT

Screening mammography in female patients provides good sensitivity in the detection of breast abnormalities but low specificity for the diagnosis of breast carcinoma. Thus many patients end up with unnecessary biopsy and/or lumpectomy. The use of nuclear medicine methods in detection of malignancy has been widely studied with various radiopharmaceuticals. The objective of this study was to study the efficacy ^{99m}Tc -MIBI scintimammography and mammography in the detection of breast carcinoma. The diagnosis would be made by pathological findings of the tissue or clinical follow up for at least 6 months. There were 33 female patients included in the study, among these there were 7 cases with known carcinoma of breast and clinically suspected of recurrent. Of all 33 cases, 14 cases was diagnosed as breast carcinoma and 19 cases as benign disease of the breasts. The results showed that sensitivity, specificity, accuracy, positive predictive value and negative predictive value of ^{99m}Tc -MIBI scintimammography in the diagnosis of breast carcinoma were 93%, 100%, 97%, 100% and 95% respectively. Sensitivity, specificity, accuracy, positive predictive value and negative predictive value of mammography were 100%, 63%, 79%, 67% and 100% respectively. We concluded that ^{99m}Tc -MIBI scintimammography has a good efficacy and increase specificity of mammography in the diagnosis of breast carcinoma. We suggested that patients should have mammography performed first, if the lesion is indeterminated by mammography then ^{99m}Tc -MIBI scintimammography will be the next step for investigation.

INTRODUCTION

Breast cancer is a very common neoplasm in women around the world. In the year 1993, International Agency for Research on Cancer reported that breast cancer ranked the third most common neoplastic disease in Thai women after cervix cancer and liver cancer with incidence rate of 11.9/100,000 population¹. In the same year 208 breast cancer patients were treated in Chulalongkorn Hospital². It comprised of 14.77%

of all cancer patients and ranked the second after cervix cancer.

Most patients present with palpable breast mass. However, physical examination alone usually unreliable for the differentiation between benign and malignant mass³. Mammography is an accepted method of choice both for screening and diagnosis of breast cancer. However, one paper reported false negative findings of up to 26.8%⁴. Further-

¹ Department of Radiology, Faculty of Medicine, Chulalongkorn University, Bangkok.

² Department of Radiology, Faculty of Medicine, Khon Kaen University, Khon Kaen.

³ Department of Surgery, Faculty of Medicine, Chulalongkorn University, Bangkok, Thailand.

more the sensitivity of mammography is lower in young patients, dense breasts, fibrocystic disease, evaluation after biopsy, surgery or radiotherapy⁵. ^{99m}Tc-methoxyisobutyl isonitrile (MIBI) is a tracer that is widely used for myocardial perfusion imaging. It has been found that ^{99m}Tc-MIBI can be used to detect different types of neoplasms such as brain gliomas, bone cancer, thyroid cancer, lung cancer, etc⁶. In 1992, there are reports of ^{99m}Tc-MIBI in the diagnosis of breast cancer^{7,8} and since then, various authors have studied the possible usefulness of ^{99m}Tc-MIBI scintimammography in the evaluation of breast cancer^{9,10,11}.

The aims of this study were to evaluate the locally produced ^{99m}Tc-MIBI in Thai women with suspicious of breast cancer and to determine whether a diagnostic protocol based on the joint use of mammography and scintimammography is capable of increasing the sensitivity and specificity in the detection of breast cancer.

MATERIAL AND METHODS

We prospectively studied 33 women of age range 30-67 years (mean \pm sd. = 46.9 \pm 8.4 years). Mammography and ^{99m}Tc-MIBI scintimammography were performed in all subjects. Inclusion criteria consisted of: a) women who were suspected of having breast cancer by physical examination and/or mammography, b) known cases of treated breast cancer with suspected of recurrence. Final diagnosis was established by biopsy or fine needle aspiration or clinical follow up for at least 6 months.

Subject was examined by surgeon then mammography and scintimammography were performed within 1 week. Mammography was performed in all subjects in craniocaudal and mediolateral oblique views. And if necessary, additional projections including magnification or spot compression techniques were used. The mammogram was evaluated by radiologist according to the findings, and the studies were divided into three group representing positive, negative or indeterminate for malignancy.

MIBI, which was produced by the Office of Atomic Energy for Peace, Thailand, was labeled with Tc-99m in the Nuclear Medicine Division, Chulalongkorn Hospital. Twenty mCi (740 MBq) was injected into patient's arm vein on the contralateral side of the affected breast. When there were clinical suspicions of having bilateral breast masses, the injection was made in the dorsal vein of foot. The same imaging sequence was performed in all subjects, beginning with the lateral view of the affected breast, followed by the contralateral breast and the anterior view of both breasts. For the lateral view, subject lied on the scanning bed on her side with gamma camera head placed underneath the bed. Planar image acquisition began 5 minutes after radiopharmaceutical administration using low-energy parallel hole, high-resolution collimator, 128x128 matrix size and 20% window centered at 140 KeV. Each image acquisition time was 10 minutes.

All focal accumulation of ^{99m}Tc-MIBI higher than the surrounding background of the breast was considered an abnormal increased uptake. Then, in such a case, "tumor uptake ratio (TUR)" was calculated.

$$\text{Tumor uptake ratio} = \frac{\text{average count per pixel in area of increased tracer accumulation}}{\text{average count per pixel in surrounding background area}}$$

RESULTS

Of 33 subjects included in this study, 26 were suspicious of primary breast cancer and 7 were suspicious of recurrent disease. Among these subjects, final diagnoses were established by surgical biopsy in 21 cases, by fine needle aspiration in 7 cases and by 8-15 months clinical follow up in 5 cases. There were 14 malignant and 19 benign conditions. One subject was diagnosed as bilateral invasive ductal carcinoma. Details of the final diagnoses were shown in table 1.

In 14 subjects with malignant disease, mammography gave positive, negative and indeterminate results in 10, 0 and 4 cases respectively. Scintimammography showed abnormal increased uptake in 13 cases with TUR between 1.48 - 3.05 (mean \pm s.d. = 2.16 ± 0.15). The size of the lesion varied from 0.5 - 5cm. The smallest mass detected by scintimammography was 1 cm. Figure 1 was a sample of a 40 years old patient with final diagnosis of invasive ductal carcinoma, scintimammography show an area of increased radiotracer accumulation in right breast with TUR of 2.0. One case with negative scintimammography, the mass size was 0.5 cm. and mammography also gave indeterminate result (Table 2). Among 7 cases of suspected recurrent, one case was found to have recurrent of ductal carcinoma with palpated mass

of 1 cm. Scintimammography result in TUR 1.8 but the lesion was indetermined by mammography (Fig. 2).

In 19 subjects with benign conditions, mammography gave positive, negative and indeterminate results in 1, 12 and 6 cases respectively. Scintimammography showed no abnormal uptake in 12 cases but 7 cases showed abnormal increased uptake with TUR between 1.13 - 1.33 (mean \pm s.d. = 1.26 ± 0.07). Figure 3 was a sample of a 46 years old patient with final diagnosis of fibroadenoma, scintimammography show an area of faintly increased radiotracer accumulation in left breast with TUR of 1.3. One case of chronic inflammation with fat necrosis, mammography gave positive result but no abnormal uptake by scintimammography (Table 3).

If we considered TUR value of 1.40, which was the value of mean ± 2 s.d. of benign condition, as diagnostic cut off value for malignant lesion, scintimammography will give only 1 false negative without false positive case (Table 2, 3). Then sensitivity and specificity of scintimammography for the diagnosis of malignancy will be 93% and 100% respectively.

Table 1 Final diagnoses in 33 subjects included into the study.

Diagnosis	number
Ductal carcinoma	14
Fibrocystic disease	4
Chronic inflammation / Fat necrosis	3
Fibroadenoma	2
Granuloma	2
Mammary dysplasia	1
No evidence of malignancy	7
Total	33

Table 2 Showed diagnostic results of mammography and scintimammography in patients with malignant diseases.

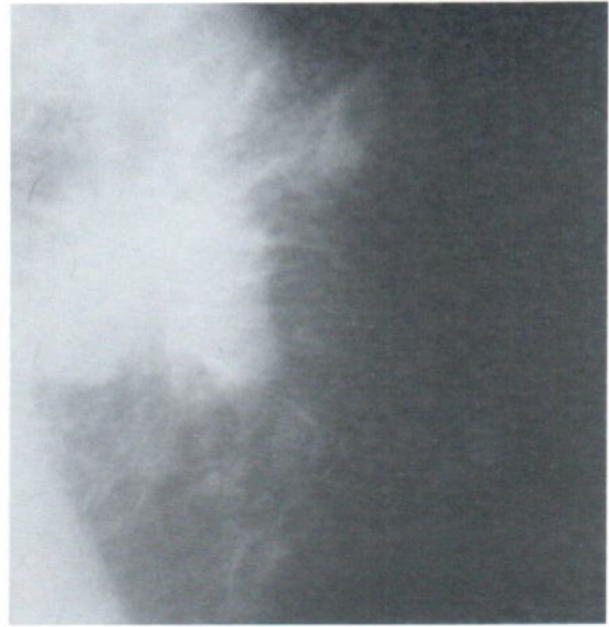
	Scintimammography		
	Abnormal increased uptake		No abnormal uptake
Mammography	TUR > 1.40	TUR < 1.40	
Positive	10	-	-
Negative	-	-	-
Indetermined	3	-	1

Table 3 Showed diagnostic results of mammography and scintimammography in patients with benign conditions.

	Scintimammography		
	Abnormal increased uptake		No abnormal uptake
Mammography	TUR > 1.40	TUR < 1.40	
Positive	-	-	1
Negative	-	3	9
Indetermined	-	4	2



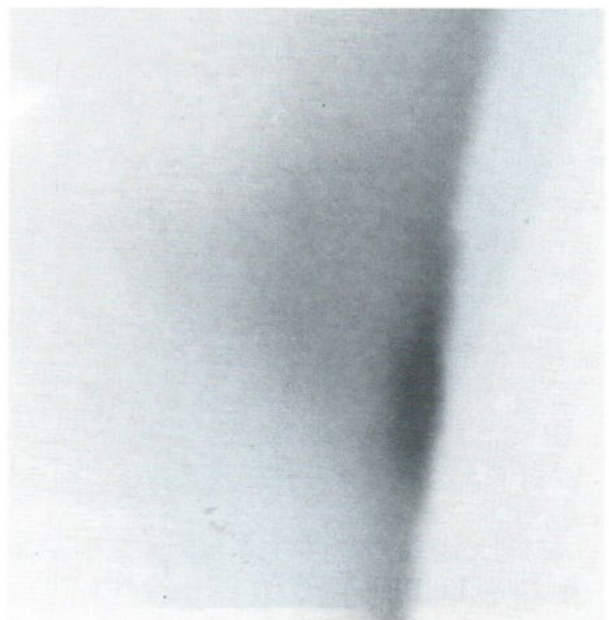
1A.



1B.



1C.



1D.

Fig. 1 A 40 years old patient with final diagnosis of invasive ductal carcinoma, mammogram of right breast (CC and MLO views) showed a microlobulated mass with spiculated border at right upper outer quadrant being highly suspicious of malignancy (A = right CC, B = right MLO). Scintimammography show a round area of increased radiotracer accumulation in right breast (arrow) with TUR of 2.0 (C = right breast, D = left breast).
MLO = mediolateral oblique, CC = craniocaudal

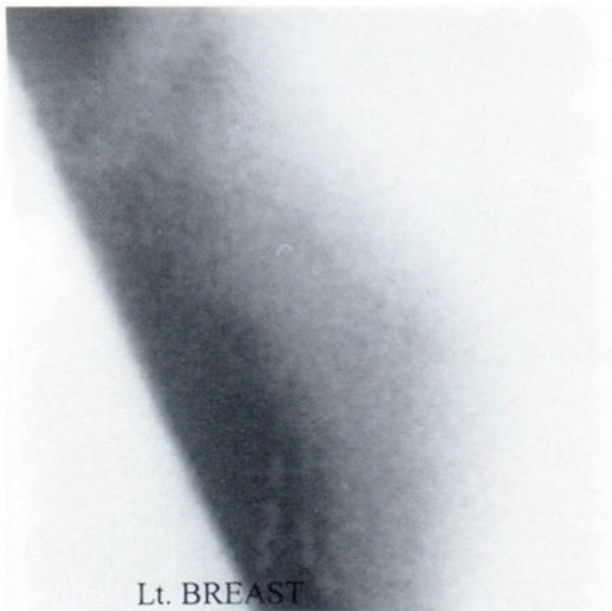
Rt. BREAST



2A.



2B.

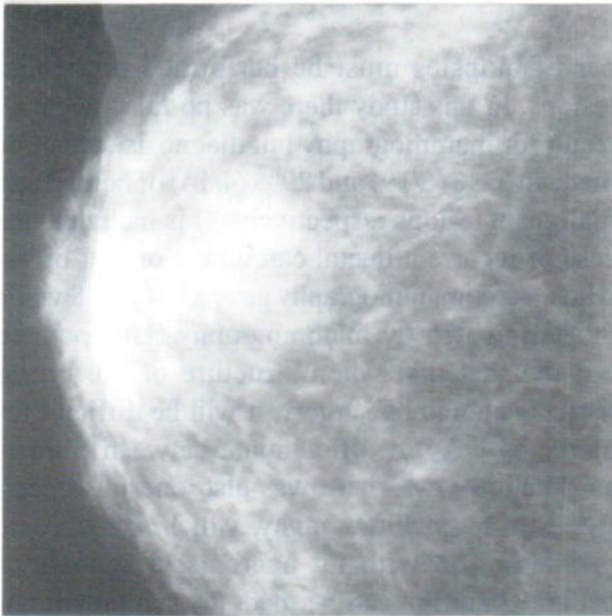


2C.



2D.

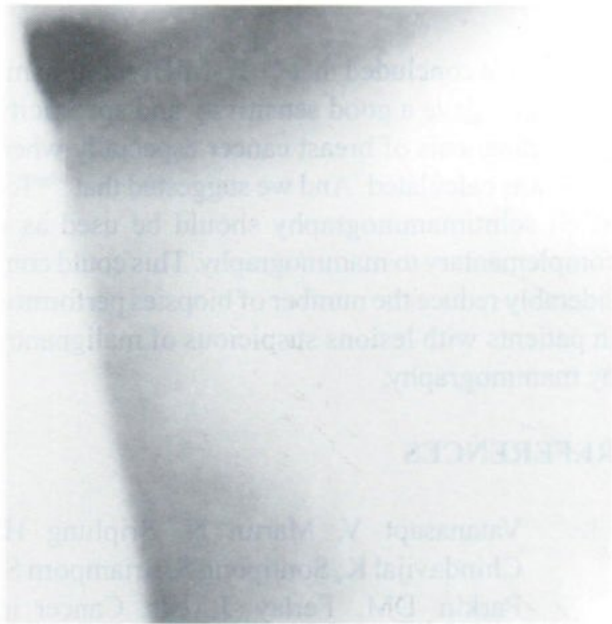
Fig. 2 A 41 years old patient who had wide excision done for breast carcinoma, on follow up recurrent of malignancy was suspected. Mammogram of left breast (CC and MLO views) showed an ill-defined opacity with radiating fibrosis strands at left upper outer quadrant, post-operative scar is possible but residual tumor cannot be definitely excluded (A = left CC, B = left MLO). Scintimammography show a round area of increased radiotracer accumulation in left breast (arrow) with TUR of 1.8 (C = right breast, D = left breast).



3A.



3B.



3C.



3D.

Fig. 3 A 46 years old patient with final diagnosis of fibroadenoma, mammogram of left breast (CC and MLO views) showed a lobulated well-defined border soft tissue mass at left upper middle quadrant without hypodensity rim, fibroadenoma is suspected but malignancy cannot be definitely excluded (A = left CC, B = left MLO). Scintimammography show an oval area of faintly increased radiotracer accumulation in left breast (arrow) with TUR of 1.3 (C = right breast, D = left breast).

DISCUSSION

During the past several years, many studies have reported the successfulness of using ^{99m}Tc -MIBI in the evaluation of breast lesions.¹²⁻¹⁷ The results of this technique in the detection of breast cancer, in general, were good with a sensitivity between 67%¹⁸ and 94%¹⁹ and a specificity between 72%²⁰ and 100%²¹. In this study the sensitivity and specificity were 93% and 63% respectively if TUR were not taken into consideration. However, if TUR of equal to or greater than 1.40 were used as the diagnostic criteria for malignancy, specificity would dramatically improve to 100%. This was because, as generally known that the accumulation of ^{99m}Tc MIBI will increase in some benign conditions with hypercellularity such as fibrocystic disease and fibroadenoma²²⁻²⁵. Such conditions have been found to be the risk of breast cancer^{26,27}. There were 2 cases of fibrocystic disease and 1 case of fibroadenoma in this study, which resulted in positive scintimammography. We also found histologically hypercellularity in each case of mammary dysplasia and chronic inflammation. However, TUR in all these cases were not greater than 1.33. In all other reports, the TUR in all but one malignant tumor were greater than 1.48. Tallifer R.²⁸, Maurer DF.²⁹, and Khalkhali I.³⁰ reported TUR for their breast cancer subjects equal to $2.2 + 0.7$, $1.82 + 0.95$ and $2.13 + 0.93$ respectively. One false negative case was invasive ductal carcinoma with a mass size of 0.5 cm. Most reports also found the smallest mass that could be detected by ^{99m}Tc -MIBI scintimammography was 0.8-1.0 cm³¹⁻³³

Mammography is an accepted technique in screening for breast cancer. However, in many occasions, distinguishing between benign and malignant lesion is unreliable. For example patient with breast prosthesis, some cases of fat necrosis and women with dense breast³⁴. And because the positive predictive value of mammography is approximately 15%-30%³⁵, a large num-

ber of biopsies must be performed on benign lesions. In this study there was no false negative result for mammography but diagnosis cannot be made in 32% (6/19) and 29% (4/14) of benign and malignant lesions respectively. This included one case of recurrent ductal carcinoma on left breast whose scintimammography gave TUR of 1.8 while indetermined by mammography. This pointed out the fact that when structure of the breast tissue is altered by surgery, it will be difficult for mammography to differentiate between fibrosis and malignancy. There was also one false positive case by mammography, which was chronic inflammation with fat necrosis, diagnosis of benign condition can be made by scintimammography.

CONCLUSION

We concluded that ^{99m}Tc -MIBI scintimammography gave a good sensitivity and specificity in the diagnosis of breast cancer especially when TUR was calculated. And we suggested that ^{99m}Tc -MIBI scintimammography should be used as a complementary to mammography. This could considerably reduce the number of biopsies performed in patients with lesions suspicious of malignancy by mammography.

REFERENCES

1. Vatanasapt V, Martin N, Sriplung H, Chindavijal K, Sontipong S, Sriamporn S, Parkin DM, Ferlay J. eds. Cancer in Thailand 1988-1991 IARC Technical report No. 16 International Agency for Research on Cancer, Lyon France, 1993 ISBN 92 832 1430 7
2. Tumor registry statistical report 1993. Faculty of medicine. Chulalongkorn hospital. Bangkok. Thailand.

3. Sickles EA. Mammographic features of 300 consecutive nonpalpable breast cancers. *AJR* 1986;146:661-3.
4. Niloff PH, Sheiner NM. False-negative mammograms in patients with breast cancer. *Canadian J Surg* 1981;24:50-2.
5. Kopans DB. The positive predictive value of Mammography. *AJR* 1992;158:521-6.
6. Abdel_Dayem HM, Scott AM, Macapinlac HA, El-Gazzar AH, Larsen SM. Role of 201Tl chloride and 99mTc sestamibi in tumor imaging. In: Freeman LM, ed. *Nuclear Medicine Annual 1994*. New York, NY: Raven Press; 1994:181-234.
7. Waxman A, Ashok G, Kooba A, et al. The use of 99mTc-methoxy isobutyl isonitrile (MIBI) in the evaluation of patients with primary carcinoma of the breast (abstract). *Clin Nucl Med* 1992;9:761.
8. Campeau RJ, Kronemer KA, Sutherland CM. Concordant uptake of Tc-99m sestamibi and Tl-201 in unsuspected breast tumor. *Clin Nucl Med* 1992;17:936-7.
9. Kao CH, Wang SJ, Liu TJ. The use of technetium-99m-methoxyisobutylisonitrile breast scintigraphy to evaluate palpable breast masses. *Eur J Nucl Med* 1994;21:432-6.
10. Palmedo H, Schomburg A, Grunwald F, Mallmann P, Krebs D, Biersack H. Technetium-99m-MIBI scintimammography for suspicious breast lesion. *J Nucl Med* 1996;37:626-30.
11. Villanueva-Meyer J, Leonard MH Jr, Briscoe F, et al. Scintimammography with technetium-99m-sestamibi in suspected breast cancer. *J Nucl Med* 1996;37:926-30.
12. Campeau RJ, Kronemer KA, Sutherland CM. Concordant uptake of Tc-99m sestamibi and Tl-201 in unsuspected breast tumor. *Clin Nucl Med* 1992;17(12):936-7.
13. Waxman A, Nagaraj N, Ashok G, et al. Sensitivity and specificity of tc-99m methoxy isonitrile (mibi) in the evaluation of primary-carcinoma of the breast - comparison of palpable and non-palpable lesions with mammography. *J Nucl Med* 1994;35(5):P22-P22 Suppl.
14. Kao CH, Wang SJ, Liu TJ. The use of technetium-99m methoxyisobutylisonitrile breast scintigraphy to evaluate palpable breast masses. *Eur J Nucl Med* 1994;21(5):432-6.
15. Khalkhali I, Cutrone J, Mena I, et al. Technetium-99m-sestamibi scintimammography of breast-lesions-clinical and pathological follow-up. *J Nucl Med* 1995;36(10):1784-9.
16. Palmedo H, Schomburg A, Grunwald F, Mallmann P, Krebs D, Biersack HJ. Technetium-99m-MIBI scintimammography for suspicious breast lesions. *J Nucl Med* 1996;37(4):626-30.
17. Becherer A, Helbich T, Staudenherz A, Jakesz R, Kubista E, Lehner R, Rudas M, Teleky B, Kletter K, Leitha T. The diagnostic value of planar and SPET scintimammography in different age groups. *Nucl Med Commun* 1997;18(8):710-8.
18. Becherer A, Helbich T, Staudenherz A, Jakesz R, Kubista E, Lehner R, Rudas M, Teleky B, Kletter K, Leitha T. The diagnostic value of planar and SPET scintimammography in different age groups. *Nucl Med Commun* 1997;18(8):710-8.
19. Khalkhali I, Cutrone J, Mena I, et al. Technetium-99m-sestamibi scintimammography of breast-lesions-clinical and pathological follow-up. *J Nucl Med* 1995;36(10):1784-9.

20. Waxman A, Nagaraj N, Ashok G, et al. Sensitivity and specificity of tc-99m methoxy isonitrile (mibi) in the evaluation of primary-carcinoma of the breast - comparison of palpable and non-palpable lesions with mammography. *J Nucl Med* 1994;35(5):P22-P22 Suppl.
21. Kao CH, Wang SJ, Liu TJ. The use of technetium-99m methoxyisobutylisonitrile breast scintigraphy to evaluate palpable breast masses. *Eur J Nucl Med* 1994;21(5):432-6
22. Khalkhali I, Cutrone J, Mena I, Diggles L, Venegas R, Vargas H, Jackson B, Klein S. Technetium-99m-sestamibi Scintimammography of breast lesions: clinical and pathological follow-up. *J Nucl Med* 1995; 36:1784-9.
23. Taillefer R, Robidoux A, Lambert R, Turpin S, Laperriere J. Technetium-99m-sestamibi prone Scintimammography to detect primary breast cancer and axillary lymph node involvement. *J Nucl Med* 1995;36:1758-65.
24. Palmedo H, Schomburg A, Grunwald F, Bender H. Scintimammography with 99mTc MIBI in patients with suspicious breast nodules: A comparison of planar and SPECT imaging techniques(Abstract). *Eur J Nucl Med* 1995;22:725.
25. Burak Z, Argon M, Yasarbas U, Memis A. Scintigraphic imaging of malignant breast masses with 201Tl and 99mTc MIBI: comparison with Mammography and ultrasonography (Abstract). *Eur J Nucl Med* 1995;22:725.
26. Dupont WD, Page DL. Risk factors for breast cancer in women with proliferative breast disease. *N Engl J Med* 1985;312: 146-51.
27. Jensen RA, Page DL, Dupont WD, Roger LW. Invasive breast cancer risk in women with sclerosing adenosis. *Cancer* 1989; 64:1977-83.
28. Taillefer R, Robidoux A, Lambert R, Turpin S, Laperriere J. Technetium-99m-sestamibi prone Scintimammography to detect primary breast cancer and axillary lymph node involvement. *J Nucl Med* 1995;36:1758-65.
29. Maurer AH, Caroline DF, Jadali FJ, Mazone TA, Maier WP, Au FC, Schnall SF. Limitations of craniocaudal thallium-201 and technetium-99m-Sestamibi Scintimammography. *J Nucl Med* 1995; 36:1696-700.
30. Khalkhali I, Cutrone J, Mena I, Diggles L, Venegas R, Vargas H, Jackson B, Klein S. Technetium-99m-sestamibi Scintimammography of breast lesions: clinical and pathological follow-up. *J Nucl Med* 1995; 36:1784-9.
31. Lu G, Shih WJ, Huang HY. et al. 99mTc-MIBI Scintimammography of breast masses: early and delayed imaging. *Nucl Med Comm* 1995;16:150-6.
32. Aktolun C, Bayhan H, Kir M. Clinical experience with 99mTc MIBI imaging in patients with malignant tumors. Preliminary results and comparison with 201Tl. *Clin Nucl Med* 1992;17:171-6.
33. Khalkhali I, Cutrone J, Mena I, Diggles L, Venegas R, Vargas H, Jackson B, Klein S. Technetium-99m-sestamibi Scintimammography of breast lesions: clinical and pathological follow-up. *J Nucl Med* 1995; 36:1784-9.
34. Jackson VP, Hendrick RE, Kerg S.A. et al. Imaging of the radiographically dense breast. *Radiology* 1993; 198: 297-301.
35. Kopans DB. The positive predictive value of Mammography. *AJR* 1992;158:521-6.

GRANULOMATOUS AMEBIC ENCEPHALITIS : REPORT OF TWO CASES WITH NEUROIMAGING FINDING.

Arkhom ARAYAWICHANONT, M.D., Orasa CHAWALPARIT, M.D.¹
Tumtip SANGRUCHI, M.D.², Vorapun SENANARONG, M.D. MRCP(U.K.)

ABSTRACT

Granulomatous amebic encephalitis is quite rare but highly fatal. We reported two cases of this disease included clinical presentation, investigations and neuroimaging finding. The disease should be differentiated from other space occupying lesions or unusual cerebritis. Because the examination is nonspecific, the neuroimaging will encourage brain biopsy for definite diagnosis.

INTRODUCTION

Free-living amebas rarely cause diseases in human, however, they can directly invade the central nervous system especially in immunosuppressed patients. *Entamoeba histolytica* is the most common amebic infection of human and also in Thailand. By contrast, primary amebic meningoencephalitis (PAM) due to *Naegleria fowleri* and granulomatous amebic encephalitis (GAE) due to *Acanthamoeba* sp and leptomyxid amebas have rarely been reported. In Thailand, the incidence of GAE is quite rare. There are only two reports of granulomatous amebic encephalitis (Jariya et al., 1992,¹ Sangruchi et al, 1994).² Our report is the third report of two cases of GAE caused by *Acanthamoeba* sp. and neuroimaging seen in GAE has been described.

CASE REPORT

CASE 1.

A 43 year-old man with underlying disease of alcoholic cirrhosis came to Siriraj Hospital with history of prolonged fever for one

month, hematemesis and confusion for one day. He also had first episode of generalized clonic-tonic seizure a month before admission, nevertheless, investigations for causes of seizure were unremarkable.

Physical examination on admission revealed body temperature of 38.5°C, respiratory rate of 24/min, pulse rate of 100/min, blood pressure of 170/100 mmHg. He was confused with partially response to command. He had moderately pale, mild jaundice, signs of chronic liver disease, no skin lesion and no superficial lymphadenopathy. Cardiovascular and respiratory system were normal. Neurological examination revealed no stiff neck, no papilledema, no motor weakness and no focal neurological deficit.

Investigations showed seronegative for HIV, hematocrit 19 percent, white blood cell count 11,400 cells/mm³ with polymorphonuclear cell predominate, platelet count 229,000 cells/mm³. Several hemoculture were negative, however, he

Division of Neurology, Department of Medicine,

¹ Department of radiology,

² Department of Pathology, Faculty of Medicine, Siriraj Hospital, Mahidol University, Bangkok 10700 THAILAND.

Correspondence : Associated Professor Orasa Chawalparit, Department of Radiology, Faculty of Medicine, Siriraj Hospital, Mahidol University, Bangkok 10700 THAILAND. Tel : (662) 419-7086 Fax : (662) 412-7785

still had intermittent fever. Treatment of upper gastrointestinal (GI) hemorrhage and hepatic encephalopathy was administered with improvement of GI hemorrhage. He still confused and developed right hemiparesis grade III/IV with bilateral Babinski sign, nine days after admission. The chest film showed bilateral peribronchial infiltration with bilateral pleural effusion. The CT brain revealed multiple hypodensity in gray matter, gray-white junction and periventricular region of cerebrum and cerebellum. Some lesions showed faint incomplete ring enhancement (Figure 1). Focal or adjacent parenchymal infarction or edema were also demonstrated. Lumbar puncture revealed an open pressure of 160 mmH₂O, white blood cell of 9 cells/mm³ with lymphocytic predominate, red blood cell of 1820 cells/mm³, cerebrospinal fluid (CSF) sugar of 18 mg/dl (blood sugar 98 mg/dl), CSF protein of 1,229 mg/dl. Gram stain, acid fast bacilli (AFB) stain and india ink preparation were negative. Cefotaxime and ampicillin high dose were administered for empirical treatment of brain abscess, however, CSF culture showed no growth. He developed sepsis syndrome and death on the eleventh day after admission. Granulomatous amebic encephalitis was diagnosed postmortem (Figure 2).

CASE 2

A 17 year-old woman with underlying disease of systemic lupus erythematosus (SLE) presented with symptoms of fever and productive cough for six days, severe generalized dull aching headache with vomiting for two days, and generalized tonic-clonic seizure one day before admission. She had no previous history of seizure. She had regularly followed up at Siriraj Hospital since her diagnosis of SLE and her last medication was oral prednisolone 15 mg per day.

Physical examination on admission revealed body temperature of 39°C, respiratory rate

of 28/min, pulse rate of 104/min, blood pressure of 120/80 mmHg, no skin lesion and no superficial lymphadenopathy. Chest examination revealed hyperpnea and medium crepitation of left lower lung field. The cardiovascular system and the abdomen were normal. Neurological examination showed neck stiffness and Kernig's sign was positive while other examinations were unremarkable.

Complete blood count showed hematocrit 28 percent, white blood cell count 6,030 cells/mm³ with polymorphonuclear cell 63 percent, platelet count 164,000 cells/mm³. Sputum examination for gram stain, AFB stain, and culture were all negative finding. Chest radiogram showed perihilar infiltration. Lumbar puncture revealed an open pressure of 380 mmH₂O, white blood cell of 56 cells/mm³ with lymphocytic predominate, red blood cell of 13 cells/mm³, CSF sugar of 30 mg/dl, CSF protein of 125 mg/dl and negative finding of gram stain, AFB stain and india ink preparation. Hemoculture and CSF culture showed no growth. Treatment of tuberculous meningitis was given. CT brain was done three days later and showed multiple hypodensity areas with no enhancement in gray matter, gray-white junction, periventricular region in cerebrum and cerebellum (Figure 3). The MRI of brain revealed multiple enhancing nodules in the corresponding regions with some focal meningeal involvement (Figure 4A,B). There was some area of nonenhanced lesion compatible with infarction (Figure 5B).

The brain biopsy was done at left frontal lobe lesion for definite diagnosis. Pathological section demonstrated acute vasculitis with cerebritis without any organisms. Intravenous co-trimoxazole was administered as empirical treatment of Nocardial brain abscess. She developed sepsis and expired sixteen days after admission. The autopsy was done and granulomatous amebic encephalitis was diagnosed later (Figure 5A, 6).

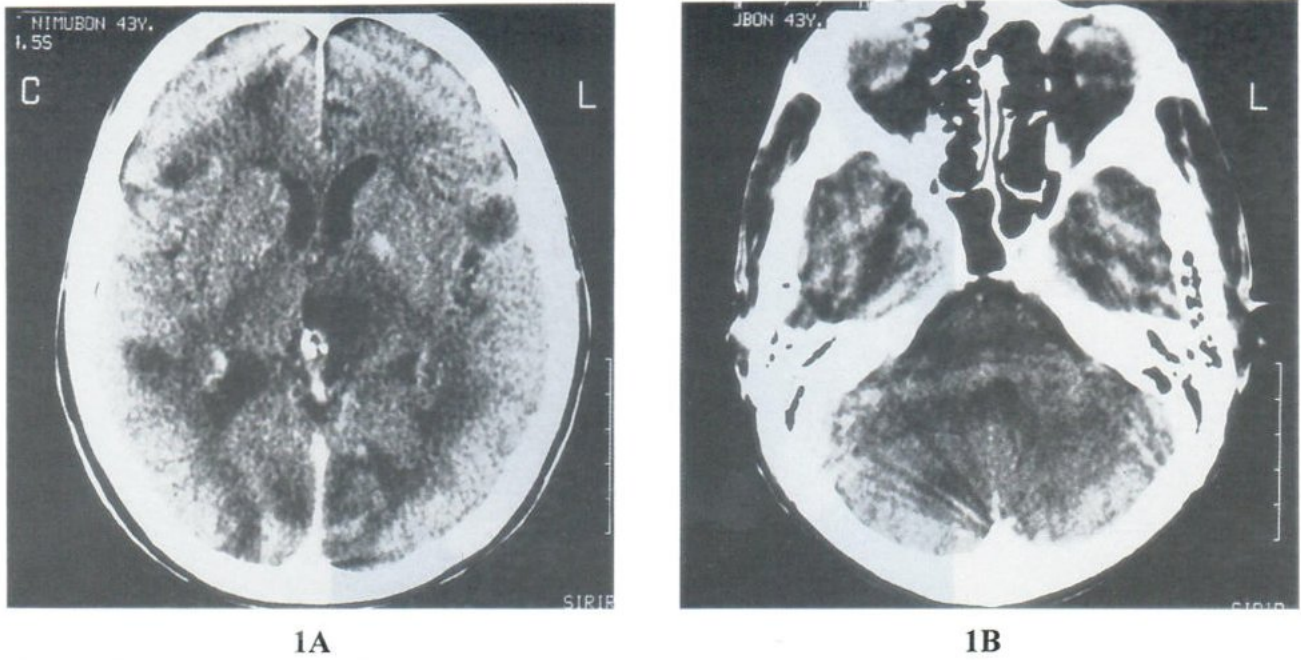


Fig. 1. Contrast enhanced CT of Case 1 (A,B) demonstrate multiple low density areas in supratentorial and infratentorial location with some faint enhancement.

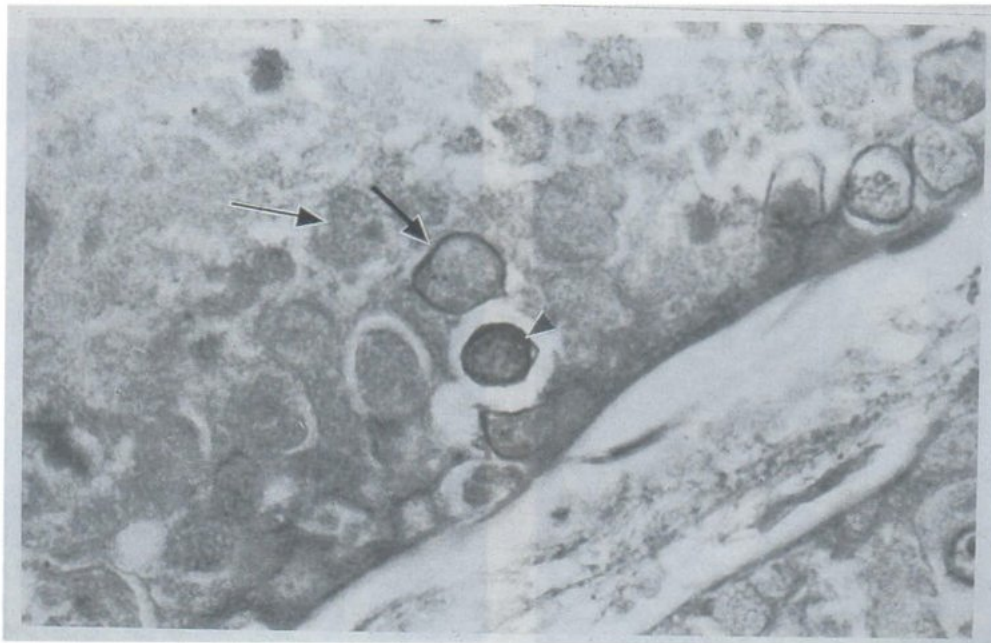


Fig. 2. Numerous trophozoites (→) and cysts (▶) were found around thrombosed vessel in brain autopsy tissue. (H&E 400X)

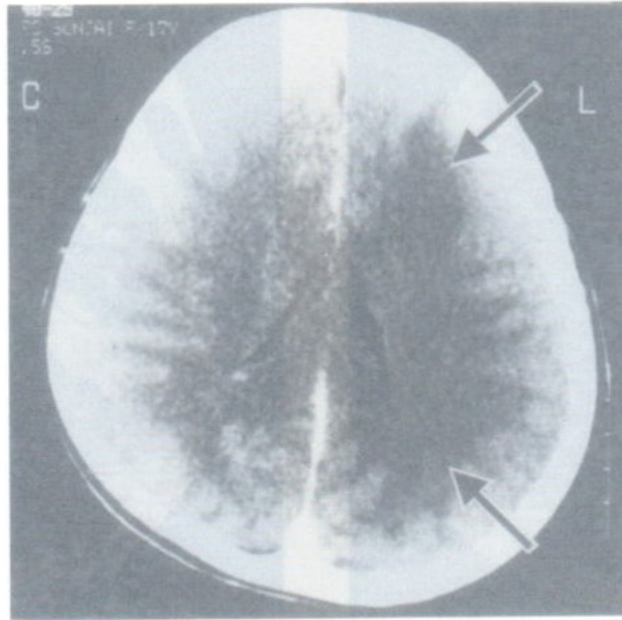
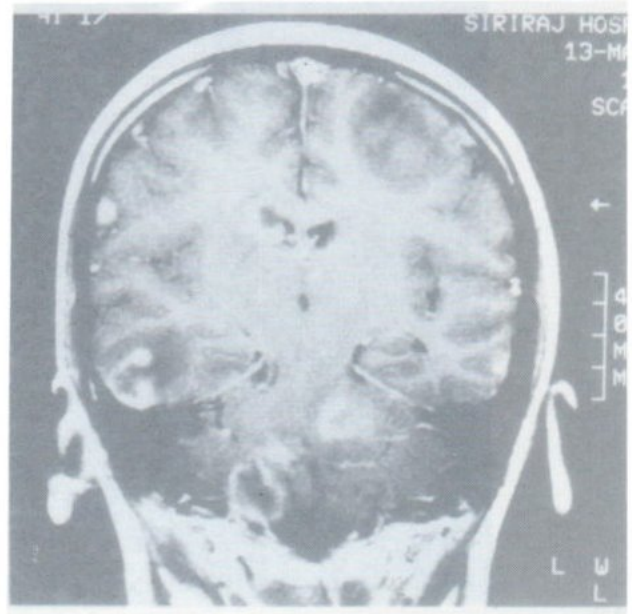


Fig. 3. Contrast enhanced CT of Case 2 reveals multiple areas of nonenhancing low density in cerebrum.



4A



4B

Fig. 4. T₂wi (A) and Gd-T₁wi (B) of Case 2 show multiple high signal intensity with enhancing nodules.

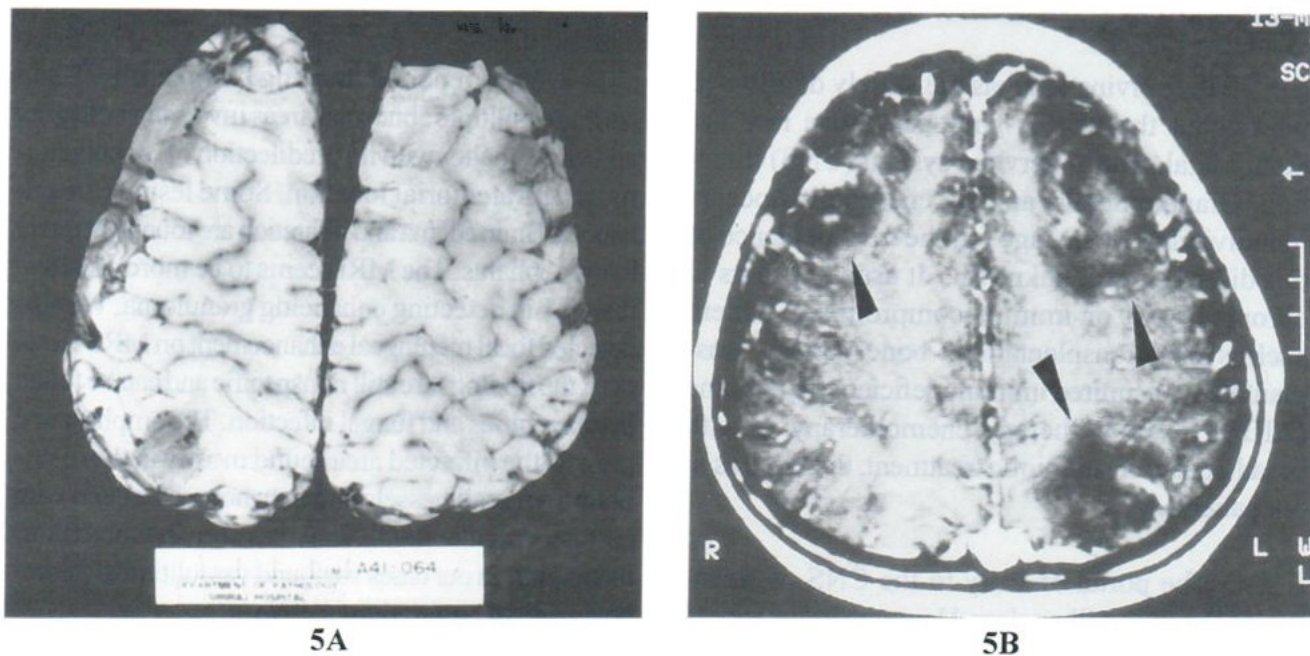


Fig. 5. Multiple necrotic nodules focally involved meningeal covering (A). The areas corresponded with infarction on MRI (B).

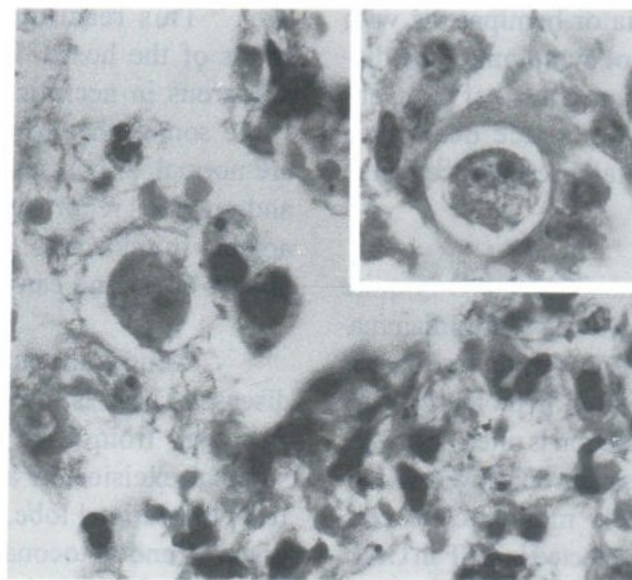


Fig. 6. A trophozoite in the lung and in a small granuloma in the brain parenchyma. (inset) (H&E 400X)

DISCUSSION

Free-living amoebae are widely distributed throughout the world. They can cause rare but highly fatal central nervous system (CNS) infection. Granulomatous amoebic encephalitis occurs in individuals of any age but the true incidence of this disease is still unknown.³ It usually occurs in chronically ill or immunocompromised patient such as renal transplantation,⁴ bone marrow transplantation,⁵ acquired immunodeficiency syndrome (AIDS),^{6,7} steroid therapy, chemotherapy, or with broad-spectrum antibiotic treatment, the same as in our patients.^{8,9}

The portal of entry to the CNS of *Acanthamoeba* sp is still unclear. Hematogenous spread from the skin or lungs has been demonstrated,¹⁰ therefore, it can directly invade the brain parenchyma. Both of our cases had foci in the lungs which seemed to be source of spreading. Clinical manifestations consist of altered mental status, fever, headache, convulsion, and focal neurological deficits such as aphasia or hemiparesis with subacute or gradual onset of symptoms. The disease may simulate the clinical course of brain abscess, brain tumor, or other space occupying lesions. Raised intracranial pressure can also occur.^{11,12,13}

Antemortem diagnosis of GAE is quite difficult. Most patients show a nonspecific inflammatory response in the CSF. An opening pressure is usually elevated, as well as high CSF protein concentration. The glucose concentration is often normal or reduced. Leukocytes are present in only low or moderate numbers predominately mononuclear cell. Because amoebae are rarely detected in CSF in GAE, specific diagnosis usually requires biopsy or autopsy specimens. Even then, the diagnosis is likely to be missed unless the pathologist is alerted in advance to consider this rare disease. However, serologic tests of *Acanthamoeba* may help to determine the diagnosis.¹⁴

Most reported imaging findings on CT and MRI are multiple abnormal areas involving both gray and white matter with no predilection of supratentorial or infratentorial location. Some lesions are enhanced. Brain edema and infarction are found but rarely hydrocephalus. The MRI seems to be more sensitive than CT in detecting enhancing granuloma. We also detected focal meningeal enhancement on MRI. However, the findings are still nonspecific and can be found in tuberculous and fungal infection. The emphasizing point is the infarcted area found mostly in the distribution of small vessels and may not associated with cortical vascular involvement as seen in tuberculous meningitis. In our cases we found vasculitis and thrombosis causing infarction.^{5,15,16,17}

The pathological findings of GAE has been described.^{2,12,13,18} Focal or extensive cerebral necrosis with wide range of granulomatous reaction were seen.

This reaction might indicate immune status of the hosts. Trophozoites and cysts are numerous in necrotic or granulomatous lesions while some other parts of the uninvolved brain are normal. A constant finding seen in our cases and previous reports is vasculitis with or without amoebic trophozoites. Thrombosis and infarction always occur and can be detected by CT or MRI.

Almost all patients with GAE died of the disease. There is only one nonfatal case report. Recovery from GAE has been described using surgical excision of a large inflammatory mass from the parietal lobe, and following by amphotericin B and ketoconazole.¹⁹ Amphotericin B or ketoconazole may be benefit in *acanthamoeba* infection.

In summary, we reported two rare cases of GAE with clinical and neuroimaging findings. The disease should be differentiated from other space

occupying lesions or unusual cerebritis. Because the examination is nonspecific, the neuroimaging will encourage brain biopsy for definite diagnosis.

REFERENCES

1. Jariya P, Lertlaituan P, Warachoon K, et al. Acanthamoeba spp : a case of chronic granulomatous amoebic meningoencephalitis. *Siriraj Hosp Gaz* 1992;44:148-53.
2. Sangruchi T, Martinez AJ, Visvesvara GS. Spontaneous granulomatous amoebic encephalitis : Report of four cases from Thailand. *Southeast Asian J Trop Med Public Health* 1994;25:309-13.
3. Visvesvara GS, Stehr-Green JK. Epidemiology of free-living amoeba infections. *J Protozool* 1990;37:25s-33s.
4. Martinez AJ. Acanthamoebiasis and immunosuppression. *J Neuropathol Exp Neurol* 1982;41:548-57.
5. Anderlini P, Przepiorka D, Luna M, et al. Acanthamoeba meningoencephalitis after bone marrow transplantation. *Bone Marrow Transplant* 1994;14:459-61.
6. Gardber HA, Martinez AJ, Visvesvara GS, Sotrel A. Granulomatous amoebic encephalitis in an AIDS patient. *Neurol* 1991;41:1993-5.
7. Gordon SM, Steinbery JP, Du Puis MH, et al. Culture isolation of Acanthamoeba species and leptomyxid amoebas from patients with amoebic meningoencephalitis, including two patients with AIDS. *Clin Inf Dis* 1992;15:1024-30.
8. Martinez AJ, Janitschke K. Acanthamoeba, and opportunistic microorganism: a review. *Infect* 1985;13:2151-6.
9. Martinez AJ. Is Acanthamoeba encephalitis an opportunistic infection. *Neurol* 1980;30:567-74.
10. Martinez AJ, Markowitz SM, Duma RJ. Experimental pneumonitis and encephalitis caused by acanthamoeba in mice: pathogenesis and ultrastructural features. *J Inf Dis* 1975;131:692-9.
11. Ma P, Visvesvara GS, Martinez AJ, et al. Naegleria and Acanthamoeba infection. *Rev Inf Dis* 1990;12:490-513.
12. Durack DT. Amebic infections In: Scheld WM, Whitley RJ, Durack DT, eds. *Infections of the central nervous system*. Philadelphia: Lippincott-Raven, 1997: 831-44.
13. Bale JF. Parasitic and rickettsial infections of the nervous system. In : Tyler KL, Martin JB, eds. *Infectious diseases of the central nervous system*. Philadelphia : F.A. Davis, 1993:266-9.
14. Gullett J, Mills J, Hadley K, et al. Disseminated granulomatous acanthamoeba infection presenting as an unusual skin lesion. *Am J Med* 1979;67:891-6.
15. Sell JJ, Rupp FW, Orrisou Jr WW. Granulomatous amoebic encephalitis caused by acanthamoeba. *Neuroradiol* 1997;39:434-36.
16. Kidney DD, Kim SH. CNS infection with free-living amoebas : neuroimaging findings. *AJR* 1998;171:809-12.
17. Schumacher DJ, Tien RD, Lane K. Neuroimaging findings in rare amoebic infections of the central nervous system. *AJNR* 1995;16:930-5.
18. Scaravilli F, Cook GC. Parasitic and fungal infections. In : Graham DI, Lantos PL, eds. *Greenfield's neuropathology*. London : Arnold, 1997;2:66-8.
19. Ofori-Kwakye SK, Sidobottom DG, Herbert J, et al. Granulomatous brain tumor caused by Acanthamoeba. *J Neurosurg* 1986;64:505-9.

Message from
Professor Dr. Kawee Tungsubutra

Editor-in-Chief, The Asean Journal of Radiology

Dear Friends ,

This is the 1st Number of Vol VI of the Asean Journal of Radiology. It has passed the goal of 5 years of regular publication so that our journal will be eligible to be entered into the Index Medicus. The 10th AAR Congress of Radiology has taken place in Bangkok, Thailand on 23-25 March in the year 2000. I have taken the Chair of the President of Asean Association of Radiology which was handed over from Singapore.

I will continue to be the editor of the AAR journal so that it will be admitted into the Index Medicus. After that I am sure that other member committee in the Royal College of Radiology will be able to continue to do the task and improve to the perfection and satisfaction.

I would like to thank to Bracco International for providing the educational grant for starting the Journal in 1955. I would like to thank in person to Dr. Zaini Ibrahim, Dr. Paul Synaeve, Dr. Maria C. Cedrini for his and her kind considerations. I would also like to thank to every body involved in the publishing of the AAR journal to be successful as it is.



Kawee Tungsubutra
January - April 2000.

AAR Journal of Radiology.
Instructions for Authors.

1. The AAR Journal of Radiology publishes the papers on Radiological Sciences, such as research work, review articles, case reports, innovations in Medical Sciences related to all branches of Radiology, and letters to the editor. The aforementioned materials can be written in English only.

2. The authors have to submit 2 copies of the manuscript and a diskette: to **Prof. Dr. Kawee Tungsubutra**. 318 Kaweevej Hospital, Taksin Road, Dhonburi, Bangkok 10600, Thailand.

3. The original copy to be submitted must be typed in a double space on one side of the page of 8.1/2" x 11.1/2" paper.

4. The format of the article must include :

- a. Title page and address of the author (s)
- b. Abstract
- c. Introduction (Background)
- d. Material and Method
- e. Results and discussion (Tables and Illustrations)
- f. Acknowledgement (if any)
- g. References (Follow the Vancouver style developed by ICMJE)

5. We will provide 25 copies of reprints for the author (s) who submit (s) an article for publication in the AAR Journal.

6. The illustrations and tables must be clearly prepared with legends in English as they are the art works to be reproduced.

7. The authors are responsible for the contents of the article as to its facts and findings.

8. Ethics.

Paper reporting studies which might be interpreted as human experimentation (e.g. controlled trials) should conform to the standards of the Declaration of Helsinki (see British Medical Journal 1964:2:177) and should indicate that, approval that such studies may proceed, has been granted by the local or hospital Ethics Committee.

When reporting experiments on animals indicate whether the institution's or the National Research Council's guide for, or any national law on, the care and use of laboratory animals was followed.



ขอขอบคุณ บริษัทต่อไปนี้ ที่ได้มีอุปการะคุณแก่

รังสีวิทยาสมาคมและราชวิทยาลัยรังสีแพทย์แห่งประเทศไทย
ในการลงโฆษณาแก่รังสีวิทยาสารตั้งแต่พิมพ์เป็นภาษาไทย และ
ASEAN JOURNAL OF RADIOLOGY ซึ่งพิมพ์เป็นภาษาอังกฤษ

คณะกรรมการรวมทั้งสมาชิกของรังสีวิทยาสมาคมและ
ราชวิทยาลัยรังสีแพทย์แห่งประเทศไทย จะถือเป็นหน้าที่ซึ่งจะต้อง
ระลึกถึงบุญคุณ และถ้ามีโอกาสจะช่วยเหลือกิจการของบริษัทต่างๆ
ที่จะกล่าวนามต่อไปนี้ พวกเราจะไม่ละเลยหรือละเว้นที่จะช่วยเหลือ
ด้วยความเต็มใจ

บริษัท แบริคโค อินเตอร์เนชันแนล จำกัด
บริษัท อินเตอร์เนชันแนล ฟาร์มาซูติคัล จำกัด (BRACCO)
บริษัท ซี.เอ็ม.ซี. ไบโอดีค จำกัด (TOSHIBA)
บริษัท ฟิลิปส์ อิเล็กทรอนิกส์ (ประเทศไทย) จำกัด
ห้างหุ้นส่วน วิมิตรกิจ จำกัด
บริษัท เซริง (กรุงเทพฯ) จำกัด
บริษัท คงศักดิ์ เอกซเรย์การแพทย์อุตสาหกรรม จำกัด
บริษัท วรไทย เมดิคอล จำกัด (HOPE THAI)
บริษัท แปซิฟิกเฮลแคร์ (ไทยแลนด์) จำกัด
บริษัท ไทยเทคนิโนเมต จำกัด
บริษัท สุพรีม โพรดักส์ จำกัด
บริษัท กมลสุโกศล อิเล็กทริก จำกัด
บริษัท เบอรัลลี่ ยูคเกอร์ จำกัด (AGFA)
บริษัท รังสีภัณฑ์ จำกัด
บริษัท ยู.เอส. สัมมิต (โอเวอร์ซีส์) จำกัด
บริษัท ฟูลิไฟด์ฟิล์ม (ไทยแลนด์) จำกัด
บริษัท โกดัก (ประเทศไทย) จำกัด
บริษัท วิทยาคม จำกัด
บริษัท ซีเมนส์ จำกัด
บริษัท อ็อกไซ เคมี (ประเทศไทย) จำกัด
บริษัท เคียววา ฮัคโค (ประเทศไทย) จำกัด
บริษัท เจ็บเซน แอนด์ เจิสเซน มาร์เก็ตติ้ง จำกัด
บริษัท เมดิคอลอินเทนซีฟแคร์ จำกัด (M.I.C)
บริษัท ไทยโพลีเมตริก จำกัด
บริษัท ไอ.ซี.ซี. อินเตอร์เนชันแนล จำกัด (มหาชน)
บริษัท เทอรูโม (ประเทศไทย) จำกัด
บริษัท ซิลลิด ฟาร์มา จำกัด (ไนโคเมต)
บริษัท อุดมเมดิคอล อีควิปเมนท์ จำกัด
บริษัท ซายน์เทค จำกัด
บริษัท เอส.ไอ. เมดิคอล จำกัด

บริษัท ไทยฮอทพิเทคส์ จำกัด
บริษัท เอส.เจ. เมดิคอล เทรตติ้ง จำกัด
บริษัท อี.อี. อินเตอร์เนชันแนล จำกัด
บริษัท ยูไนเต็ด 4 จำกัด
บริษัท ธเนศพัฒนา จำกัด
บริษัท ไปโอจีเน็ทเทคส์ จำกัด
บริษัท ทรานส์เมตริก จำกัด
บริษัท ยูนิเมต จำกัด
บริษัท โชวิค จำกัด
บริษัท บอร์เนียว (ประเทศไทย) จำกัด
บริษัท ไทยอินดัสเตรียลแก๊ส จำกัด
บริษัท เมดิคอล อินดัสเทียล โดเมสติกส์ จำกัด
บริษัท ไทย จี แอล จำกัด
ห้างหุ้นส่วนจำกัด ปทุมการช่างเอกซเรย์
บริษัท บีกริม เฮลแคร์ จำกัด
บริษัท แองโกล-ไทย จำกัด
บริษัท จอนห์สัน แอนด์ จอนห์สัน (ประเทศไทย) จำกัด
บริษัท โอเร็กซ์เทรตติ้ง จำกัด
บริษัท เมย์แอนด์เบเกอร์ จำกัด
บริษัท เดลตา แล็บบอราตอรี จำกัด
บริษัท นำสินเทรตติ้ง จำกัด
ห้างหุ้นส่วน นริกุล จำกัด
บริษัท สยาม ฟาร์มาซูติคัล จำกัด
บริษัท 3เอ็ม (ประเทศไทย) จำกัด
บริษัท โดมอนด์ ฟิลด์ จำกัด
บริษัท สเตอริลิง ดรัค อินเตอร์เนชันแนล จำกัด
บริษัท เอส.บี. เมดิโค จำกัด
บริษัท พิคเกอร์ อินเตอร์เนชันแนล จำกัด
บริษัท ไทยยูนิค จำกัด
บริษัท ไทยก๊อส จำกัด
บริษัท ประมวลมิตร จำกัด
ห้างหุ้นส่วนจำกัด สุรียา แอนด์ แกแล็กซี่ กรุ๊ป จำกัด
บริษัท ดีทแฮล์ม จำกัด
บริษัท เมดิคอลมีเดียโปรดักส์ จำกัด
บริษัท ไทยเมต-เทค จำกัด (SCHNEIDER)
บริษัท เจ.เอฟ.แอตวาน เมต จำกัด
บริษัท ไพร้ม เมดิคอล จำกัด
บริษัท เอเป็กซ์เมดิคอล เทคโนโลยีส์ (ประเทศไทย) จำกัด
บริษัท เมดิทอป จำกัด



***THE BOARD OF EDITORS OF THE AAR JOURNAL ,
THE JOURNAL OF THE RADIOLOGICAL SOCIETY OF THAILAND ,
AND THE ROYAL COLLEGE OF RADIOLOGISTS OF THAILAND.***

WE WOULD LIKE TO EXTEND OUR GRATITUDE AND APPRECIATION FOR THE KIND CONSIDERATIONS TO BE HELPFUL IN THE PUBLISHING OF THE JOURNAL OF THE RADIOLOGICAL SOCIETY OF THAILAND IN THAI LANGUAGE AND THE ASEAN JOURNAL OF RADIOLOGY IN ENGLISH, TO THOSE COMPANIES OF DIFFERENT BUSINESSES IN THAILAND AND ABOARD.

IF THERE IS ANY THING WE CAN DO TO PROMOTE YOUR BUSINESSES IN THAILAND, PLEASE DON'T HESITATE TO LET US KNOW.

THE BRACCO INTERNATIONAL CO.,LTD.
INTERNATIONAL PHARMACEUTICAL CO.,LTD. (BRACCO)
C.M.C. BIOTECH CO.,LTD. (TOSHIBA)
PHILIPS ELECTRICAL CO. OF THAILAND LTD.
VIMITKIJ LTD. PARTNERSHIP
SCHERING (BANGKOK) CO.,LTD.
KONGSAK X-RAY MEDICAL INDUSTRY CO.,LTD.
HOPE THAI MEDICAL CO.,LTD.
PACIFIC HEALTH CARE (THAILAND) CO.,LTD.
THAI TECHNOMED CO.,LTD.
SUPREME PRODUCTS CO.,LTD.
KAMOL SUKOSOL ELECTRIC CO.,LTD.
BERLI JUCKER CO.,LTD. (AGFA)
RADIOLOGICAL EQUIPMENT CO.,LTD.
U.S. SUMMIT CO.,LTD.
FUJI PHOTO FILM (THAILAND) CO., LTD.
KODAK (THAILAND) CO.,LTD.
VIDHAYAKOM CO.,LTD.
SIEMENS CO.,LTD.
OXO CHEMIE CO.,LTD.
KYUOWA HAKKHO (THAILAND) CO.,LTD.
JEBSEN & JESSEN CO.,LTD.
MEDICAL INTENSIVE CARE CO.,LTD.
THAI POLY MEDIC CO.,LTD.
INTERNATIONAL COSMETICS CO.,LTD.
TERUMO (THAILAND) CO.,LTD.
ZUELLIG PHARMA CO.,LTD. (NYCOMED)
UDOM MEDICAL EQUIPMENT CO.,LTD.
SCIENCE TECH CO.,LTD.
S.I. MEDICAL (DU PONT FAR EAST INC.)

THAI HOSPITEX CO.,LTD.
S.J. MEDICAL TRADING CO.,LTD.
G.E. INTERNATIONAL OPERATIONS CO.,LTD.
UNITED 4 CO.,LTD.
THANETPATTANA CO.,LTD.
BIO JINITECH CO.,LTD.
TRANMEDIC CO.,LTD.
UNIMED CO.,LTD.
XOVIC CO.,LTD.
BORNEO (THAILAND) CO.,LTD.
THAI INDUSTRIAL GLASS CO.,LTD.
MEDICAL INDUSTRIAL DOMESTIC CO.,LTD.
THAI GL. CO.,LTD.
PHATUMKARNCHANG X-RAY PARTNERSHIP
B-GRIMM HEALTH CARE CO.,LTD.
ANGLO-THAI (THAILAND) CO.,LTD.
JOHNSON & JOHNSON (THAILAND) CO.,LTD.
OREX TRADING CO.,LTD.
MAY & BAKER CO.,LTD.
DELTA LABORATOIRE CO.,LTD.
NAMSIN TRADING CO.,LTD.
HARIKUL LTD. PARTNERSHIP
SIAM PHARMACEUTICALS CO.,LTD.
3M (THAILAND) CO.,LTD.
DIAMOND FIELD CO.,LTD.
STERLING DRUG INTERNATIONAL INC.
S.B. MEDICO CO.,LTD.
PICKER INTERNATIONAL (THAILAND) CO.,LTD.
THAI UNIQUE CO.,LTD.
THAI GAUZE CO.,LTD.
PRAMUANMIT CO.,LTD.
SURIYA & GALAXY GROUP LTD. PARTNERSHIP
DIETHELM CO.,LTD.
MEDICAL MEDIA PRODUCT CO.,LTD.
THAIMED TECH CO.,LTD. (SCHNEIDER)
J.F. ADVANCE MED CO.,LTD.
PRIME MEDICAL CO.,LTD.
APEX MEDICAL TECHNOLOGY (THAILAND) CO.,LTD.
MEDITOP CO.,LTD.

